Weathering of plastics in terrestrial environments

Max Groß [a,*], Matthias Mail [b,c,d], Rafaela Debastiani [b,c], Torsten Scherer [b,c], Melanie Braun [a]

[a] Institute of Crop Science and Resource Conservation (INRES) - Soil Science and Soil Ecology, University of Bonn, Nussallee 13, Bonn, 53115, Germany
[b] Institute of Nanotechnology (INT), Karlsruhe Institute of Technology (KIT), Hermann-von-Helmholtz-Platz 1, Eggenstein-Leopoldshafen, 76344, Germany
[c] Karlsruhe Nano Micro Facility (KNMFi), Karlsruhe Institute of Technology (KIT), Hermann-von-Helmholtz-Platz 1, Eggenstein-Leopoldshafen, 76344, Germany
[d] Tescan GmbH, Zum Lonnenhohl 46, Dortmund, 44319, Germany

Keywords:
Scanning electron microscopy
Degradation
Ageing
Soil
Compost
Landfill
Wastewater

A B S T R A C T

When plastics accumulate in the terrestrial environment, they undergo weathering, which alters their properties and causes them to fragment into micro- and submicron plastics. Although various analytical methods exist to study these processes, a comprehensive overview of their application and the alterations of plastics under field conditions across different terrestrial systems is missing. This review summarises analytical approaches for assessing surface, structural, chemical and mechanical changes in weathered plastics, focusing on scanning electron microscopy. We examine plastic alterations in short-term (e.g., composting, wastewater treatment) and long-term (e.g., landfills, soils) systems. As sample treatment can substantially alter analyses, we provide recommendations for assessing these changes. Plastic weathering leads to significant, but comparable, changes across terrestrial systems, with plastic properties as key influencing factors. While most data come from landfill studies, research in soils remains limited. Understanding long-term weathering is essential for evaluating the environmental fate of plastics, emphasizing the need for extended studies in diverse terrestrial environments.

Abbreviations

AFM	Atomic Force Microscopy
2D-COS	Two-Dimensional Correlation Spectroscopy
AES	Auger Electron Spectroscopy
Al	Aluminium
Al_2O_3	Aluminium (III) oxide
AOP	Advanced oxidation process
As	Arsenic
Au	Gold
Ba	Barium
Be	Beryllium
BET	Brunauer-Emmett-Teller
BOPP	Bi-Oriented Polypropylene
Br	Bromine
C	Carbon
C═C	Carbon-carbon double bond
C═O	Carbonyl group
Ca	Calcium
Cd	Cadmium
CH═CH2	Vinyl group
CH_2	Methylene group
CH_3	Methyl group
CI	Carbonyl index
Cl	Chlorine
CLSM	Confocal Laser Scanning Microscopy
Co	Cobalt
C–O	Carbon–oxygen bond
CO_2	Carbon dioxide
C–*O*–C	Ether group
Cr	Chromium
CT	X-ray Computed Tomography
Cu	Copper
DSC	Differential Scanning Calorimetry
EDX	Energy-Dispersive X-ray Spectroscopy
Fe	Iron
F	Fluorine
FTIR	Fourier Transform Infrared Spectroscopy
GPC	Gel Permeation Chromatography
H_2O	Water
HDPE	High-density Polyethylene
HI	Hydroxyl index
IR	Infrared
K	Potassium
LDPE	Low-density Polyethylene
LIBS	Laser-Induced Breakdown Spectroscopy
LLDPE	Linear Low-density Polyethylene
Mg	Magnesium
Mn	Manganese

(*continued on next column*)

(*continued*)

(*continued on next page*)

* Corresponding author.
E-mail address: max.gross@uni-bonn.de (M. Groß).

(*continued*)

MP	Microplastic
MS	Mass Spectrometry
N	Nitrogen
Na	Sodium
N–H	Nitrogen hydrogen group
NIRS	Near-Infrared Spectroscopy
NMR	Nuclear Magnetic Resonance Spectroscopy
O	Oxygen
O/C	Oxygen/Carbon
O–H	Hydroxyl group
OM	Optical Microscopy
Os	Osmium
P	Phosphate
PA	Polyamide
Pb	Lead
PBS	Phosphate-buffered saline buffer
PE	Polyethylene
PET	Polyethylene terephthalate
PP	Polypropylene
PS	Polystyrene
Pt	Platinum
PU	Polyurethane
PVC	Polyvinyl chloride
ROS	Reactive oxygen species
Ru	Ruthenium
S	Sulphur
SEM	Scanning Electron Microscopy
Si	Silicon
SiO_2	Silicon dioxide
Sn	Tin
TEM	Transmission Electron Microscopy
TGA	Thermogravimetric Analysis
Ti	Titanium
UV	Ultraviolet
UV–Vis	Ultraviolet–Visible
WCA	Water Contact Angle
WWTP	Wastewater treatment plant
XPS	X-ray Photoelectron Spectroscopy
XRD	X-ray Diffraction
XRF	X-ray Fluorescence Spectroscopy
Zn	Zinc
$ZnCl_2$	Zinc chloride

1. Introduction

In recent years, plastic production has increased exponentially, from 1.5 million tonnes in 1950 to 413.8 million tonnes in 2023 [1,2]. A rise in waste generation has accompanied this increase in production. Only a small proportion of plastic waste is recycled, while the majority ends up in landfills or the environment [3,4]. Once plastics enter the environment, their persistence leads to an accumulation in various environmental systems. There, they are exposed to a variety of processes, that can alter their ecological impacts and environmental fate [5]. These processes - collectively termed degradation, alteration, ageing or weathering - describe changes in the properties of plastics. Noteworthy, fixed terms like 'ultraviolet (UV) degradation' or 'biodegradation' used in many studies do not describe a complete degradation or mineralisation, i.e., the breakdown into small molecules, mainly carbon dioxide (CO_2) and water (H_2O) [6], but rather a weathering of plastics. Also the term ageing, in soil science defined as the decrease of extractability of, e.g., pollutants with increasing residence time in soil [7–9] is in many studies used to describe plastic alterations (recently summarised in He et al. [10], Wang et al. [11] and Lu et al. [12]). To avoid misunderstandings, we will use the term weathering or alteration to describe changes of plastic particles, like their surface or structure, except for fixed terms like UV degradation or biodegradation.

Plastic weathering can be divided into abiotic and biotic processes. Abiotic processes involve interactions between the polymer and physicochemical agents, resulting in photodegradation, hydrolysis, oxidation or thermal weathering. These processes typically increase the surface area of plastics, fostering biodegradation through the activity of (micro) organisms [13,14]. The complex interplay of abiotic and biotic weathering processes, which depends on the specific environmental conditions, ultimately leads to the fragmentation of larger plastics into smaller particles, such as microplastics (MPs) (1 μm–5 mm) and submicron plastics (1 nm-1 μm) or even nanoplastics (1 nm–100 nm) [15,16].

A range of analytical methods, including microscopic, spectroscopic, and thermoanalytical techniques, is used to study plastic weathering in the environment, assessing changes in surface morphology, structural integrity, mechanical properties, and chemical composition (recently reviewed in Shi et al. [17] and Tian et al. [18]). However, despite the widespread use of techniques like scanning electron microscopy (SEM), significant uncertainty remains regarding their implementation and standardization. This includes variations in pre-treatment methods such as plastic extraction and fixation, as well as differences in SEM settings. Evaluating the effects of these factors is essential to ensure the comparability of SEM-based studies.

To understand the fate of plastics in the environment, acquiring a more profound understanding of their weathering is critical. Zhang et al. [5] and Andrady et al. [15] recently summarised the weathering processes in the marine environment, highlighting that a significant proportion of fragmented plastics found in marine environments likely originated from land-based sources. In addition, both studies point out the challenges of extrapolating laboratory weathering data to real-world environmental conditions due to the complexity and variability of natural environments. Binda et al. [13] and Wang et al. [11] just recently reviewed different weathering processes of plastic in the environment, focusing on laboratory studies under accelerated simulated conditions. These studies summarised commonly used artificial ageing methods, elucidate the underlying mechanisms, and evaluate their effects on plastic properties and implications for MP analysis. Laboratory studies are important for estimating polymer lifetimes but fail to capture the complexity of real-world environmental conditions and often describe only a very short exposure period, not accounting for long residence times in landfills or soils [11,16]. However, a detailed understanding of how plastics alter in the terrestrial environment - one of the largest global reservoir of plastics [19]- under real conditions is still missing, as well as an overview on how this weathering may differ between single systems.

In the terrestrial environment, plastics accumulate in various systems where they undergo weathering. These systems can be categorized based on their residence time: long-term reservoirs, such as landfills and soils, and short-term reservoirs, such as composting, digestion, and wastewater treatment facilities. Landfills remain the most common method of waste disposal, accounting for nearly 40 % of global waste [20,21]. Consequently, significant quantities of plastics are intentionally stored in these sites [22]. In soil, plastics are introduced through several input pathways, including agricultural practices such as sludge and compost application and the intentional use of plastics, termed "plasticulture". But also, diffuse sources such as littering, atmospheric deposition or flooding contribute to the plastic loads of soil [23]. Hence, in most cases, plastic items are already pre-altered during composting, digestion and water treatment before reaching soil where they undergo further weathering. Plastics, entering composting and digestion facilities, mainly originate from the improper disposal of waste [24,25]. Wastewater contains high concentrations of plastics from a variety of sources. Depending on the properties of the plastic and the wastewater treatment processes, they may either accumulate in sewage sludge or remain in the treated wastewater [26]. Additionally, plastics may undergo weathering during transportation or their service life before reaching these short-term systems. The extent and types of the respective weathering processes depend on the properties of the specific compartment and the duration of the plastic's residence time.

Accordingly, this review aims to (i) summarise current methods for characterising the effects of weathering on plastics in the environment, with particular emphasis on SEM, and (ii) elucidate the weathering

processes of plastics in both natural and artificial terrestrial systems in the terrestrial environment (excluding laboratory-scale studies as they have been recently summarised by Binda et al. [13] and Wang et al. [11]). Terrestrial systems include long-term systems (landfills and soils) and short-term systems (composting and digestion facilities, wastewater treatment plants). The focus is on the most commercially relevant plastics: polyethylene (PE), polypropylene (PP), polyamide (PA), polystyrene (PS), polyvinyl chloride (PVC), polyurethane (PU) and polyethylene terephthalate (PET) [2].

2. Literature search, selection and data extraction

The final literature search was conducted in March 2025, in Web of Science using the words 'plastic' and 'microplastic' in combination with the respective environments and the keywords 'degradation', 'biodegradation', 'corrosion', 'alteration', 'surface change', 'modification', 'ageing' and 'weathering'. Studies were included if they were conducted under real environmental conditions, such as natural soils, industrial composting, biogas and wastewater treatment plants, as well as landfills actually used for waste treatment. Studies conducted under artificial conditions or at a laboratory scale were excluded. No specific size parameters were set, so all studies describing changes in, e.g., microplastics, mesoplastic and macroplastics were included. The polymers in scope were the most commercially relevant conventional plastics: PE, PP, PET, PVC, PA, PS and PU, which account for nearly 75 % of all plastics produced globally in 2023 [2]. Polymers with non-common, specific additives were not considered. To focus on real environmental settings, also artificially pre-weathered plastic particles, for example, with UV radiation or heat and blends of the polymers were excluded in this review. As a result, a total of 70 studies were reviewed.

3. Results & discussion

3.1. Methods used to describe the weathering of plastics in the terrestrial environment

A total of 19 different methods were used to assess the weathering of plastics in the terrestrial environment (Fig. 1). Most of the analyses focused on surface (43 %) and chemical changes (38 %) of plastics after environmental exposure (Fig. 1). Structural or mechanical properties were analysed less frequently, 9 % and 10 % respectively. Above all, scanning electron microscopy (SEM) and Fourier transform infrared spectroscopy (FTIR) proved to be the most common methods. Notably, most studies employed a multimodal approach, combining different methods to analyse chemical and surface properties, such as FTIR and SEM. Additionally, surface characterization was often enhanced by coupling SEM with energy-dispersive X-ray spectroscopy (EDX), contributing to its widespread use.

Before weathering analysis, 89 % of the studies provided details on the extraction and cleaning of the plastics analysed. Of these, only 37 % used a gentle extraction and cleaning process that involved manual removal of plastics followed by rinsing with tap water, distilled water or ultrapure water and, if necessary, ultrasound or shaking. In contrast, 63 % of the studies analysed plastic particles that had undergone MP extraction, including density fractionation and/or approaches for organic matter removal. These extraction methods, however, can alter surface properties, modify FTIR spectra, alter mass and molecular weight distributions, and contribute to plastic fragmentation, depending on the type of plastic [27–29]. As a result, studies examining the weathering of such extracted particles may overestimate the effects of environmental weathering. To ensure accuracy, researchers should compare extracted particles with pristine plastic particles subjected to the same extraction methods, if possible.

To minimise the effects of extraction, it is important to carefully

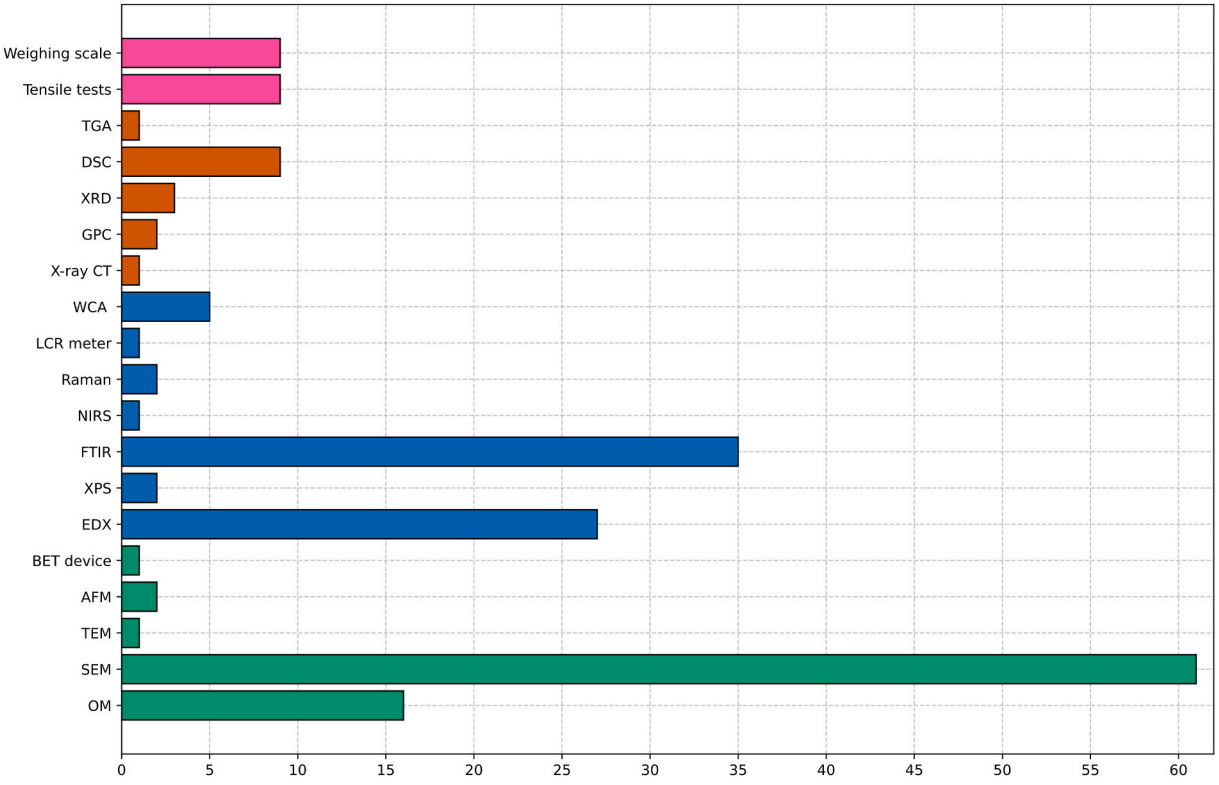

Fig. 1. Frequency (given as number of studies) of methods used to analyse weathering of plastic particles exposed in terrestrial systems, including analyses focusing on surface (green), chemical (blue), structural (orange) and mechanical (pink) alterations of plastics. (For interpretation of the references to colour in this figure legend, the reader is referred to the Web version of this article.)

consider whether extraction is necessary and, if so, to select the least invasive method. For larger plastic particles, extraction is usually unnecessary as they can be sorted manually. This is also true for controlled experiments, where plastics are often secured in holders [30], containers [31] or mesh bags [32]. However, even cleaning procedures such as, acetone treatment can cause material changes that need to be carefully considered [33]. Where extraction is necessary, particularly for smaller particles such as MPs, researchers should avoid corrosive substances and oxidative chemicals [34]. Instead, they should opt for less aggressive alternatives, such as potassium formate solutions or enzymatic digestion, to preserve the integrity of the plastic and ensure accurate analysis [35,36]. However, it is important to note that elements in density solutions can interfere with subsequent elemental analyses, as the use of Zinc chloride ($ZnCl_2$) might increase the Zinc (Zn) levels on the plastic surface and hence falsify SEM-EDX results [37].

3.1.1. Optical microscopy (OM

Optical microscopy was a commonly applied technique in the reviewed studies (16 times), in which light from a source is focused onto a specimen (Fig. 1). Optical microscopes typically provide magnifications of up to 1000×, depending on the lens used, with some advanced systems providing even higher magnifications [38]. Several advanced techniques, such as polarization, phase contrast, dark-field, fluorescence and differential interference contrast microscopy, can be applied to enhance imaging [39]. When describing the weathering of plastics, optical microscopy was used to assess a range of features, including surface characteristics, textural changes, microbial colonisation and the attachment of organic and inorganic materials [40,41] (Fig. 1 and Tables 2–5). A more advanced optical-microscopic technique is Confocal Laser Scanning Microscopy (CLSM), in which a focused laser beam is employed and scanned across the sample surface, creating high-resolution, optically sectioned images. Image quality and contrast are enhanced by eliminating out-of-focus light, while stimulated emission depletion microscopy and structured illumination microscopy provide even higher resolutions [42,43]. CLSM has mainly been used to study fungal and microbial growth patterns, as well as biofilm formation on plastics after exposure in terrestrial environments [33,44]. In addition, CLSM can assess material homogeneity by examining layer structures and detecting inhomogeneities in coated or multilayer plastics, reconstruct three-dimensional structures of plastic samples, and visualize colour distributions, additives, or fluorescently labelled contaminants in fluorescence studies [45].

3.1.2. Scanning electron microscopy (SEM

Scanning electron microscopy is the most widely used method (61 studies) for assessing the weathering of plastics (Fig. 1 and Tables 2–5), as it can provide information on the surface topography, crystalline structure, chemical composition and electrical behaviour of a sample with a resolution up to 1 nm [46,47]. Because of its crucial role in the analysis of weathered plastics, we reviewed the studies regarding pre-treatments, SEM equipment and settings, detectors and magnifications used in more detail (Table 1) and concluded about the implications for surface analysis.

To conserve surface structures, such as biological attachments (e.g., microbial colonisation), samples often underwent a special treatment, like dehydration in ethanol or critical point drying (Table 1). Several preparation methods can be applied to study plastic samples in more detail. Breaking and etching are typical methods used to assess the morphology of polymer blends [48]. Staining improves the ability to assess the weathering of plastics in greater detail by increasing the contrast in imaging techniques. Heavy atoms, such as osmium (Os) and ruthenium (Ru), selectively bind to specific phases of the resin, enhancing the signals in SEM or transmission electron microscopy (TEM) due to their higher atomic numbers. This allows for enhanced visibility of microstructural and chemical changes [48]. Additionally, staining can stabilize plastics for electron microscopy, but it may also alter their structure by significantly changing their physicochemical surface properties, especially in weathered particles. a) Chemical changes occur when stains react with surface functional groups or embed themselves, especially in weathered particles whose surfaces are more reactive. b) Physical changes include swelling, surface roughness, or deformation of sensitive polymers like PE or PS, with weathered particles being more susceptible due to cracks or porous structures. c) Changes in surface charge and wettability happen as weathered particles, often containing more polar groups, interact more strongly with stains. d) Material dependence is evident as hydrophilic plastics like PA are more sensitive, but weathered hydrophobic plastics like PE can also be significantly affected due to new polar groups. Special care is required for MPs as their small size, large surface area, and weathering make them highly susceptible to chemical and physical changes. Mild staining protocols, such as low concentration, short duration, and moderate temperature, should be used to preserve particle integrity and ensure accurate results [49].

Table 1
Sample treatment and SEM settings in the reviewed studies.

Parameter	Nr. of studies[a]	Examples
Preparation	30/61	Dehydration in ethanol Critical point drying Phosphate-buffered saline buffer and a fixative solution (PBS buffer and glutaraldehyde) Removal of biofilm with a sterile physiological solution Fixes on carbon tape, graphite, conductive silver Surface coating (Au, Pt, C, Au–Pd) with a thickness 2–30 nm
SEM- Device	49/61	SEM, FESEM, ESEM from various companies: ZEISS, FEI, Hitachi, TESCAN, ThermoFisher, Phillips, JEOL, KYKY
SEM-Voltage	47/61	Acceleration voltage of 1–30 kV, most 5, 10, 20 kV
SEM- Detector	24/61	SE1, SE2, BSE, InLens
Pixel size/ Magnification	30/61	2867–19.11 nm 35-12000 x
EDX-Device	8/27	EDX detectors from Horiba and Oxford instruments
EDX-Voltage	3/27	5, 14, 15 kV

[a] Number of studies: first number relates to studies that give information regarding this parameter; last number refers to the total number of studies.

Depending on the type of SEM, sample preparation may also involve coating the sample with heavy elements such as gold (Au), platinum (Pt) or chromium (Cr) to reduce charge and electron beam damage (Table 1). Alternatively, carbon (C) coating is often preferred for plastics as it minimises X-ray absorption by heavy metals and increases the X-ray quantum yield for EDX while remaining negligible for plastics analysis [50]. Of the reviewed articles, 51 % of the studies described the sample preparation methods used (Table 1).

In an SEM, primary electrons (electron beam) are emitted from the electron source (cathode), accelerated by a voltage commonly in the range of 0.05–30 kV between the cathode and anode, pass through a set of electromagnetic lenses/coils and are focused to a small spot (typical sizes: 1 μm to 1 nm) on the surface of the sample [48]. When the electron beam hits the surface, secondary (low energy (<50 eV)) and backscattered (high energy (>50 eV)) electrons are emitted together with Auger electrons, cathodoluminescence and characteristic X-rays during interaction with and penetration into a sample [48]. The emitted X-rays provide information about the local elemental composition of the sample and are used in EDX. EDX is a spectroscopic technique that enables qualitative or quantitative elemental analysis of a selected region and facilitates the mapping of elemental distributions in conjunction with SEM imaging. [47]. Of the 61 studies using SEM, 27 combined it with EDX (Table 1). However, only limited information was provided on the

Table 2
Reviewed studies for landfills.

Landfills	Country	Polymers	Methods	Analysis	Study
Samples were buried 1.2 m below the landfill surface. Sampling was carried out after 2, 4, 6, 9, 13, 18 and 24 months of exposure.	USA	LDPE, LLDPE, HDPE, PP	Universal testing machine, weighing scale	• Weight change • tensile strength at break • percentage elongation	[56]
30 waste samples were collected from 4 municipal solid waste landfills at depths between 5 and 55 m. The samples were grouped according to age: <10 years (7 samples) and >10 years (23 samples).	UK	PE, PP	ESEM-EDX, FTIR, DSC	• Surface analysis • CI • Degree of crystallinity	[132]
Leachate samples were collected from 10 landfills ranging in age from 4 to 24 years.	China	Various polymer types found, SEM-EDX for PVC	SEM-EDX	• Surface analysis • Elemental analysis	[143]
Samples were taken at a depth of 20 cm at two different locations in a controlled landfill.	Brazil	No info about the analysed polymer type	OM, SEM,	• Surface analysis	[133]
Topsoil samples were collected from two landfill sites in Siaya Central. In addition, topsoil samples were collected from a roadside in Mbaga village, the Ramba marketplace and a courtyard in Aringo Estate (see Table 5).	Kenya	–	SEM, OM	• Surface analysis	[44]
Sampling was carried out in cell compartments covering the age of the landfill from 7 to 31 years. Samples were collected at depths of 2, 4 and 8 m. Collected samples were divided into 6 groups according to their age: <10, 10–15, 15–20, 20–25, 25–30, >30 years.	China	Various polymer types found. SEM, XPS and WCA of no specific polymer type. FTIR of PE, PP, and PS.	SEM, FTIR, XPS, WCA measuring device	• Number of MPs' • Surface analysis • Generation rate of MPs for different plastics • Changes in WCA • Changes in FTIR spectra • CI • Analysis of C1s spectra	[84]
Samples were taken from a practical landfill in Shanghai after 10 years of landfilling.	China	PE	SEM, AFM, FTIR, GPC	• Changes in FTIR spectra • Surface analysis and surface roughness • molecular weight distribution	[61]
Samples were buried for 11 months at a depth of 2 m in a 5 year old cell (methanogenic phase) of a solid waste landfill.	Brazil	PP	OM, FESEM, FTIR, DSC, TGA, weighing scale	• Changes thermal behaviour and melting temperature • Changes in FTIR spectra. • Changes in isotacticity • ketone CI, methylene group index • Surface analysis	[73]
Stratified random sampling was used and the site was divided into three strata: stratum 1 (area with oldest waste), stratum 2 (monsoon dumping) and stratum 3 (current dumping). And further divided according to age: ⩾25 years, 20–24 years, 15–19 years, 10–14 years, 5–9 years and ⩽4 years.	India	Various polymer types found, but analysis for LDPE	SEM-EDX, FTIR,	• Surface analysis • Elemental analysis • CI • Changes in FTIR spectra	[140]
Collection of leachate samples from a landfill receiving 500 tonnes of municipal solid waste.	Iran	Various polymer types found, but no information about analysed polymer	SEM-EDX	• Surface and elemental analysis	[134]
Sampling from a closed section of a landfill for municipal solid waste. The site has not received waste for at least 5 years.	Poland	PP	SEM, OM, FTIR, DSC	• Surface analysis and evaluation of microorganism colonisation • Changes in FTIR spectra • CI and HI • Size of plastic particles • Degree of crystallinity, melting temperature and DSC thermogram	[33]
A total of 15 film samples were taken, with 3 samples per colour: black, white, red, green and yellow.	Italy	PE	ESEM-EDX, FTIR, Raman, DSC, XRF	• Differences in FTIR spectra • DSC thermogram, melting peaks • Differences in Raman spectra • Surface and elemental analysis • XRF*: although the authors mention XRF, they do not present any result using XRF or mention it on methods section	[98]
Samples were collected from a leachate treatment plant (3 raw leachate, 6 leachate ponds and 3 treated leachate samples, respectively)	Bangladesh	Various polymer types found; no information about the analysed polymer	SEM	• Surface analysis	[137]
Samples were taken from different depths in a municipal waste landfill. The age of the samples was 1.5, 5, 7.5, 30, 50 and 60 years.	Poland	PE, LDPE, HDPE, LLDPE	FTIR, DSC, SEM, OM	• Surface analysis and evaluation of microorganism colonisation • Crystallinity • Changes in FTIR spectra • CI and HI	[139]
Samples in mesh bags were incubated for 5, 9, 14 months at a depth of approximately 1 m in the slope of a 5–8-year-old landfill.	Germany	PE, PP, PS, PA, PET	SEM, OM	• Surface analysis and evaluation of microorganism colonisation	[32]
Sampling was carried out in three cells of different ages for a regional non-hazardous waste landfill: old (years 1973–2000), middle-aged (years	Lithuania	Various polymer types found, FTIR analysis for PE	FTIR	• Number of particles • CI	[146]

(*continued on next page*)

Table 2 (*continued*)

Landfills	Country	Polymers	Methods	Analysis	Study
2000–2008) and young (2008-present). Three replicate samples were taken every 2 m to a depth of 10 m in the old, up to 20 m in the middle-aged and up to 14 m in the young section.					
Leachate and refuse samples were collected from a landfill in China at depths of 0.5, 1 and 1.5 m. The landfill was divided into different zones according to the age of the landfill: young (<3 years), middle-aged landfill (~10 years) and old landfill (>20 years).	China	Various polymer types found, OM of no specific polymer type and FTIR analysis of PE	FTIR, OM	• Number of particles • Changes in FTIR spectra and CI	[144]
Sampling was carried out in a municipal soild waste landfill. The age of the excavated waste was 0, 4, 8, 13 and 18 years.	China	Various polymer types found; FTIR, SEM-EDX and Universal testing machine of PE, PP and PET	FTIR, SEM-EDX, Universal testing machine	• Changes in FTIR spectra • CI • Surface and elemental analysis • Tensile tests	[142]
Leachate and landfill waste were collected at a depth of 4.5–14 m.	China	Various polymer types found. FTIR of PE, SEM no info	SEM, FTIR	• Number of particles • Surface analysis • Changes in FTIR spectra	[135]
Sampling at a depth of 2 m in a municipal waste landfill (age 7–30 years).	China	Various polymer types found; Analysis for PE and PP	SEM-EDX, FTIR, DSC, Universal testing machine, WCA measuring device	• Changes in FTIR spectra • CI and HI • Surface and elemental analysis • Number of particles • Changes in DSC thermogram, melting temperature and degree of crystallinity • Evaluation of failure load, tensile strength and elastic modulus • WCA	[85]
A total of 20 mineralised waste and 23 leachate samples were collected from a landfill, which was divided into four zones according to the age of the landfill, with landfill ages of 9–10 years, 5–6 years, 1–3 years and <1 year.	China	Various polymer types found; FTIR of PE	FTIR	• Number and size of particles • Changes in FTIR spectra and CI	[147]
A total of 10 samples from the leachate treatment plant (4 anaerobic pond leachates, 3 aerobic pond leachates and 3 discharge leachates) of a municipal solid waste landfill were taken.	Bangladesh	Various polymer types found, but no information about analysed polymer	SEM	• Particle number • Surface analysis	[136]

Table 3
Reviewed studies for composting and digestion.

Composting/Digestion conditions	Country	Polymers	Methods	Analysis	Study
Composting of a mix of digestate (from organic waste) and raw organic waste for 28 days. Anaerobic digestion of organic waste for 24 days at a temperature of 41.1 ± 1.0 °C.	Germany	LDPE	SEM-EDX weighing scale, FTIR, NIR, DSC, Universal testing machine	• Surface and elemental analysis • Changes in FTIR and NIRS spectra • Degree of crystallinity and melting peak • Evaluation of elastic modules, tensile strength at yield tensile strength stress at break, strain at break and elongation at break	[30]
Industrial tunnel composting of organic household waste (286 t) for 25 days with temperatures of up to 70 °C.	Germany	PP	SEM, FTIR, X-ray CT	• Surface analysis • Structural changes • Changes in FTIR spectra and CI	[31]
Composting of pre-treated (manual sorting, crushing and pressing) rural domestic waste for 35 days in aerobic bins with forced ventilation and overturning. Samples were taken at two stations:	China	Various polymer types found; no information about the analysed polymer	SEM	• Number and size of particles • Surface analysis	[162]
Open windrow composting of green waste with natural aeration and periodic reloading for 8 months.	Lithuania	HDPE, LDPE, PS, PP	SEM, FTIR, weighing scale	• Number of particles • Weight change • Changes in FTIR spectra	[106]
Sampling in municipal composting yards of two cities in India.	India	Various polymer types found; no information the analysed polymer	SEM	• Surface analysis	[165]
Sampling of three composting and two digestion facilities.	China	Various polymer types found; SEM and OM of PE, PP, PET	OM, SEM	• Number and size of particles • Surface analysis	[164]
Analysis of municipal solid waste (MSW) compost, issued from the composting of the residual fraction of household waste after packaging sorting.	France	–	TEM-EDX	• Surface, morphological and elemental	[58]

EDX detectors (30 % of studies) and the applied voltages (11 %) (Table 1). Cathodoluminescence detection has been utilised in the past for the identification of various types of plastic, as well as to evaluate the presence of dyes, additives and contaminants [51,52]. However, this method was not applied in the reviewed studies. Several types of SEMs are available, which differ in their electron source, including tungsten filaments, lanthanum hexaboride cathodes and field emission guns, or in their electron optics, such as potential tubes and immersion lenses.

Table 4
Reviewed studies for wastewater treatment plants.

Sludge/WWTP	Country	Polymers	Methods	Analysis	Study
Sampling during three different days in three different months at a WWTP in Spain.	Spain	Various polymer types found; FTIR of PE and PP	FTIR	• Number and size of particles • Changes in FTIR spectra	[178]
Samples were taken from the influent, effluent treated by lamellar settling and the treated effluent of a WWTP in Morocco.	Morocco	Various polymer types found; no information about the analysed polymer	SEM-EDX	• Particle number • Surface and elemental analysis	[191]
A total of 99 samples taken from the influent, effluent and sludge of eleven wastewater treatment plants.	Bangladesh	Various polymer types found; no information about the analysed polymer	SEM	• Number of particles • Surface analysis	[177]
Samples were collected from the influent, grit chamber, primary sedimentation, aeration, secondary sedimentation and final effluent units of the WWTP for 1 month in spring and winter and analysed after mixing.	Iran	Various polymer types found; no information about the analysed polymer	SEM	• Particle number • Surface analysis	[181]
A total of 79 dewatered sludge samples from 28 WWTPs in 11 provinces in China were analysed.	China	Various polymer types found; no information of the analysed polymer	SEM	• Number of particles • Surface analysis	[180]
Sludge samples were collected from municipal wastewater treatment plants in 4 cities in China. Sludge samples were analysed before and after anaerobic digestion (AD), thermal drying (TD), thermal hydrolysis (TH) and from five stages (initial phase, heating phase, thermophilic phase, cooling phase and maturing phase) of aerobic composting (AC).	China	Various polymer types found; FTIR of PA, PE, PP, PS; Specific surface area for PA, PE, PP, PS; SEM of unknown polymer,	FTIR, SEM, BET device	• Metal adsorption • Surface analysis • Specific surface area • Changes in FTIR spectra (Two-Dimensional Correlation Spectroscopy)	[64]
Sludge samples were collected from municipal wastewater treatment plants in 4 cities in China. Sludge samples were analysed before and after anaerobic digestion (AD), thermal drying (TD), thermal hydrolysis (TH) and from five stages (initial phase, heating phase, thermophilic phase, cooling phase and maturing phase) of aerobic composting (AC).	China	Various polymer types found; no information about the analysed polymer	FESEM-EDX	• Number of particles • Surface and elemental analysis	[185]
Samples were taken from the effluent from intake, effluent from grid, effluent from oxidation ditch, effluent from secondary sedimentation tank, effluent from deep treatment and from dewatered sludge.	China	Various polymer types found; no information about the analysed polymer	SEM	• Number of particles • Surface analysis	[184]
Sludge samples after various treatments including thermal drying (TD), anaerobic digestion (AD) and lime stabilisation (LS) were collected from seven WWTPs.	Ireland	Various polymer types found; SEM analysis of HDPE, PE and items of unknown polymer types	SEM	• Number and size of particles • Surface analysis	[186]
Samples were taken over a three-month period in a WWTP in Poland.	Poland	Various polymer types found; no information about the analysed polymer	SEM	• Surface analysis	[182]
Sludge samples were sampled at a WWTP in China at 4 different treatment stages: sedimentation tank sludge, dewatered sludge, biogas residue of sedimentation tank sludge and biogas slurry of sedimentation tank sludge.	China	Various polymer types found; SEM and OM of PE, PP, PET	OM, SEM	• Number and size of particles • Surface analysis	[164]
Fresh municipal sludge (FSS1), mixed sludge (FSS2) and hot (320–420 °C) air-dried municipal sludge (DSS) were applied to a paddy soil (Haplic-stagnic Anthrosol) in a long-term application experiment (see also Table 5).	China	No analysis of MPs derived from sludge samples, just for soil		• Number of particles	[179]
The sewage sludge tested was derived from fermented sludge from a domestic wastewater treatment plant (see also Table 5).	China	Various polymer types found; no information about the analysed polymer	SEM	• Surface analysis	[183]

Specialised systems, such as environmental SEMs, operate under low vacuum (10 to several thousand Pa) and often use water vapour or nitrogen (N) to mitigate sample charging and protect sensitive samples from high vacuum [47,48].

Monte Carlo simulations, along with the Kanaya-Okayama formula, are valuable tools for estimating electron penetration depth and trajectory [48,53,54]. Monte Carlo simulations [54] demonstrated that the elemental composition and density of the plastics (Fig. 2 and Table S1) significantly influence lateral and axial electron propagation, as well as backscattered electron generation, at the same acceleration voltage.

Furthermore, SEM settings significantly impact the resulting images. One critical parameter influencing the penetration depth and the signal contribution from both surface and subsurface layers is the applied acceleration voltage, which ranged from 1 to 30 kV in the reviewed studies (Table 1). Commonly applied voltages include 5, 10, and 20 kV, each affecting the charging effects on the sample and the efficiency of secondary electron detection. Lower voltage settings (1–5 kV) are ideal to minimise damage and charge build-up, while higher voltages (10–20 kV) offer deeper penetration for bulk analysis but can cause more charge effects and less surface detail (Fig. 3) [50].

Coatings are essential for preventing charge effects, with their impact depending on material and thickness. For example, increasing the thickness of the gold coating reduces the penetration depth for the same acceleration voltage. Additionally, coating materials influence signal yield due to differences in atomic number (Fig. 3). As well as possible charging effects due to differing conductivities (Fig. 4).

Acceleration voltage and coating are critical to the accuracy of EDX analysis. At 1 kV, EDX is severely limited as the electrons lack the energy to ionise inner shells, although light elements remain detectable due to reduced background radiation. A 5 kV acceleration voltage allows a wider range of elements to be detected while maintaining an acceptable sample charge. To ensure accuracy, a ~5 nm C coating provides conductivity without interfering with detection (Fig. 4). At 5 kV elements from beryllium (Be) to calcium (Ca) can be reliably measured, with light elements (e.g., C, N, oxygen (O), fluorine (F), sodium (Na), magnesium (Mg) and aluminium (Al)) being optimally detectable and medium heavy elements (e.g., silicon (Si), phosphate (P), sulphur (S), chlorine (Cl), potassium (K) and Ca) being analysable with slightly reduced sensitivity. Carbon coating is preferred for accurate analysis, while gold is unsuitable as it masks C signals and introduces artefacts into the EDX spectra.

Common challenges in interpreting SEM-EDX data include charging artefacts and image drift, which can distort image and spectral data (Figs. 3 and 4). To minimise radiation damage, high beam currents and

Table 5
Reviewed studies for soil.

Soil	Country	Polymers	Methods	Analysis	Study
47 samples along the Yellow River basin in fields with 5–10, 10–20, 20–30 and ≥ 30 years of mulching.	China	Various polymer types found, FTIR for LDPE	FTIR	• Number and size of particles • CI and HI	[240]
Sampling in two orchards in Argentina, where no plastic film had been used for 7 years prior to sampling.	Argentina	Various polymer types found; OM no specific polymer, SEM, FTIR, DSC of PE	OM, SEM, FTIR, DSC	• Surface analysis • Changes in FTIR spectra • Changes in thermal properties	[40]
Soil samples were taken from arable fields cultivated with mulch film for 5 ± 1, 10 ± 1, 15 ± 1 and 20 ± 1 consecutive years without prior use of plastic mulch	China	LDPE	SEM, FTIR, OM	• Number and size of particles • Surface analysis • Changes in FTIR spectra	[212]
Samples were taken at the surface and at a depth of 20 cm for two sampling points of a park soil in Brazil.	Brazil	Various polymer types found, No info	OM, SEM	• Surface analysis	[133]
Sampling of two soils in the summer of 2014 in a subtropical region. The first soil was a coarse sandy clay loam and the second soil was a fine sandy clay loam. Strips of film 1 m long and 15 cm wide were placed over these soils.	Australia	PE	Manual stress application	• Elongation at break based on film embrittlement	[102]
Topsoil samples were collected from two dumpsites in Siaya Central. Topsoil samples were also collected from a roadside in Mbaga village, the Ramba market place and a courtyard in Aringo Estate (see Table 2).	Kenya	–	SEM, OM	• see Table 2	[44]
Burial of two films (transparent LLDPE:LDPE films with thicknesses of 5.7 and 10.18 μm) in nylon mesh bags at a depth of 10 cm in two soils (loess orthic entisols and loess-like loam). Samples were taken after 3, 6, 12, 15, 18, 24, 27 and 30 months of burial.	China	LLDPE	FTIR, weighing scale, WCA measuring device, Universal testing machine	• Evaluation in nominal tensile and strain at break • Changes in WCA • Keto carbonyl bond, ester carbonyl bond, vinyl bond and internal double bond index • Changes in FTIR spectra • Degree of crystallinity • Weight change	[74]
Soil samples were taken from the top 10 cm of the farmland, with sample sites characterised by riverside locations, flood-prone areas, close to highways, adjacent to urban areas and different types of cropping.	Bangladesh	Various polymer types found; SEM no information about polymer type; EDX for PE, PP, PET, PVC, PS	SEM-EDX	• Number of particles • Surface and elemental analysis	[237]
Samples were taken at depths of 0–10 cm, 11–20 cm and 21–30 cm in 4 soils with up to 10 years of plastic mulch.	India	–	SEM-EDX,	• Number of particles • Surface and elemental analysis	[236]
Samples were collected from chilli and potato fields mulched with PE film in northern China. This sampling region has been using PE mulch film for >2 years.	China	PE	SEM	• Surface analysis	[225]
The sampling site was a long-term plastic film mulching and fertiliser experiment in China. The soil is a Haplic-Udic Alfisol in the US soil taxonomy. Samples were collected at depths of 0–10 cm, 10–20 cm, 20–40 cm, 40–60 cm, 60–80 cm and 80–100 cm.	China	Various polymer types found; SEM of PE, PP, PET,	SEM-EDX,	• Number of particles • Surface analysis	[232]
Three types of PE-based mulch films, white (0.006 mm thick), black (0.012 mm thick) and silver-black (0.012 mm thick), were applied to the soil surface and buried in the soil at a depth of 20 cm for 9 months.	China	PE	SEM-EDX, Universal testing machine, FTIR, XPS, WCA measuring device, XRD	• Surface and elemental analysis • Changes in FTIR spectra • Changes in WCA • Degree of crystallinity • Evaluation of tensile strength	[66].
Sampling at 0–5 and 5–10 cm depth at six sampling sites. 2 sites were traditional open field agricultural areas. While 4 sites used covering film, mulching film, and/or sunshade nets.	China	Various polymer types; SEM-EDX of PP, PE, PS	SEM-EDX	• Surface and elemental analysis	[227]
PE films were wrapped in nylon nets and buried at a depth of 2 cm in a mangrove soil and two forest soils for 112 days.	Malaysia	PE	Weighing scale	• Weight change	[230]
57 agricultural soil samples were collected from 0 to 20 cm depth around a waste treatment centre in China.	China	Various polymer types found No info about analysed polymer	SEM-EDX	• Number and size of particles • Surface and elemental analysis	[242]
Weathered plastic mulch debris was collected from five agricultural fields. The fields were characterised by intensive horticultural production and a history of plastic use at least twice a year over the last decade.	Spain	LDPE	Raman, FTIR, SEM-EDX	• Changes in FTIR spectra • CI • Changes in Raman spectra • Elemental analysis	[80]
Samples were taken (0–30 cm) from fields under plastic mulch application for 1–6, 7–11, 12–16, 17–21 and 22–30 years.	China	PE	SEM, FTIR	• Particle number • Changes in FTIR spectra • Surface and elemental analysis	[238]

(*continued on next page*)

Table 5 (*continued*)

Soil	Country	Polymers	Methods	Analysis	Study
4 different LDPE films (white, black, thin transparent and thick and thick transparent) were buried in soil at a depth of 7.5 cm for 22 months. A sample was taken every 2 months.	Bangladesh	LDPE	OM, SEM	• Surface analysis	[41]
Four different LDPE films were evaluated: a white film (0.019 mm thick), an opaque black film (0.010 mm thick), a thick transparent film (0.050 mm thick) and a thin transparent film (0.015 mm thick). The films were buried in a silty loam soil at a depth of approximately 7.5 cm. The study lasted 22 months, with samples taken at 1, 3, 5, 7, 9, 11, 13, 15, 17, 19 and 22 months.	–	LDPE	SEM, FTIR, Universal testing machine, weighing scale, XRD, LCR meter	• Weight change • Surface analysis • Evaluation of stress-strain curve and strain at maximum • Changes in FTIR spectra • CI • Dielectric properties • Degree of crystallinity	[81]
Transparent PS cup, LDPE fragments with a thickness of 60 μm, LDPE juice bag and LDPE film with a thickness of 60 μm were buried for 32–37 years in garden soil in Japan at a depth of 10 and 50 cm.	Japan	PVC, PS, LDPE	OM, SEM, DSC, XRD	• Surface analysis • Changes in FTIR spectra • Oxidation temperature, • Degree of crystallinity	[93]
Samples (0–15, 15–30 cm) were taken from agricultural fields near a landfill.	Bangladesh	Various polymer types found; OM of unknown polymer type; SEM-EDX of PE, PP, PS, PVC	OM, SEM-EDX	• Surface and elemental analysis	[37]
Sampling at three field with annual application of biosolids since 8, 7 and 2 years and an additional control field.	Australia	Various polymer types found; no information about the analysed polymer	SEM-EDX	• Surface and elemental analysis	[233]
Two-year field trial with 0.016 mm and 0.010 mm thick LDPE film. Films were incorporated before the first and second growing seasons.	China	LDPE	FTIR, weighing scale, SEM	• Surface analysis • Changes in FTIR spectra • CI	[239]
Sampling was carried out every 5 cm to a depth of 60 cm on an agricultural field which received unsorted household waste in 1990. The soil was a well-drained cambisol enriched in pebbles and developed from alluvial deposits. Since 2005 the field was used as a meadow.	China	Various polymers found. FTIR from PE, PP, PS, PVC; SEM-EDX no polymer type	SEM-EDX, FTIR	• Surface and chemical analysis • Changes in FTIR spectra • CI	[226]
Soil samples were taken from the surface layer (0–27 cm) of one control and one amended plot (application of MSW compost for 10 years), each sample consisting of 10 pooled subsamples. The soil was a loamy luvisol to a depth >1.2 m and developed on carbonated loess of aeolian origin.	France	–	TEM-EDX	• Surface, morphological and elemental	[58]
Two-year field trial in China. In which 4 different commercial LDPE films with thicknesses of 0.015, 0.010, 0.008 and 0.006 mm respectively were applied to a grey desert soil.	China	LDPE	SEM, FTIR, Universal testing machine, weighing scale	• Surface analysis • Evaluation of tensile force, maximum tensile strength and elongation at break • Changes in FTIR spectra	[105]
Sampling in three areas of intensive agricultural use in China. Each sampling site included at least three types of management: vegetable fields, greenhouses and arable fields. The soils sampled were phaozems and fulvo-aquic soils. Samples were taken at a depth of 20 cm and an area of 1 m × 1 m per sampling point.	China	LDPE	SEM, FTIR, GPC	• Number of particles • Surface analysis • Changes in FTIR spectra • Molecular distribution	[91]
Sampling in cotton fields in northwestern China. Samples were collected from 60 sampling points in cotton fields with 5, 10, 15, 20, 25 and 30 years of continuous mulching. Samples were taken in 10 cm increments to a depth of 60 cm.	China	PE	SEM-EDX, OM	• Number of particles • Surface, morphological and elemental analysis	[231]
Fresh municipal sludge (FSS1), mixed sludge (FSS2) and hot (320–420 °C) air-dried municipal sludge (DSS) were applied to a paddy soil (Haplic-stagnic Anthrosol) in a long-term application experiment. Samples were taken at a depth of ~20 cm (see also).	China	Various polymer types found; No specific type	SEM	• Surface analysis • Number of particles	[179]
The test soil was derived from Quaterny red clay. Samples were taken from an experimental plot where 1.69 t ha-1 of pig manure had been applied for 22 years and from an unfertilised control plot. Analysis of manure for particle number, shape and colour.	China	PE, PP	SEM-EDX, FTIR	• Number of particles • Surface and elemental analysis • Changes in FTIR spectra	[234]
Sampling on Hydragric Anthroso/paddy soil with a depth of cultivation of 18 cm. There were three treatments: non-mulched soil (never mulched, NF), mulched paddy soil for 4 years (2012–2015; F4), and paddy soil continuously mulched for 10 years (from 2009 to 2019; F10). The used PE film was transparent and had athickness of 0.004 mm.	China	PE	SEM-EDX, FTIR, AFM, WCA measuring device	• Number of particles • Surface, roughness and elemental analysis • Changes in WCA • Vinyl, carbonyl and hydroxyl indices	[86]
LDPE film (0.008 mm thick and 1.4 m wide) ploughed into the first 30 cm of three concentrations (75 kg/ha, 150 kg/ha and 300 kg/ha) of Heima soil (Calcic Kastanozems, FAO taxonomy) with a field water	China	LDPE	SEM, FTIR	• Surface analysis • CI	[224]

(*continued on next page*)

Table 5 (*continued*)

Soil	Country	Polymers	Methods	Analysis	Study
holding capacity (FWHC) of 23 %, an average bulk density in the upper 100 cm soil layer of 1.20 g/cm3 and a gravimetric water content of 6.2 % at the permanent wilting point. The soil consists of 38 % clay (<0.002 mm), 58 % silt (0.002–0.05 mm) and 4 % sand (0.05–2.0 mm). The soil from 0 to 20 cm depth contains 5.9 g/kg organic carbon and 0.36 g/kg total nitrogen, with a pH of 7.8. Extraction was carried out after 2 years.					
Soil samples (0–100 cm in 10 cm increments) were taken from a greenhouse cropping experiment with five different treatments, including the control, chemical fertilizers, chicken manure compost, soil testing and local agricultural practices.	China	Various polymer types found; no information about the analysed polymer	SEM-EDX	• Particle number • Surface analysis • Elemental analysis	[235]
Soil samples (0–20, 20–40 cm) were taken from a long-term field trial with eight different treatments, including fertilizer and sludge application.	China	Various polymer types found; no information about the analysed polymer	SEM-EDX	• Surface and elemental analysis	[183]

acceleration voltages should be kept as low as possible, as they can cause polymer shrinkage and complicate analysis [50].

There are also other strategies to avoid charging effects and improve the image quality. On the one hand, the time the beam stays on each point of the sample plays an important role. If this so-called dwell time is too long, charging effects are amplified. A shorter dwell time ensures less charging but also more noise [50,55]. Accumulating several images with a short dwell time is, therefore, a good method of reducing noise while at the same time preventing charging artefacts. In addition, working in a low vacuum is also a common method for avoiding charging.

A further method that can be employed, for instance, to visualize ultra-thin sections of the interior of a specimen, or the morphology of the surface and subsurface of a specimen using ultra-thin sections of the surface, is scanning transmission electron microscopy (STEM). Electron-transparent ultra-thin samples (thickness <100 nm) with sufficient contrast between components are required for successful application [48,56].

3.1.3. Transmission electron microscopy (TEM)

Similar to STEM, transmission electron microscopy (TEM) is primarily used to evaluate the surface and subsurface morphology of ultrathin sections, which can be applied, for example, to evaluate the crystalline lamellae of semicrystalline polymers [48,57]. However, TEM micrographs typically offer lower contrast than STEM images, due to the higher acceleration voltage used and the resolution of TEM. Additionally, TEM-based EDX measurements can achieve higher resolution results compared to SEM-EDX [48]. For examining polymer surface morphology, TEM plays a minor role compared to SEM (Fig. 1 and Tables 2–5). Watteau et al. [58] used TEM-EDX successfully to provide morphological characteristics of MPs in soil.

3.1.4. Atomic force microscopy (AFM)

Atomic force microscopy (AFM), a type of scanning probe microscopy, does not create an image by focusing light or electrons on a surface, but instead images the surface of a polymer by measuring the deflection of a cantilever that holds a very fine probe (radius of curvature 10–20 nm) positioned close to the surface [47]. From the reviewed studies only two used AFM, although this method shares the advantage that it provides additional height information of the surface, rather than just two-dimensional images of a sample surface [59]. Under ideal conditions these images have an atomic resolution [60]. An advantage compared to electron microscopic techniques is the simpler sample preparation, as the sample does not need to be coated, electrically grounded, coloured or transparent [59]. For example, landfilled PE has shown an increase in average surface roughness of more than 2.5 times that of virgin PE [61].

3.1.5. Brunauer-Emmett-Teller (BET) device

A Brunauer-Emmett-Teller (BET) device is used to determine the specific surface area, a key property of solid surfaces. It is estimated using the BET equation, which calculates the specific surface area based on the amount of gas molecules adsorbed on the solid surface [62,63]. The specific surface area has only been calculated once (Fig. 1) and showed that sludge-derived MPs had a specific surface area up to 10 times higher than virgin MPs [64].

3.1.6. X-ray photoelectron spectroscopy (XPS)

X-ray photoelectron spectroscopy (XPS) is a technique used for the analysis of the chemical composition of the outmost atomic layers of a material. XPS is based on the photoelectric effect: using a monochromatic soft X-ray beam (~1 keV) to irradiate the sample, the X-rays provide enough energy to overcome the binding energy of the electrons and eject them. As the binding energy is characteristic of each element, it is possible to identify the elements present in the sample. Due to small shifts in the binding energy, it is also possible to identify the chemical state (bonding) of the element. [65]. To analyse plastic weathering in the environment, XPS was only used in two studies (Fig. 1 and Tables 2–5). For example, Liang et al. [66] could successfully quantify plastic weathering based on the calculation of the oxygen/carbon (O/C) ratio of PE films after 9 months of soil burial and soil surface exposure.

3.1.7. Fourier transform infrared spectroscopy (FTIR)

Infrared (IR) Spectroscopy is used to analyse the interaction of a sample with IR light (14000–4 cm^{-1}). The Fourier transform infrared (FTIR) spectroscope is the most commonly used instrument for identifying the polymer type [67,68], as well as, chemical alterations during weathering (Fig. 1 and Tables 2–5) in the terrestrial environment. When IR radiation (4000-600 cm^{-1}) interacts with a sample, it can be absorbed, causing chemical bonds in the material to vibrate. A particular functional group will always absorb the radiation at the same wavenumber, regardless of the rest of the molecule's structure. By measuring the amount of IR radiation absorbed at different frequencies, an absorption spectrum can be produced from which the structure of a molecule can be deduced. Since a particular type of polymer is made up of a particular combination of atoms, the resulting absorption spectrum is specific to that polymer type [67,68]. In addition to simply identifying the type of polymer, it is also possible to assess chemical alterations from FTIR spectra by analysing the formation and disappearance of functional groups (applied in 35 studies, Fig. 1). In particular, two-dimensional correlation spectroscopy (2D-COS) can be used to establish a relationship between spectral change and exposure time [69,70]. In addition, to measure the formation of certain functional groups produced during oxidation, various indices have been developed in the past, where the ratio between a specific peak/area and a reference peak/area is

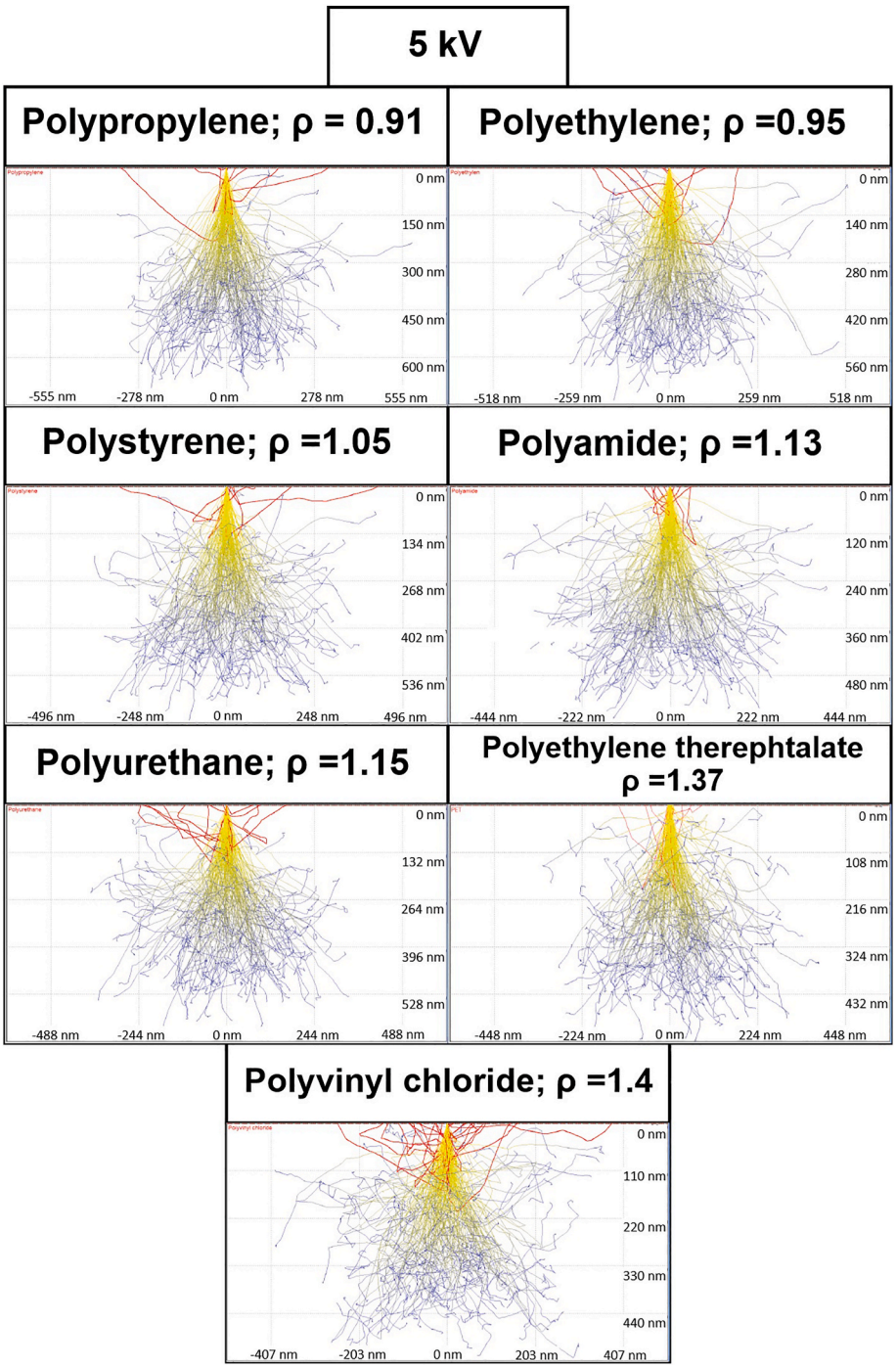

Fig. 2. Simulation of electron trajectories for different polymer types (ρ: density of polymers in g cm^{-3}) at 5 kV and spot size of 1.5 nm with Casino v2.48 [54], Yellow trajectories represent high energy loss of the electrons, blue trajectories represent low energy loss and red trajectories represent the backscattered electrons. (For interpretation of the references to colour in this figure legend, the reader is referred to the Web version of this article.)

determined [71] (Fig. 5). A variety of indices were calculated in the reviewed studies, of which the carbonyl index (CI) was the most common (Fig. 5). The CI was used in several studies as an indicator of weathering (Fig. 5). For example, a significant increase in the CI of PP was reported during industrial composting [31]. However, the calculation method varied considerably in the different studies, which makes it difficult to compare the results, as recently shown by Almond et al. [71] and Gomes et al. [72]. In rare cases, FTIR spectra were further used to assess the crystallinity or the isotacticity of plastics [73,74].

3.1.8. *Near-infrared spectroscopy (NIRS)*

Near-Infrared Spectroscopy (NIRS) works unlike FTIR (operating primarily in the mid-IR region), in the near-IR region (12500-4000 cm^{1}). In this region, bands arise from overtones and combination modes of molecular vibrations, which are generally weaker and less distinct than the fundamental vibrations observed in FTIR. NIRS is a non-destructive, non-contact method that can be applied to samples in various states, shapes, and thicknesses [75]. NIRS, only once used to determine weathering effects in the terrestrial environment (Fig. 1), confirmed the formation of new functional groups in bulk LDPE following composting and digestion [30].

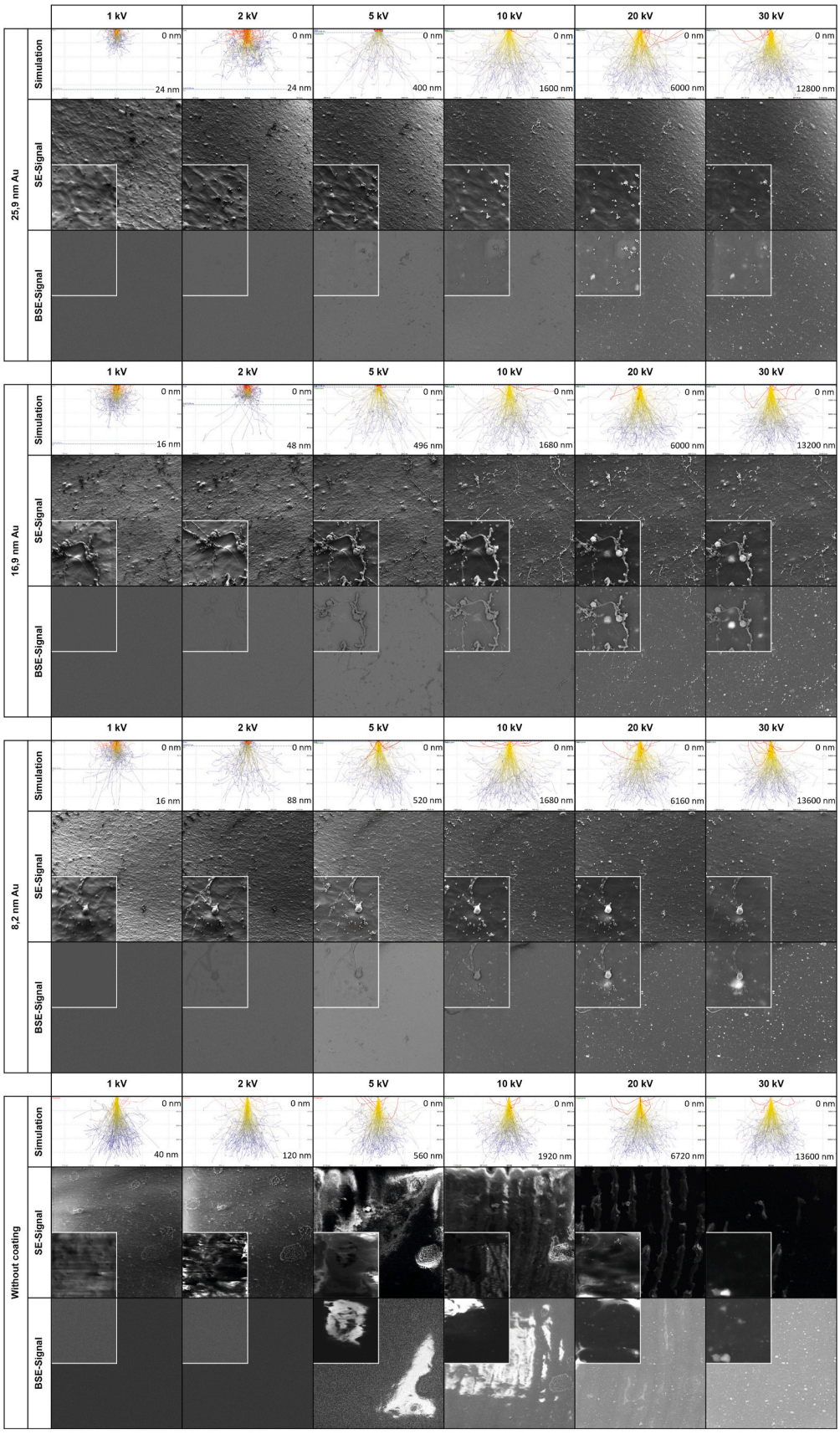

Fig. 3. Images of 4 samples (all from the same PE foil). One covered with a thick gold layer (25.9 nm), one with a medium thick layer (16.9 nm), one with a thin layer (8.2 nm) and one without any coating. For 6 different acceleration voltages the corresponding simulation [54] as well as the secondary electron and backscattered electron images are shown. The field of view of the images is 750 µm, the field of view of the small insets is 50 µm. (For interpretation of the references to colour in this figure legend, the reader is referred to the Web version of this article.)

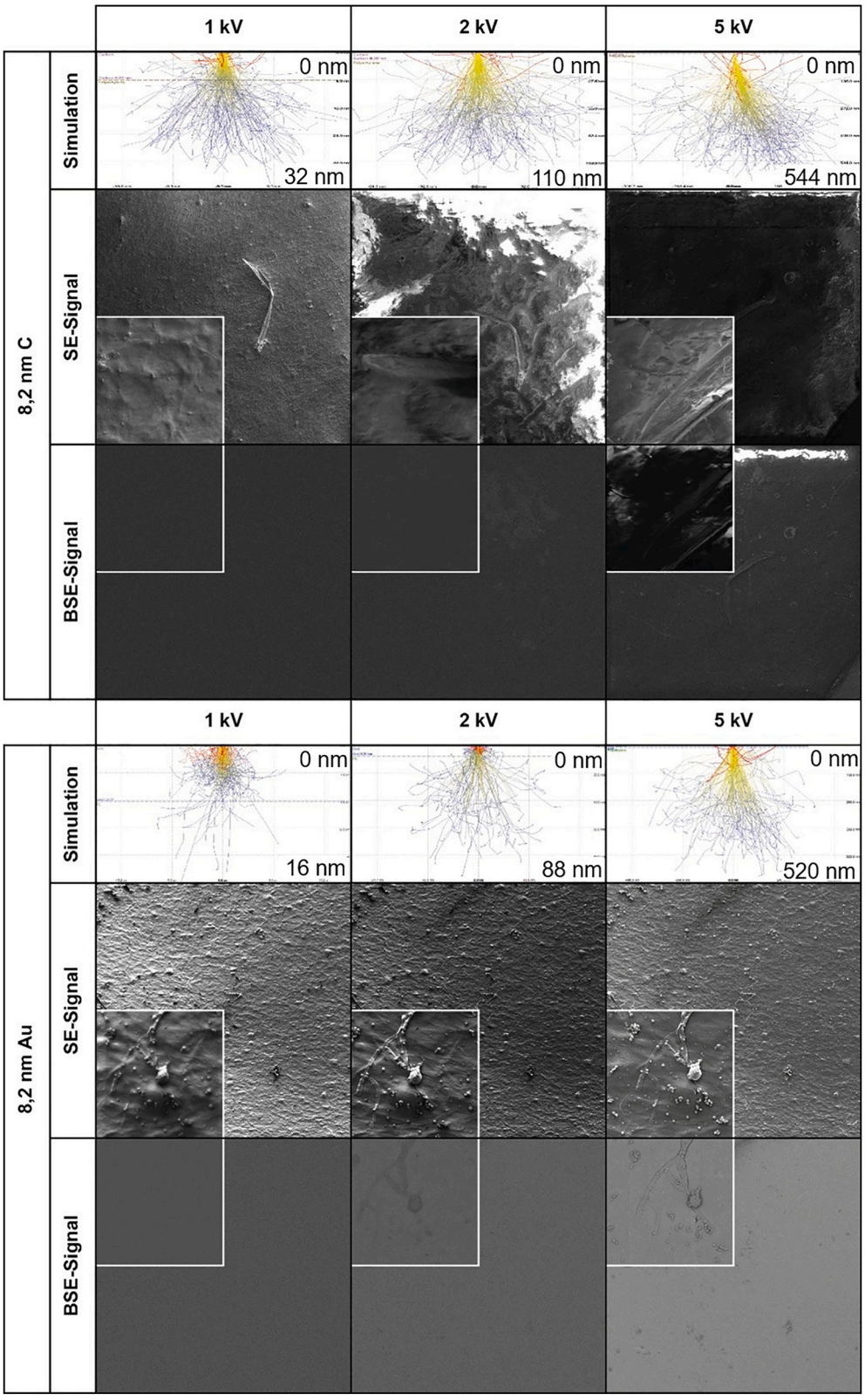

Fig. 4. Images of two samples taken from the same PE film: one coated with an 8.2 nm thick gold layer and the other with a carbon layer of the same thickness. For three different acceleration voltages (1 kV, 2 kV, and 5 kV), the corresponding simulations [54], as well as secondary electron and backscattered electron images, are shown. The field of view for the main images is 750 µm, while the insets have a field of view of 50 µm. (For interpretation of the references to colour in this figure legend, the reader is referred to the Web version of this article.)

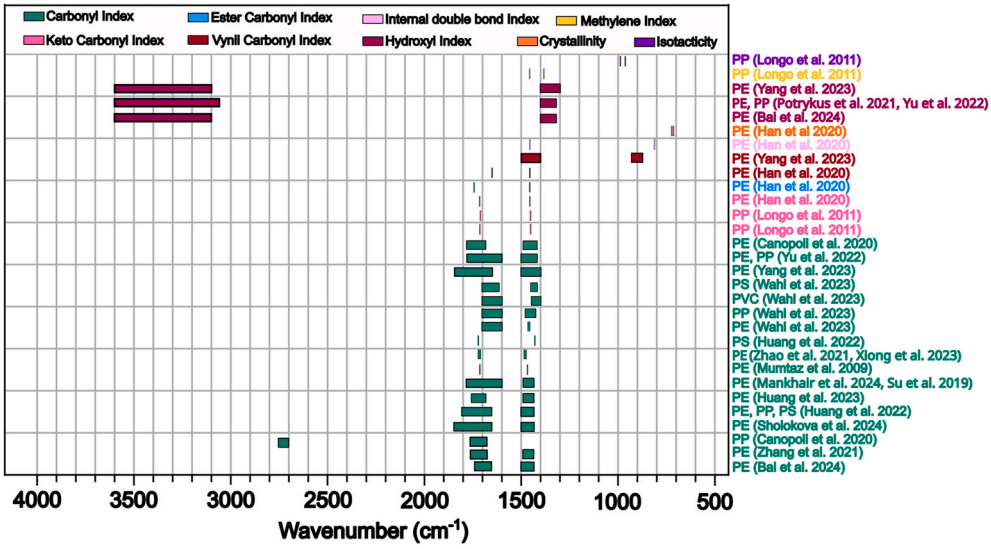

Fig. 5. The different indices and the corresponding bands used for calculation. The different colours reflect the different indices. In addition, the different polymers for which these indices were calculated, as well as the corresponding studies, are shown on the right y-axis. (For interpretation of the references to colour in this figure legend, the reader is referred to the Web version of this article.)

3.1.9. Raman spectroscopy

Raman Spectroscopy is a complementary technique to IR and identifies molecules present in the sample, with a typical Raman shift in the range from 50 to 4000 cm ^{1}. A monochromatic beam, usually a laser, irradiates the sample. During irradiation, a small fraction of the photons interacts inelastically with the vibrational modes of the molecules. This causes a shift in the photon energy due to the loss or gain of energy during the interaction. These energy shifts correspond to specific rotational or vibrational modes in the molecules and are used to determine the chemical composition and molecular structures of the samples [76]. For the analysis of polymers, no sample preparation is required, although the cleaning of the sample surface is necessary to avoid interferences mainly caused by organic matter [34,77]. Similar to FTIR, Raman spectroscopy is a widely used technique for identifying the polymer type and assessing weathering-induced changes in the spectra [78,79]. Among the studies reviewed, Raman spectroscopy was applied only twice. For example, Macan et al. [80] observed additional Raman signals from LDPE films after soil exposure, which could be related to changes in crystallinity.

3.1.10. LCR meter

LCR meters are used to evaluate dielectric properties of plastics, especially capacitance, loss tangent and dielectric constant [81,82]. In the reviewed studies, only one study (Fig. 1) used an LCR meter to detect changes in the dielectric spectra, evident as shifts in the transition peaks toward lower temperatures, indicating alterations in the molecular structure of PE after soil burial [81].

3.1.11. Water contact angle (WCA) measuring device

The contact angle measures the wettability of a solid surface, defined as the angle at the intersection of the liquid-vapour and solid-liquid tangents. On hydrophilic surfaces, the droplet spreads out, resulting in a contact angle close to zero. Less hydrophilic surfaces have angles up to 90°, while hydrophobic surfaces exceed 90°. Angles greater than 150° indicate superhydrophobic surfaces [48,83]. The water contact angle can be measured directly using optical goniometry or indirectly via force tensiometry [48,66,84]. The WCA, analysed in 5 of the reviewed studies (Fig. 1), typically decreased after exposure to various terrestrial environments [74,85,86].

3.1.12. X-ray computed tomography (CT)

X-ray Computed Tomography (CT) is a non-destructive, three-dimensional X-ray imaging method [87,88]. The 2D X-ray photographs of the sample are collected with equal angle increment over 180° or more and are reconstructed through an algorithm to create a 3D model of the scanned object [89]. The X-ray passes through the sample and part of it is absorbed by the material. The X-ray absorption depends on the density of the materials in the sample, with high-density materials absorbing more than low-density materials. This is expressed by different greyscale values in the resulting image. For light materials such as polymers, the absorption is very weak and the contrast between material and air may not be enough to determine the structures and polymer weathering, such as porosity. For this, X-ray phase contrast imaging is required and can be acquired through different processes, depending on the device. The phase contrast arises from differences in the refractive index of the materials and results in an edge enhancement in the resulting image. CT-scanners in the submillimeter voxel resolution range, are divided into mini-CT (voxel resolutions: 200–50 μm), micro-CT (voxel resolutions: 50–1 μm) and nano-CT, also known as X-ray microscope (voxel resolutions: 1–0.1 μm) [88]. Although CT offers the possibility of analysing both the bulk polymer and the surface, they were only used once in the studies investigated. Groß et al. [31] observed an increase in the pore structure of PP with extended composting time using nano-CT, as well as a 550-fold increase in surface attachments detected through micro-CT.

3.1.13. Gel permeation chromatography (GPC)

Gel Permeation Chromatography (GPC) is a technique used to determine the full molecular weight distribution of a polymer. In this method, a dilute polymer solution flows through a column packed with porous gel beads, where molecules are separated based on their hydrodynamic volume. Smaller polymer molecules enter most of the pores, taking a longer flow path, while larger molecules are excluded from all but the largest pores. As a result, polymer molecules elute from the column in decreasing order of molecular size [90]. Although GPC is widely used in polymer science, it was applied in only two of the reviewed studies (Fig. 1). These studies observed a shift in the molecular weight distribution [61] and a reduction in the high molecular weight fraction [91] of plastics following exposure in terrestrial environments.

3.1.14. X-ray diffraction (XRD

X-ray diffraction (XRD) is used to determine the crystallinity of a material. XRD is based in the interaction between X-rays and the regular atomic arrays in crystalline materials. This technique is based on Bragg's law, which describes how the incident X-ray beam is diffracted by the atoms in the crystalline structure. When the path difference between the reflected X-rays from successive atomic planes results in constructive interference, the spacing between the successive atomic planes d can be determined by measuring the diffraction angle θ. This spacing d is then used to characterize the crystalline structure of the sample [92]. In the reviewed studies, XRD was employed to evaluate differences in crystallinity of weathered PE following soil exposure [41,66,93]. Similarly, techniques such as electron diffraction and neutron diffraction can be used to assess the crystallinity of plastics, providing complementary information about their structural properties [94,95].

3.1.15. Differential scanning calorimetry (DSC

Differential scanning calorimetry (DSC) is a thermoanalytical technique that measures the heat flow in and out of the respective polymer sample relative to a reference [96]. The thermogram provides plastic physical properties such as the temperatures at the glass transition, onset of melting, peak of melting, and enthalpy of fusion, used to calculate crystallinity [97]. DSC was the most frequently applied structural analysis technique, used in 9 studies. It revealed changes in the DSC thermogram, including the appearance of an additional shoulder melting peak, shifts in melting temperature, and variations in crystallinity [85,98].

3.1.16. Thermogravimetric analysis (TGA

In thermogravimetric analysis (TGA), the plastic sample under investigation is weighed as it is heated at a predetermined rate. The weighted plastic is recorded as a function of time or temperature. The thermogram produced shows the percentage of weight lost at different stages as the temperature rises. This can provide information about the composition of the sample and its thermal stability [99]. TGA was applied only once (Fig. 1) to assess the thermal behaviour of PP and bioriented PP (BOPP) after soil burial, revealing differences between the samples attributed to their chain orientation [73]. In addition to DSC and TGA, several other thermal techniques are available, including dynamic mechanical analysis, differential thermal analysis and evolved gas analysis. These methods allow the assessment of heat flow, mass change, size and volume deformation, conductivity and release of volatile components during thermal processes [100].

3.1.17. Universal testing machine/Universal tensile machine

Tensile tests in universal testing machines are methods used to determine the mechanical properties of plastics according to standardized procedures such as ASTM D638 and ISO 527. In total, 9 studies applied tensile testing in the reviewed studies. One end of the sample, typically in a "dumbbell" or "dogbone" shape, is clamped in a stationary grip of a universal testing machine, while the other end is subjected to controlled displacement. After positioning the sample between the grips, it is stretched at a predetermined rate. The load cell connected to the moving end measures the load corresponding to the displacement. From the resulting stress-strain curve, various material properties, such as elongation at break, modulus of elasticity, and tensile strength, were estimated in the reviewed studies [66,85,101]. One of the eight studies applied a simplified form of tensile testing, in which the authors assessed the embrittlement of soil surface exposed PE films, which was defined as the point where the weathering time had elapsed to the extent that the film fractured in multiple directions when a small stress was manually applied normal to the film plane [102]. This point corresponds to the condition where the elongation at break was reduced to less than 5 % of the original film [103].

In addition, other mechanical parameters – such as flexural strength, impact resistance and compressive strength – can be assessed using complementary standardised ISO and ASTM test methods tailored to specific stress conditions [104].

3.1.18. Weighing scale

Weight change, the simplest and most direct method for measuring plastic degradation [16] through a weighing scale, was assessed in nine studies. The plastic samples were weighed with a scale before and after exposure in the respective environment. To account for any material adhering to the surface, the plastics were typically cleaned with water and ultrasound and then dried afterwards before weighing, revealing mixed results after exposure in terrestrial environments [105,106].

3.1.19. Additional methods for potential weathering analyses that have not been applied in the reviewed studies

3.1.19.1. Zeta potential. The zeta potential represents the electrical potential difference between the double layer surrounding an electrophoretically mobile particle and the dispersant layer at the slipping plane [107]. Observations of the zeta potential as a function of pH, for example, showed that the isoelectric point of three different plastics shifts to lower pH values with weathering, due to changes in surface functional groups [108].

3.1.19.2. Nuclear magnetic resonance spectroscopy (NMR). NMR spectra provide insight into the chemical structure of the polymer chain, including the number of end groups, degree of branching, tacticity, molecular mobility, degree of crystallinity and possible changes in these parameters after weathering [90,100,109].

3.1.19.3. Glossmeter. Gloss, or specular gloss, measures the reflectivity of a surface. Weathering and surface abrasion can affect gloss levels, which can be assessed using a glossmeter or lustremeter. The gloss data of an environmentally exposed sample are compared to a reference sample [101,104].

3.1.19.4. Yellowness index. The yellowness index, as defined by ASTM E313 and ISO 17223, is a standard test procedure used to determine the colour change of plastics as they turn yellow due to environmental exposure. This is achieved by analysing spectrophotometric data from comparative measurements [101].

3.1.19.5. Mass spectrometry (MS). Mass spectrometry, allowing for precise identification and quantification of chemical constituents, is often combined with complementary techniques such as chromatography (e.g., gas and liquid chromatography), thermal methods (e.g., pyrolysis gas chromatography and TGA), spectroscopy (TGA-FTIR-MS) or matrix-assisted laser desorption/ionisation, among others. These methods allow for a detailed characterization of polymers, such as the quantification of end groups, the identification of volatile compounds and degradation products, as well as the determination of molar mass distribution [110–112]. Mass spectrometry of secondary ions produced by surface bombardment with energetic primary particles is commonly used in time-of-flight secondary ion mass spectrometry [113]. This method allows the assessment of chemical changes on plastic surfaces by exploiting its high spatial resolution and sensitivity to molecular species, including distinct peaks corresponding to oxidised fragments [114,115].

3.1.19.6. Laser-induced breakdown spectroscopy (LIBS). Laser-induced breakdown spectroscopy (LIBS) allows qualitative and quantitative determination of the elemental composition of a sample [116,117]. In addition to identification [118], LIBS was used to analyse plastic weathering along a depth profile, where the intensity of the C_2 Swan band and oxygen (O) emission lines were evaluated to assess changes in the polymer [117].

3.1.19.7. Ultraviolet–visible (UV–Vis spectroscopy. UV–Vis spectroscopy is particularly valuable for the quantitative analysis of specific functional groups, called chromophores, and their modification by auxochromes, which can influence absorption properties [100]. Additionally, this technique can determine the percentage of transmittance and the degree of absorbance of radiation within the UV–visible spectral range [119].

3.1.19.8. Auger electron spectroscopy (AES. Auger electron spectroscopy (AES) is a highly sensitive technique for surface analysis. The emitted Auger electrons provide elemental information about the surface, allowing detailed chemical analysis of the surface composition of the material [120].

*3.1.19.9. X-ray fluorescence spectroscopy (XRF).*X-ray fluorescence (XRF) is a spectroscopic technique that can identify and quantify the elemental composition of a sample based on the emitted X-rays, which have characteristic energies specific to the elements [121].

3.2. Effects of exposure in terrestrial systems

In total, 70 studies were found during the literature search (Tables 2–5). Of these, 63 studies dealt with one, 6 studies with two and 1 study with three environmental systems. The majority focused on soil, followed by landfills, compost and wastewater treatment plants (WWTPs), and least frequently, digestate (Fig. 6). The majority of studies were conducted in Asia (47), with almost half coming from China alone. Europe accounted for 21 % of the studies, while research in other regions was particularly scarce. North America (1 study), South America (3 studies), Australia (2 studies) and Africa (2 studies) were significantly underrepresented (Tables 2–5).

Depending on the system, different periods of environmental exposure were considered in the studies, ranging from a few days (compost and digestate) to several decades (soil and landfills) (Tables 2–5, Tables S2-5 and Fig. 7). There is also a clear difference in the study design: the majority of the studies analysed plastics that were already present in the environment (79 %) (Fig. 7); the age estimation of these environmental plastics is based on information about the utilisation of the soil, process parameters of industrial plants or the construction and closure of landfill compartments. In contrast, 21 % of the studies specifically introduced plastic into the environment and analysed it after defined periods ('experimental plastic'). For experimental plastics, the observed changes can be more precisely related to an exact period than for environmental plastics. PE (including linear low-density PE (LLDPE), low-density PE (LDPE) and high-density PE (HDPE)) and PP are the most commonly analysed plastics in the reviewed studies, reflecting their high production volumes [2]. These polymers were studied across all terrestrial systems. In contrast, the lower production volumes of other polymers [2] may explain the limited research on their weathering. For example, PVC was analysed only in soil and landfills, PA in sludge landfills (Tables 2–5 and Tables S2-5) and PU, despite accounting for 5.3 % of global plastics production in 2023 [2], was not investigated in any study (Fig. 7). Many studies focusing on environmental plastics also did not report the polymer type (Fig. 7). Although FTIR or Raman spectroscopy was often used to identify specific polymers, subsequent analyses such as microscopy were often performed on unspecified particles (Tables 2–5 and Tables S2-5). Although general weathering effects can still be inferred, degradation is polymer-specific, i.e., the degradation mechanisms of plastics with a carbon-carbon backbone (e.g., PE, PP, PS and PVC) differ significantly from those with heteroatoms in the main chain (e.g., PET and PU) [122].

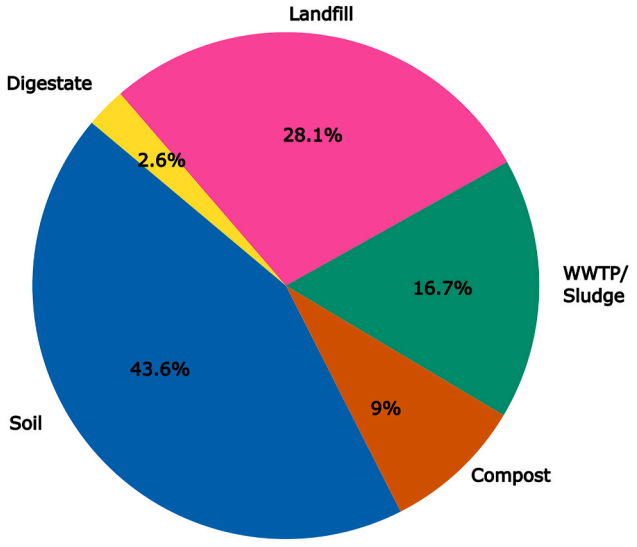

Fig. 6. Percentage of studies addressing plastic particle exposure in the different terrestrial systems.

3.2.1. Landfills

Modern sanitary landfills are equipped with bottom liners made of impermeable material to separate the waste from the underlying soil [21]. However, these liners can degrade over time; in this case, the prevention of leachate entering the underlying aquifers or neighbouring rivers might be limited [123]. In addition, leachate collection systems are installed to treat pollutants in percolating precipitation before disposal, as well as gas extraction systems to reduce fire risk and greenhouse gas emissions from anaerobic digestion processes [21]. When the operating volume is reached, landfills are covered with a final layer of soil and an additional barrier layer [21,123,124]. Some landfills are designed as bioreactors that use leachate recirculation to promote waste stabilisation under varying aerobic conditions, affecting the microbial community and gas and leachate composition [123]. Unsanitary landfills or open dumps, on the other hand, are unmanaged and pose increased environmental risks. In particular, the lack of liners and barriers increases the risk of leachate-containing MPs or additives seeping into the soil and macroplastics being transported by wind, runoff or flooding [125].

A total of 22 studies were available reporting on plastics in landfills, with durations ranging from 60 days to 60 years, which is the longest duration of all studies reviewed (Table 2, Table S2 Figs. 6 and 7).

As the plastics are usually at the end of their service life, they are often altered before being disposed of in landfills [61]. In landfills, weathering processes will continue for decades, depending on the respective landfill conditions. As there are different types of sanitary and non-sanitary landfills, conditions such as O content, moisture, waste type, leachate, corrosive chemicals, temperature and pH vary greatly [22]. In addition, the types of plastics entering landfills, their pre-alteration and local weather conditions differ (Table 2, Table S2 and Fig. 8).

Mechanical stress caused by waste compaction prevails in all landfills. After the organic material is broken down, the waste slowly collapses, resulting in friction and shear forces [61], followed by mechanical abrasion caused by the flow of leachate and gas under high pore pressure [61]. In addition, in the presence of UV radiation and O, photo-oxidation processes can take place on the landfill's surface [22]. In aerobic landfills, thermo-oxidative processes are the main degradation pathway [22], especially with high temperatures of up to 90 °C inside the landfill cell [126]. Transition metals (e.g., iron (Fe), copper (Cu), titanium (Ti) and Cr) in the landfill can increase the rate at which hydroperoxide intermediates decompose into radicals, ultimately accelerating the oxidation processes of hydrocarbons [127,128]. The combination of mechanical and thermo-oxidative processes results in an enhanced weathering of plastics [129]. In anaerobic landfills, other pathways are common. Polymers can be broken down into smaller,

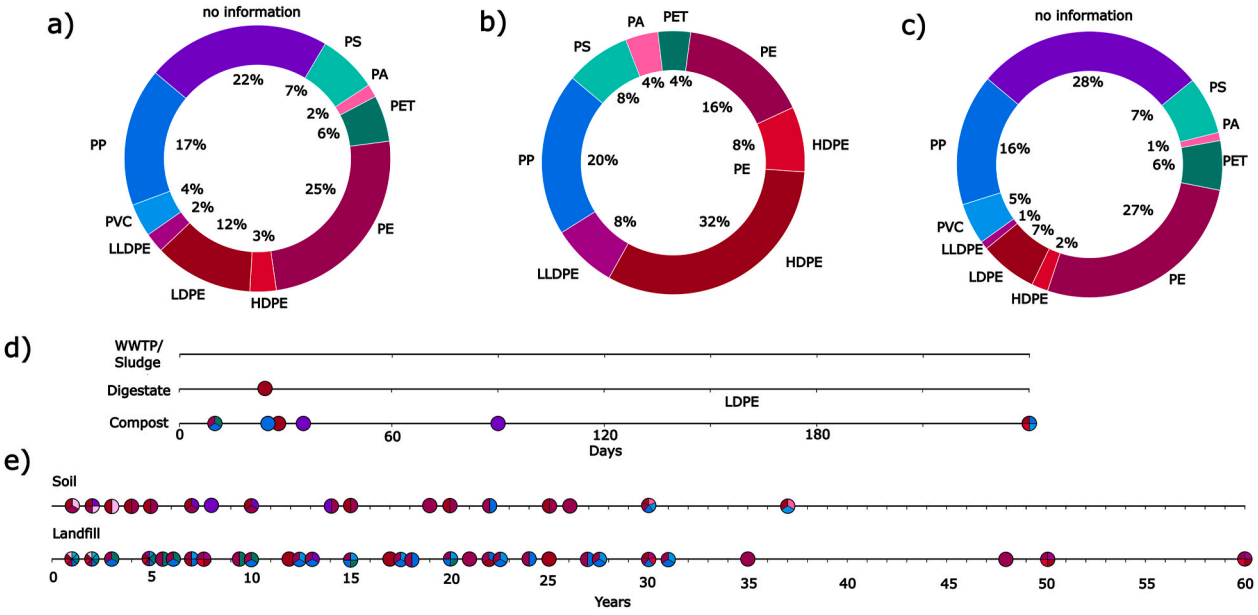

Fig. 7. The polymer types across all studies (a), differentiated by experimental (b) and environmental plastics (c). Exposure times of the analysed plastics in wastewater treatment plants (WWTPs)/sewage sludge, digestate and compost (d), as well as in soil and landfill (e). The colours on the timelines correspond to the colours of the polymer types in a-c. The number of studies per time point is not reflected. (For interpretation of the references to colour in this figure legend, the reader is referred to the Web version of this article.)

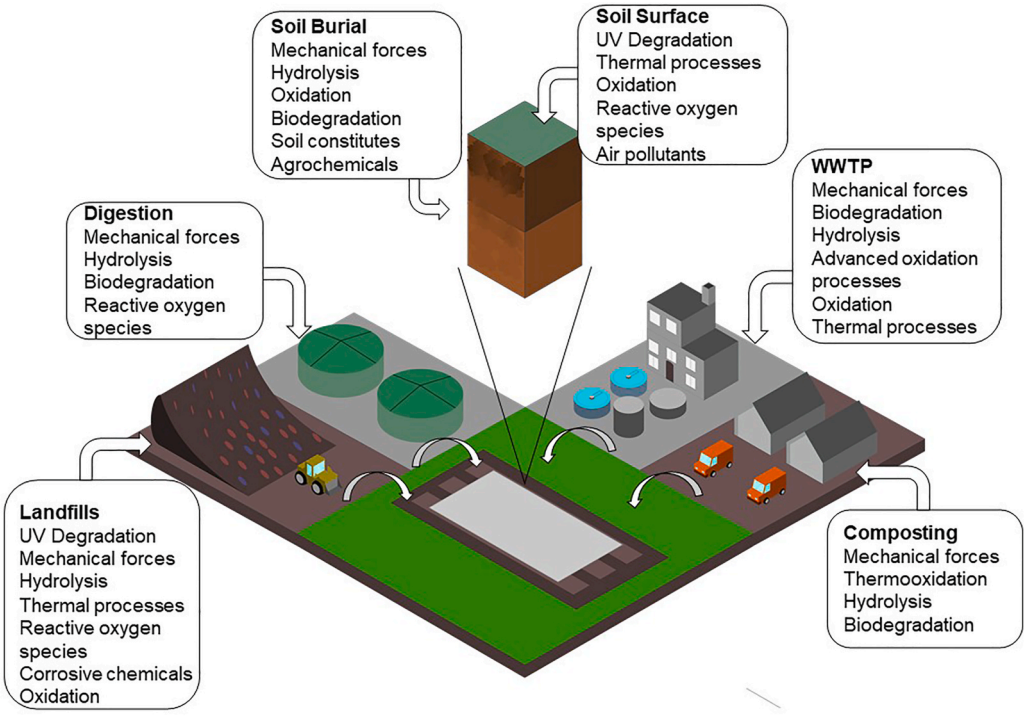

Fig. 8. Different factors can potentially affect plastic particles in different terrestrial systems. Plastics enter the soil through a variety of pathways and may be pre-altered.

short-chain molecules by exoenzymes from anaerobic consortia of microorganisms and used as a source of carbon or energy [130]. For polymers containing hydrolysable covalent bonds in functional groups such as ester, ether, anhydride, amide, carbamide (urea), ester amide (urethane) and others, hydrolysis is an important chemical pathway that depends on parameters such as water activity, temperature, pH and time [131]. Dissolved organic matter in the leachate can form, even under dark conditions, reactive oxygen species (ROS), which trigger the oxidation of plastics. Fulvic acids promote weathering more than humic acids as their generation rate of ROS is higher, caused by molecular structural differences [129]. In addition, substances such as hydrogen sulphide can be produced in landfills at low pH, leading to the corrosion of specific plastics [22] (Fig. 8).

All these processes led to macroscopic as well as microscopic changes in plastics. Macroscopic changes include the loss of gloss, yellowing, fading of printing, reduced elasticity and embrittlement [33,85,132]. On

a microscopic level, plastics displayed signs of surface deterioration such as pits, cracks and holes [133–137], which led to an increase in surface roughness and later fragmentation, resulting in the formation of smaller plastic particles [84,85]. In contrast, virgin reference plastics had smooth surfaces with virtually no signs of weathering, except for mechanical wear caused by processing [33,85]. In addition, the aged plastic particles were colonised by a variety of microorganisms, which developed a patchy coating together with lipopolysaccharides and soil organic carbon. Most of the microorganisms found were viable, suggesting biodegradation processes [32,33,44], which depend on various factors such as temperature, alkalinity, O and moisture content [138], but also on the age of the plastic waste [139]. While 1.5-year-old plastics contained only viable microorganisms, 60-year-old plastics contained approximately equal numbers of living and dead microorganisms that formed distinct colonies around areas of severe delamination on the landfilled plastics [139]. The high pressure caused by the continuous compaction of the waste, combined with the elevated temperatures, favoured the accumulation and embedding of inorganic and organic material on the plastic surface, which led to an increase in weight during the residence time in landfills [56,140]. This weight increase is further fuelled by the water absorption of aged plastics [56,141]. The various elements (C, O, P, Fe, Cl, Si, Ca, Al, Na, cobalt (Co), Mg and Ti) found on the surface reflect the diversity of the accumulated material [85,140,142,143]. Si and Al, for example, may be indicative of soil minerals such as silicon dioxide (SiO_2) and aluminium oxide (Al_2O_3) [132]. Others are used as pigments, additives, fillers or during plastic production [104,132,140]. Puglisi et al. [98] hypothesised that the chemical distribution on the surface of the polymers and their different affinity to bacteria influenced the morphology of holes, as heavier elements such as Na, Mg, P, Si, Ca or Fe remained in the cavities on the surface of the severely altered samples. Therefore, different coloured samples showed different degrees of weathering, as they contain different dyes and additives with varying elemental compositions [98,104].

A clear correlation between the extent of surface alteration and the duration of storage could not be established: while Canopoli et al. [132] found no clear difference in the extent of surface changes between younger (<10 years) and older (>10 years) samples, others noticed an increase in surface weathering with increasing storage time [84,85,139,143]. The latter assessment was also based on the correlation between the surface roughness and the O/C ratio, i.e., with increasing surface degradation the proportion of C decreased and the proportion of O increased [85,140,142]. This shift was then confirmed by FTIR spectra of landfilled plastics. In detail, PE and PP showed the formation of carbonyl (C═O) and hydroxyl groups (O–H), along with the appearance of carbon–oxygen bond (C–O) and carbon-carbon double bond (C═C) stretching in the spectra of landfill samples [33,61,84,98,132,142]. Additionally, bioriented polypropylene (BOPP) and PP exhibited the appearance of cyclic ether (C–*O*–C) linkages and CH═CH_2 (vinyl groups). Specifically for PP, also C–O–C linkages were detected [73]. The formation of oxygenated functional groups was also observed for landfilled PET [142]. The FTIR results highlight chemical changes and an increase in O-containing functional groups such as aldehydes, ketones, carboxylic acids, hydroperoxides, and alcohols [6,141].

Deconvolution of the C1s peak through XPS in PE resulted in three distinct peaks: C–C, C–O and C═O. The area of the C═O peak increased with increasing disposal age, indicating oxidation of the polymer [84]. Furthermore, PE showed increasing absorbance at C═O and C–H bonds, while the absorbance at its characteristic double and single peaks decreased. Both PE and PP presented decreasing intensities for the CH_2 group, indicating chain scission [61,73,98,132,140].

In addition, in PP and BOPP ketone and methyl (CH_3) groups decreased over time, caused by the degradation primarily at primary and tertiary carbon sites [73]. This was particularly evident in PP samples older than 10 years, with the reduced CH_3 intensity attributed to the loss of volatile products during degradation [132]. Interestingly, despite these trends, higher absorption values for asymmetric CH_3 and symmetric CH_2 stretching vibrations were observed in aged PP in one study [144]. For PET, weathering resulted in increased absorbance, indicative of aromatic C–H bonds and C–*O*–C ester linkages, and a decrease in C═O stretching in ester C═O groups, suggesting oxidation or even structural reorganization [144].

Finally, 2D-COS analysis of plastic films aged under artificial conditions revealed a sequence of functional group changes during weathering: C–H > C–O > C═O. This sequence shows that C–H bonds are cleaved first, leading to the formation of C–O bonds by oxidation, which are then further oxidised to form C═O groups [61].

The introduction of new O-containing functional groups led to a steady decrease in the water contact angle with increasing deposition time [85]. This increasing hydrophilicity of the material favours the adhesion of microorganisms to its surface [141] and the hydrolysis rate [145]. Although these analyses indicated degradation processes, no consistent trends were observed in the calculation of CI and hydroxyl index (HI). Most studies reported that CI and HI increased with landfill age for PE [84,139,140,142,144,146,147], PP [33,84] and PS [84], while others found either a non-significant decrease in CI for PE [132] or no correlation between HI and PP deposition age [85]. Additionally, CI also increased with increasing landfill depth, presumably due to higher pressure and heat in lower strata [146].

Chain scission breaks down longer polymer chains into shorter fragments, leading to a reduction in the molecular weight of aged plastics and the appearance of an additional shoulder melting peak in the DSC thermogram [85,98]. However, no significant differences in the melting point between fresh and aged PE and PP were found [85]. Better quantification of degradation was possible by the ratio of enthalpies between the lower shoulder peak (60–100 °C) and higher major peak (110–120 °C), showing that mainly the colour of plastics affected the degradation of PE, with yellow, green and black samples showing the highest level of degradation [98]. These differences may be due to the role of pigments in weathering. For example, TiO_2 can act simultaneously as a thermo- and photocatalyst, accelerating degradation processes, and as a UV absorber, potentially stabilising the polymer under certain conditions [148]. Similarly, TGA of aged PP revealed two distinct mass loss events, indicating the presence of degradation products or new phases, likely from the breakdown of polymer chains into smaller, more volatile compounds that decompose at lower temperatures [100]. In contrast, BOPP maintained a single mass loss in both aged and fresh samples, suggesting higher thermal stability due to its chain orientation [73].

Changes in crystallinity were polymer-specific, however, without consistent trends, neither for PP nor PE. For PP most studies indicate an increase in crystallinity over time [33,85], even if one study found similar values for aged and virgin PP [132]. Contrastingly, Longo et al. [73] observed a decrease in crystallinity after 11 months in a landfill, which was more pronounced in PP compared to BOPP. In the same study, the isotacticity of PP—reflecting the regular arrangement of CH_3 groups along the polymer backbone [109] - decreased significantly, indicating a structural change and reduced molecular order, consistent with the loss of crystallinity [73]. Conversely, BOPP increased in isotacticity, possibly due to chain reorganization during degradation [73]. For PE, an increase in crystallinity over time, from 39 % (fresh) to 45 % (<10 years) and 51 % (>10 years) [132] was detected, but also a decrease with increasing landfill time for samples up to 60 years old [85,139]. The decrease in crystallinity from 55.6 % to 20.8 % of a sample after 27 years of landfilling was mainly attributed to the splitting of longer polymer chains into shorter ones by biological enzymes and the rearrangement of the PE carbon chain molecules [85]. Redko et al. [139], attributed the loss of crystallinity in up to 60 years of landfilled PE to chemical degradation unique to landfill conditions. In semi-crystalline polymers such as PE and PP, oxidation, biodegradation and mechanical stress preferably affect the amorphous regions, which increases fractional crystallinity [6,130,132]. Additionally, shorter fragments of the polymer chain can crystallize through

chemi-crystallisation, forming new thin lamellae [149,150]. While these two processes typically result in increased crystallinity, a decrease in crystallinity, which was also observed in the reviewed studies, was potentially caused by increased cross-linking during the later stages of weathering or in the absence of O [6,151]. Degradation is also not confined to the amorphous phase alone. Over time, lamellae boundaries are affected, destroying the crystallites and resulting in a reduction of crystallinity after reaching a maximum during degradation [152].

While Tao et al. [142] reported a general decrease in mechanical properties of PET, PP and PE with increasing landfill time; other studies show more nuanced results. For example, tensile strength at break gradually decreased for LLDPE and LDPE after 24 months in landfills, while HDPE and PP showed no changes [56]. Compared to LLDPE and LDPE, HDPE is made up of linear chains with few branches, which allows the chains to be packed more tightly, increasing density, mass, strength and rigidity [109]. However, after long-term storage in landfills (22 and 24 years, respectively), the tensile strength of both PE and PP decreased [85]. The percent elongation at break followed a different pattern: while it decreased for PE in both studies, Yu et al. [85] reported an increase in elongation for PP, whereas Breslin [56] noted a decrease. The elongation at break decreased for PE and increased for PP. An opposite trend was observed for the modulus of elasticity, which increased for PE and decreased for PP. The changes are highly dependent on the polymer [152] and the time scale of environmental exposure, as shown by the contrasting results reported by Breslin [56] and Yu et al. [85] for PP.

The degradation and subsequent alteration of plastics in landfills led to their fragmentation into smaller plastic particles, such as MPs [33]. The concentration of MPs in landfill refuse and leachate varied widely, ranging from 580 to 653,100 pieces kg $^{-1}$ in refuse and 4 to 350 pieces l $^{-1}$ in leachates [84,135–137,144]. There is evidence of a significant positive correlation between landfill age and MP generation, with MP concentrations increasing exponentially over time. For example, MP abundance increased from 71.3 ± 17.7 pieces g $^{-1}$ plastic in landfills younger than 10 years to 653.1 ± 191.5 pieces g $^{-1}$ plastic in landfills older than 30 years [84]. This ongoing fragmentation process is further supported by a decrease in MP size with landfill age [84,144]. However, conflicting results have also been reported, showing contradictory or no clear correlations between landfill age and the number of MPs [144,146]. For example, the lowest MP concentrations in refuse and leachate were observed in the oldest landfill zones, while middle-aged and younger zones displayed two to three times higher concentrations [144,146]. These discrepancies highlight the impact of increased plastic use in recent years, resulting in more MP formation despite shorter deposition times. The lack of correlations could also be due to the high heterogeneity of waste within a landfill or between landfills, as the generation rate of MP already depends on the type of plastic [84,135]. For instance, PE (28.4 pieces g $^{-1}$ of plastic) generates significantly more MP per year than PP (15.0 pieces g $^{-1}$ of plastic) or PS (9.6 pieces g $^{-1}$ of plastic) [84]. Another critical factor is the movement of MPs within the landfill. Precipitation percolating through the landfill transports MPs to deeper layers, leading to their accumulation in lower strata [146]. In unsanitary landfills or those with damaged liners, this can result in the migration of MPs into the underlying soil, providing yet another pathway for MPs to enter the environment [135].

3.2.2. *Composting and digestion*

In particular, food and green waste, which make up the largest share of global waste (44 %) [20] can be easily treated in composting and digestion plants as an environmentally friendly alternative to landfilling. Composting and digestion are both methods of decomposing organic material. During composting, microorganisms break down organic material in the presence of O, producing CO_2, heat, water vapour and compost [153]. During digestion, this breakdown is achieved under controlled anaerobic conditions, resulting in the production of biogas and digestate [154]. Compost and digestate are used as soil amendments to improve soil health and quality [154,155], but are potentially contaminated with plastics [156]. The plastics originate from the feedstock (e.g., food waste, green waste, organic household waste) [24,156] and often come from food packaging, containers, bags, product labels and service items that are inadvertently released into the waste stream [157]. Despite strategies within the facility to reduce the plastic amount, such as manual picking, screening machines, separators, or de-packagers [158] some plastics still enter the actual composting or digestion process. Mainly because small items cannot be removed, and larger plastic particles may be mechanically fragmented by screening and sorting processes [158].

The composting and digestion conditions of the reviewed studies reflect this diversity in the process settings. For composting, besides different screening processes, factors such as the design of the composting facilities (including shredding and sieving processes), the type of feedstock, the duration, the maximum temperature or the average humidity varied [159–161] (Table 3, Table S3 and Fig. 7).

A total of seven studies examined the alteration of plastics in compost, while two focused on plastics in digestion. In composting environments, exposure times ranged from 10 days to 8 months, whereas for digestion, only one study reported a duration, which was 24 days (Table 3, Table S3 and Figs. 7 and 8).

During composting, plastic particles are affected by mechanical processes such as screening or turning the pile, and by chemical and biological degradation processes. After pre-treatment (manual sorting, shredding and pressing), the number of particles increased from 800 ± 200 particles kg $^{-1}$ dry weight in rural household waste to 1,133 ± 115 particles kg $^{-1}$ dry weight [162]. The environmental conditions, in particular the high temperatures (up to 75 °C), the simultaneous supply of O and the high humidity (36.8 ± 2.8 %) [30], can lead to thermo-oxidative and hydrolytic degradation processes [16]. These processes introduce hydrophilic groups and thus promote the attachment of microorganisms to the plastic surface, which is the first step of biodegradation [163]. The effects of these processes are manifested in both, the surface morphology and the chemical composition of the plastic particle. Yellowing, which is the result of the accumulation of degradation products of the polymer or from thermal stabilizers used [6] was only observed for LDPE, PS, PP film and rigid PP, but not for HDPE and recycled LDPE after composting [106]. In contrast, all analysed plastics developed new morphological features such as cracks, grooves, dents and holes, and a larger specific surface area [31,162,164]. In addition, hyphae, prokaryotic cells and organic as well as inorganic residues, such as titanium oxide Ca, Ba or silicates of the composted material were observed [31,58,165]. The attachments on the plastic can have large extensions, as, e.g., found for composted fruit stickers, where the volume was more than 550 times larger (3.52×10^6 μm^3) than that of the original sticker (6.24×10^3 μm^3). However, the intensity of surface changes did not depend on the duration of composting (11 or 25 days after composting) [31], but rather on the thickness of the sample, as the type of surface changes varied between thicker (cracks, scratches and ploughing) and thinner samples (cracks and holes) [106]. Although the accumulation of material on the surface of plastics, similar to landfilled samples, might suggest an increase in weight, composted samples lost weight, which in turn was negatively correlated with sample thickness [106]. Thin plastic films lost more weight than rigid plastics [106]. For PE, however, the results on weight change were conflicting, as an insignificant weight gain was also observed, which may also be due to water absorption [30]. The FTIR spectra of composted plastics displayed the formation of O–H and C═O groups. In addition, the intensity of C–H bonds for PP and PS increased, probably due to chain scission. For HDPE, C–H deformation and stretching vibrations, associated with alkene C═C groups, appeared [31,106]. Furthermore, PE revealed the formation of new peaks and changes in peak intensity in the 12,500 to 4,000 cm $^{-1}$ region, indicating a decrease in methylene (CH_2) groups, an increase in CH_3 and C–H bonds, as well as an increase in O content (2.54 %) [30]. Similarly, the mean CI of

composted PP increased with increasing composting time from 1.15 ± 0.12 to 1.25 ± 0.24 to 1.45 ± 0.24 (uncomposted, 11- and 25-day composted PP stickers, respectively), with significant differences ($p < 0.05$) between the original and 25-day composted PP. These findings were confirmed by nano-CT imaging, which revealed an increase in the pore volume in PP stickers as composting progressed, from 16.7 % (original) to 21.3 % (11-day composted) and 26.3 % (25-day composted) [31].

Various plastics released particles during composting, the number was depending on the thickness of the material. Film-like plastics released more particles than more rigid PP and PS food containers [106]. The formation of MPs (size 30 and 95 μm) was also observed on PP fruit stickers, which was attributed to a delimitation process on the surface of the stickers [31]. This resulted in a 2.3–2.4-fold increase in the number of particles after composting compared to the feedstock, while the size of the particles found decreased, indicating fragmentation [162,164]. In addition, the crystallinity decreased from 43.3 % (original PE) to 42.0 % (composted PE), as did the elastic modulus, strain at break and elongation at break. In contrast, the tensile strength at yield, the tensile strength and the stress at break increased [30]. These mechanical changes could be the reason for the physical fragmentation of the plastic into smaller particles. This suggests that the remaining material, although more brittle, may have become harder as in the course of the composting process.

While the conditions for digestion are similar to composting in terms of mechanical processes, such as screening and stirring [154], they differ significantly in terms of temperature and O availability (Table 3, Table S3 and Figs. 7 and 8). During digestion, temperatures are lower compared to composting and O is absent [30]. Oxidation processes due to the presence of O can therefore be excluded. However, other factors such as biodegradation, hydrolytic, thermal and chemical processes play a crucial role, especially in the presence of enzymes and anions, as already highlighted above for anaerobic conditions in landfills (3.2.1) [30]. These processes led to significant changes in the plastic particles. After digestion, PE revealed an increased roughness and delamination [30], simultaneously the increase in O content (9.35 %) exceeded that of composted PE samples. This was confirmed by IR spectra, where higher transmission values were recorded for C–H stretching and CH_2 rocking. New peaks appeared, indicating O–H bending and C═C stretching for alkenes. Additionally, peaks corresponding to C–H bending of CH_2 and CH_3 groups were absent. Similar to composted PE, new functional groups formed in the near-IR range, with higher intensity observed for digested plastics compared to composted ones. Additionally, a decrease in CH_2 groups and an increase in CH_3 and C–H bonds were observed. DSC analysis revealed a decrease in crystallinity from 43.3 % (original) to 38.7 % (digested). And a second melting peak at 164 °C, which, in contrast to landfilled samples, did not indicate shorter polymer chains but rather material contamination [30]. The results of the mechanical tests reflected the same trend as for composted plastics. This deterioration in mechanical properties contributes to particle fragmentation and a decrease in particle size [30]. However, the number of particles found after digestion depended on the feedstock. For example, the digestion of food waste resulted in a slight decrease in the number of particles, whereas the digestion of cow manure resulted in a slight increase. Despite these variations, particle size consistently decreased in both processes [164]. In general, plastics that have already been pre-aged typically show stronger reactions to environmental exposure [166,167]. In concordance, plastics that were composted after the digestion process showed stronger alterations than plastics that underwent either process alone. In detail, digested and composted PE had a higher O content (+10.0 %) and higher peak intensity than digested PE, while the peak formation in the IR spectra was similar. Also, a stronger decrease in crystallinity (36.4 %) and mechanical properties was observed for digested and composted PE, together with the appearance of a second melting peak [30].

3.2.3. *Wastewater treatment plants*

Worldwide, large volumes of wastewater are generated annually, amounting to 359.4 billion m^3 per year. However, only 52 % of this is treated, with the remainder discharged untreated into the environment [168]. Wastewater contains high concentrations of plastics due to the direct release of MPs from personal care products, the release of synthetic fibres during laundering, and plastic particles released from other processes (e.g., tyre wear) and subsequently entering the wastewater system [26,169]. To reduce the concentration of plastics, solids and other pollutants in wastewater, WWTPs use a combination of physical, chemical and biological processes. The treatment process typically consists of five steps [170]. (1) In the preliminary stage, large debris are separated by screens of various sizes [171]. (2) In primary treatment, suspended solids are removed by physicochemical and chemical processes such as sedimentation, chemical coagulation or filtration [170,171]. (3) The secondary treatment stage is effective for treating dissolved organic matter and nutrients by microorganisms [171]. (4) The remaining pathogens and pollutants are removed in the tertiary treatment stage by physical and chemical processes such as filtration, absorption, chlorination or advanced oxidation processes (AOPs) [172]. (5) Finally, the sludge produced is treated through various methods [172,173].

A total of thirteen studies investigated plastic weathering during wastewater treatment, though none provided information on the duration of the processes (Table 4, Table S4 and Fig. 7).

Likely, plastics have already been pre-altered during transportation when entering WWTPs. At the pre-treatment stage, mechanical stress leads to further physical degradation (Fig. 8). In the secondary treatment stage, organic material, including organic pollutants, is degraded by high microbiological activity under mainly aerobic conditions [171,174], which also favours the biodegradation of plastic particles [175]. Among tertiary treatment processes used in WWTPs, mainly AOPs, which include the use of oxidants such as ozone, hydrogen peroxide and O, as well as catalysts and/or UV radiation, will lead to substantial alteration of plastics [172,176]. AOPs are used to remove persistent and toxic organic compounds by generating highly reactive hydroxyl radicals [172], which can also attack the polymer chains of plastics, leading to chain scission [176]. During wastewater treatment, MPs can be removed at rates of 23.5 % [177] to 94.0 % [178], with WWTPS having a third treatment achieving the highest removal rates [26]. All MPs removed from wastewater, however, end up in the sludge [177,178]. The plastic concentration of the wastewater and the sludge depends, hence, on the treatment, but also on the initial plastic load of wastewater, which in turn depends on the wastewater source and seasonality [179] (Table 4 and Table S4).

After wastewater treatment - regardless of whether removed from wastewater and retained in sludge or staying in the treated water - plastics generally exhibit signs of weathering, such as uneven surfaces with grooves, dents, large cracks and small detached fragments, as well as biofilm formation [64,164,177,180–184]. In concordance, a larger specific surface area was observed for most plastic types [64]. The extent and nature of surface alterations of plastics retained in sludge largely depend on the specific sludge treatment method applied. Thermal drying resulted in blistering, wrinkling, melting and fracturing [185,186], which is attributed to the high temperatures of up to 200 °C during the process [187]. In comparison, thermal hydrolysis created deep cracks on the surface of the MPs. Compared to the effect of thermal drying, the crack surface and edges were more blurred, and melting and spalling occurred, caused by the high pressure (6–9 bar) and temperatures (140–170 °C) [185,188]. These cracks allow for deeper degradation of the bulk polymer, potentially leading to the fragmentation of plastics [61,189]. Lime stabilisation is commonly used for the reduction of pathogens and odours by raising the pH to 12 [173], resulting in MPs with a more shredded and flaked appearance compared to plastics that underwent thermal drying [186]. Alkaline conditions foster hydrolysis as the hydrogen ions attack hydrolysable covalent bonds, leading to

chain scission and surface erosion [131,190], which presumably causes the different appearance. In contrast, anaerobic digestion favoured the weathering of plastics [185], with deep cleavage, micropores and filaments, resulting in a large specific surface area that could act as attachment sites for microorganisms [164,186]. Aerobic composting of sewage sludge caused surface damage and erosion, with complex morphological changes such as tears and cracks [185]. But in contrast to composting of municipal waste, this did not lead to the fragmentation of larger plastics [185].

After sludge treatment, the FTIR spectra of PE and PP revealed the formation of C═O and O–H groups, as well as evidence of C–O stretching, C═C stretching, and C–H deformation. Similarly, PS displayed signs of C–H bending and C–O stretching, while PA exhibited a double peak in the 2350–2450 cm ^{1} region, likely associated with material accumulation [64,178].

A 2D-COS analysis of MPs originating from sludge demonstrated that C–O and N–H functional groups played a more significant role in cadmium adsorption than C–H groups, explaining the enhanced heavy metal adsorption capacity observed in aged MPs due to physicochemical changes [64]. Heavy metals like Ti, manganese (Mn), cadmium (Cd), lead (Pb), and Co, as well as other elements like Ca, Fe, Na, Mg, Si, Cl and Al, were found to accumulate on the MP surface [64,185,191]. This accumulation is also fostered through the use of Al and Fe during the coagulation-flocculation process in many WWTPs [175].

The fragmentation of MPs is dependent on the respective sludge treatment process. For anaerobic digestion [164,185], thermal drying [178,179,185] and aerobic composting, no significant changes in particle number and therefore fragmentation could be observed [185]. In contrast, mechanical dewatering [164] and thermal hydrolysis [185] led to a significant increase in the number of MPs, with particle sizes decreasing notably after mechanical dewatering [164]. The fragmentation is presumably caused by forces excreted on the plastic particles during dewatering through filtration, compaction or centrifugation [173].

3.2.4. Soils

Plastic particles entering the soil environment may already be significantly altered due to prior degradation processes in the course of, e.g., sludge or waste treatment as described above (Fig. 8). Further degradation in the soil, which, unlike the controlled environments of composting and digestion facilities, WWTPs or landfills, varies with factors such as geographical location, weather and climate conditions (including temperature and moisture, day/night cycles and seasonal changes), but depends also on soil properties and soil management [152, 192,193]. Further, the alteration is mostly dependent on the position within the soil profile. At the soil surface, plastics are directly exposed to sunlight, initiating photo-oxidative reactions [194]. This exposure can cause thermal oxidation as direct sunlight raises the surface temperature of plastics, especially for darker coloured plastics, above the ambient air temperature (up to 80 °C) due to heat build-up [195–197]. The combined effect of temperature and UV exposure produces a synergistic acceleration in the rate of plastic weathering [12,198]. In addition, particularly in urban environments, ozone and other air pollutants can promote further weathering processes [109,199] (Fig. 8).

The exposition of plastics on the soil surface led to weathering in the form of cracks and holes, which was dependent on the colour of the film, with white films showing more surface changes compared to silver-black and black films [66]. At the same time, the thickness of the film, which was also detrimental during composting, was an important factor, as the susceptibility to surface alterations like cracks increased with decreasing thickness of the film. In detail, thicker films (0.015 and 0.010 mm) showed only small dot cracks, whereas thinner samples (0.008 and 0.006 mm) showed a large number of blocky cracks of larger diameters, indicating increased weathering in a domino effect [105]. As oxidation processes depend on the diffusion rate of O through the polymer, thicker samples are more likely to experience diffusion limitations. This limitation creates a gradient of oxidation, resulting in increased chain scission concentrated on the surface layer compared to the bulk. In contrast, O diffusion in thinner films is more uniform, allowing oxidation to affect both the surface and the bulk more evenly, leading to more severe cracking [198–200]. Besides UV radiation, temperature, and rainfall, soil properties such as organic matter content or texture affect photo-oxidation on the soil surface [102]. Despite almost identical temperatures, Gauthier et al. [102] observed that on a fine-textured soil, with 3.9 % organic matter, the total solar radiation dose to reach embrittlement was more than twice as high as on a coarser textured soil with a higher organic matter content (4.4 %). In a following laboratory study, the photo-oxidation increased with the presence of water and organic matter beneath the films [102]. Water droplets that condense on the underside of transparent films, due to soil moisture evaporation, scatter and reflect incident light [201], effectively increasing the light exposure to the film and accelerating photodegradation [102]. Conversely, water droplets that form on the surface of plastic particles—whether from rain or irrigation—can function as both an O barrier and refractive element [202], as the transmission of light is reduced on average by 15 % compared with dry films [201]. Further, the rate of photo-oxidation reactions is strongly influenced by the availability of O [203,204], making O the limiting factor that ultimately controls the rate of photodegradation [202]. Organic matter displays complex behaviour in influencing ROS production, as it can either promote or inhibit ROS generation [205]. Photogeneration of hydroxyl radicals from organic matter has been observed to increase oxidation levels of plastic particles [129,206]. However, organic matter can also reduce photodegradation by scavenging ROS and acting as an optical filter, due to special molecular structures of fulvic and humic acids, including chromophores such as aromatic ketones, aldehydes, quinones, and phenolic compounds, which block UV radiation from reaching the plastic surface [207]. Additionally, organic matter may inhibit plastic weathering by facilitating reactions of intermediate radical cations with itself, rather than with ROS [205,208]. It might also interact with plastic particles through chelation and hydrogen bonding, slowing photo-oxidation [209,210]. Beyond organic matter, other soil constituents, such as iron oxides (hematite > goethite), pyrite or clay (kaolinit > montmorrilite), significantly foster photo-oxidation of plastics [210,211], highlighting the critical role of soil constituents in the weathering of plastics. In the reviewed studies, LDPE films exhibited the formation of C═O functional groups and an increase in CI following soil surface exposure [80]. Notably, PE films of different colour showed differences in FTIR peak formation [66] and intensity [212]. White films developed distinct peaks reflecting the formation of alkoxyl, C═O, O–H, and diketone groups. In contrast, silver-black films showed the formation of alkoxyl and diketone groups, while black films exhibited only the formation of alkoxyl groups [66]. Diketone groups are not common in PE and may indicate the presence of additives [213]. In addition, film thickness had a significant influence, with thicker films showing less reduction in surface tension, tension strength and elongation at break than thinner films. This is due to an initial durability advantage, as thicker mulching films generally exhibit greater tension strength and elongation at break [105]. The properties of the LDPE films also varied depending on the sampling site. Differences in crystallinity, elemental composition (e.g. Ti, Si, Ca, S, Al) and dominant microbial taxa were observed, possibly due to variations in inorganic additives such as TiO_2 [80].

In deeper soil layers, with the absence of sunlight [202], other degradation mechanisms dominate. Once incorporated into soils, plastics interact with a complex matrix of mineral and organic materials and varying levels of air and water within the soil pore spaces [214]. This soil composition largely determines the environmental conditions and influences specific factors affecting plastics through direct contact with surrounding soil constituents as well as soil organisms [202,215]. Mechanical forces such as natural shrink-swell cycles, freeze-thaw cycles, soil erosion and abrasion, and human activities such as tillage and compaction act on plastic particles [216–218]. Tillage and erosion can

bring plastic particles back to the soil surface, where they are re-exposed to sunlight. During the termination phase of the initial photo-oxidative processes, functional groups such as olefins, aldehydes and ketones are formed within the polymer, making it more susceptible to further degradation as these groups are highly photolabile [122,199]. Plastic weathering in soil is influenced by several key factors, including temperature, water content, pH and residence time [219–221] (Table 5, Table S5 and Figs. 7 and 8). These varying conditions are also evident in the 29 studies reviewed, where exposure durations ranged from 3 months to 37 years. Notably, most studies spanned less than 10 years (Fig. 7). Within the soil, water content controls processes such as hydrolysis, solute transport and also microbial activity, with low and high moisture levels slowing down degradation processes [219]. In addition, water can penetrate the weathered surface layers of plastics, potentially causing swelling. This swelling behaviour may differ from the underlying bulk polymer, and after repeated wetting and drying cycles, it can lead to delamination of the surface layer [6,222]. Further, hydrolysis is influenced by pH [131], as under acidic or alkaline conditions, hydrolysable covalent bonds in plastics are attacked, which increases the rate of hydrolysis compared to neutral conditions [190,222]. Temperature accelerates weathering by enhancing chemical and biochemical reactions, with higher temperatures accelerating microbial activity and reaction rates [220]. On the other hand, extremely low temperatures below the glass transition temperature of the respective plastic will lead to brittleness and facilitated fracture and fragmentation [109]. In managed soils, the presence of agrochemicals might foster weathering processes [223]. The complex interaction of all named factors affects the rate and extent of plastic weathering in different soils.

At a macroscopic level, transparent LDPE films became opaque, brittle and eventually fragmented during soil burial. In detail, black LDPE films lost their gloss, perforations formed and the white films showed signs of yellowing [81,212]. Initially, virgin plastics exhibited a smooth surface [41,91,179,224], while virgin films containing a variety of additives had a rougher surface structure [66]. After soil burial, plastic surfaces exhibited signs of extensive weathering, including scratches, holes, cracks and depressions, which resulted in increased surface roughness [40,133,179,183,224–226]. The degree of weathering increased with increasing burial time [86]. Additionally, the detachment of small flakes was observed, as a result of a major erosion of the amorphous regions of PE [41,81,91,227]. Several studies observed honeycomb structures due to additive leaching under moist soil conditions [66,93,227]. For phthalic acid esters, for example, up to 38 % of bulk material was released into the soil after two years of soil exposure [105]. The position in the soil body and the contact with the soil matrix also play a decisive role: LDPE samples from 10 cm depth had many holes and part of the film lost its shape as well as a higher degree of whitening compared to samples from deeper soil layers (40–60 cm) [93]. In general, soil microbial biomass and diversity correlate with the availability of C substrates, which are typically the highest in soil surface layers, resulting in higher microbial activity and degradation potential in topsoil compared to deeper soil layers [228,229]. The observed garden soil, however, had similar conditions (moisture, pH) in the two soil layers, with an even higher percentage of organic matter in the lower soil layer [93]. Therefore, other factors such as temperature or aeration of the upper soil layer might influence microbial activity and, therefore, biodegradation of plastics [214]. Plastics that were in direct contact with soil had severe degradation and whitening, whereas the other part was still transparent. In addition, a lot of holes (20–200 nm in diameter) passing through LDPE films, a variety of hyphae and ditches as a result of the metabolic action of bacteria occurred [93]. Other studies also observed the colonisation of plastics with a variety of fungal organisms and bacteria [41,44,58], associated with organic matter, clay and soil aggregates on the surface [226,230,231]. Interestingly, fungi developed germinating spores and conidiophores, which indicates fungal reproduction [44]. The attachments of various structures and substances are also reflected in the variety of elements found that could be assigned to soil constitutes, such as C, N, O, Fe, Ca, K, Mg, Al, and Mn, to additives, like Ti and Br (used in plastic production) and other elements such as arsenic (As), Cr, Cd, Cu, Pb, Sn (Tin) and Zn [37,86,227,232–235]. The concentration of found elements accumulating on the surface generally increases with increasing exposure time [236] and depends also on the polymer type [237]. In particular, the atomic proportions for O displayed a high variability for the different polymer types, ranging from 11.3 % to 26.4 % [227]. The resulting O/C ratios were 0.366 (PP), 0.321 (PS) and 0.264 (PE), indicating the highest weathering status of PP from soil [227]. FTIR spectra of PE revealed the formation of C═O and O–H groups together with C–H bending and deformation and C–O stretching, indicative of oxidative processes. Spectra of PP, PS and PVC showed evidence of C═O stretching, with additional contributions of O–H and C–O stretching observed in PP [40,81,91,226,231,234]. A peak at about 1030 cm^{-1} in both PE and PP was attributed to the attachment of polysaccharides [226] or clay particles [234] on the polymer surface. The width of the peak at 1100 cm^{-1} (O–H and C═O) increased with time for PE [91]. Miao et al. [238] also observed halogen-associated absorption peaks in FTIR spectra of PE, which might be due to the adsorption of halogenated contaminants. Interestingly, different parts of the same samples showed different band formations, indicating the heterogeneous conditions in the soil environment. The whitened part of a PE film displayed peak formations at 1715 cm^{-1} (C═O) and 1640 cm^{-1} (C═C), as signs of biodegradation, which were not observed on the transparent part. Both parts showed the formation of hydroperoxide (3600 cm^{-1}) while the intensity of the broad hydroxy peak (3400 cm^{-1}) was stronger for the whitened part [93]. The formation of polar groups through weathering processes was also observed through shifts and intensifications of the dielectric loss peaks of LDPE [81], as well as the WCA. The WCA of two LDPE films gradually decreased with time during soil burial, showing similar trends in two different soils with no significant effect of film thickness [74]. Film thickness, however, significantly affected the intensity of the asymmetric (2910-2920 cm^{-1}) and symmetric (2840-2860 cm^{-1}) stretching bands in PE, with thicker films showing higher peak intensities [105]. While in contrast to the other studies no new functional groups were detected in any of the films [105,239], all films showed a reduction in the intensities of the asymmetric and symmetric stretching bands, bending vibration peaks (1450-1480 cm^{-1}), CH_2 as well as CH_3 peaks. Notably, these intensities decreased less for thicker films over time [81,105]. PVC MPs displayed a reduced intensity at 1720 cm^{-1}, suggesting possible volatilisation of phthalate ester, although no conclusive evidence of weathering was observed [93].

With increasing soil exposure time, both the vinyl index [86] and the HI [86,240] increased. Keto carbonyl, ester carbonyl, vinyl bond and internal double bond index did not change significantly after 27 months of soil burial in two different soils [74]. The CI did not show a consistent trend across studies. Yang et al. [86] and Uzamurera et al. [239] found no significant difference in CI, whereas Bai et al. [240] observed a gradual increase and Mumtaz et al. [81] a decrease in CI with prolonged exposure time. Film thickness did not significantly affect CI, as films of different thicknesses did not show significant differences after identical exposure times [105,239]. Similarly, different plastic concentrations did not result in measurable differences in CI [224]. Interestingly, soil depth had a variable effect on plastic weathering. For example, PP and PE had the highest CI at a depth of 15–20 cm, while PET had the lowest CI at this depth compared to 0–5 cm and 30–35 cm. PS, on the other hand, had a significantly lower CI at 30–35 cm compared to other depths [226]. The impact of soil burial on crystallinity varied based on soil type. In two soils, burial resulted in a decrease in crystallinity [66,74], while in two other soils, no significant changes were observed [74,81]. The decrease in crystallinity was also influenced by the thickness of the film, with thinner films showing greater reductions [74].

The crystallinity of a transparent part of an LDPE sample was higher than that of a more degraded, whitened part of the same samples [93], which could reflect the latter stages of weathering due to cross-linking

[6]. This was also reflected in the initial oxidation temperature, which decreased in both sections compared to a fresh film. However, the oxidation temperature of the transparent section of a buried LDPE sample was about 15 °C lower, while the more degraded, whitened section showed an even greater reduction of about 25 °C [93]. Similarly, Berenstein et al. [40] reported a decrease in fusion enthalpy for all soil-derived plastic films, reflecting the changes in thermal properties. Soil burial resulted in a decrease in viscosity average molecular weight over time, with reductions of approximately 7.0 % after three years and 13.8 % after five years. While the high molecular weight fraction showed a marked decrease, correlating with the time spent buried in fluvo-aquic and phaeozem soils, the low molecular weight fraction remained relatively stable throughout the burial period [91]. Despite the change in molecular weight, studies on LDPE films exposed to soil have shown mixed results for weight loss over time. Two studies did not find apparent weight loss for most LDPE films in soil exposure under various conditions [74,81]. The exception was a 0.05 mm-thick, transparent LDPE film, which began to lose weight after 9 months, eventually losing 10 % of its weight by 16 months [81]. Conversely, Uzamurera et al. [239] found earlier weight loss in LDPE films, with reductions observed as early as 6 months. By 24 months, thinner LDPE films (0.010 mm) had lost 3.08 % of their weight, significantly more than thicker films (0.016 mm), which lost 1.71 % [239]. The results suggest that the thickness, the exposure time and the type of soil may have different effects on the weight change of LDPE.

The load-extension curves showed that as soil burial time increases, PE samples break more readily. Across all samples, the percentage strain at maximum load reached its lowest values after 15–17 months of burial. Additionally, maximum stress (N mm ^{2}) declined to its minimum within 3 and 13 months, depending on the specific sample type [81]. Similarly, the nominal tensile strain at breaking for two LDPE films (0.005 mm and 0.010 mm thick) decreased significantly after 30 months of soil burial, with a slightly greater decline in loess orthic Entisols compared to loess-like loam soil [74].

Liang et al. [66] compared buried and surface-exposed plastic films, revealing notable differences in their properties. For instance, the peak intensity of the asymmetric C–H stretch (CH_2) decreased by up to 76.6 % for films aged on the soil surface, compared to a 29.0 % reduction for those buried in the soil, which was attributed to carbon-chain breakage caused by free radical attack [66]. Additional XPS analysis revealed an increase in initially low O/C ratios after both soil-surface and soil-burial exposure. Interestingly, the different films responded variably to environmental exposure. White and black films showed higher O/C ratios in soil-surface weathering than in soil-burial, while silver-black films showed the opposite pattern. During weathering, initial C–O groups gradually formed and partially oxidised to C═O groups, with this oxidation process accompanied by a reduction in C–C bonds. White film was most susceptible to oxidation and showed the highest levels of C–O and C═O in both virgin and aged samples, which might be due to its lower thickness (0.006 mm thick) compared to the other two films (0.012 mm thick). White and black films were more affected by soil surface exposure, whereas silver-black film formed fewer oxygenated groups on the surface, probably due to its high reflectivity to sunlight [66]. Despite increased O/C ratios, white (0.006 mm thick) and black (0.012 mm thick) films showed an increase in WCA after 12 months of soil surface exposure. Whereas the WCA of all three samples decreased consistently with soil burial time, aligning with findings from Han et al. [74]. This variation was attributed to increased crystallisation in the surface-exposed samples compared to untreated reference films [66]. Films exposed on the soil surface exhibited an increase of crystallinity for white (0.006 mm thick) and black (0.012 mm thick), but not for silver-black LDPE films [66]. Differences in crystallinity were attributed to the lack of O in soil [66]. O diffuses primarily through amorphous regions, promoting chain scission and enhancing chain mobility, which fosters chemi-crystallisation [152,241]. When O is scarce, the likelihood increases that polymer radicals combine, creating a crosslink rather than reacting with O [151], which reduces the crystallinity in PE films [66].

Both exposure types significantly reduced the tensile strength of white film (0.006 mm thick). However, the tensile strength of black and silver-black films (0.012 mm thick) decreased on soil surface exposure, but increased during soil burial, likely due to crosslinking, which can temporarily enhance strength. However, elongation at break declined for both black and silver-black films (0.012 mm thick) in both treatments, with a more substantial decrease observed under soil surface exposure [66].

The loss of mechanical properties observed both on the soil surface and within the soil was also evident in the fragmentation of plastics, widely utilised in various agricultural practices [194]. The concentration of plastic particles found in the soil increased with increasing duration of plastic mulching [86,231,236,238,240]. Typically, the highest concentrations of plastics were found in the top 10–20 cm of soil, gradually decreasing with depth, as they were applied on the soil surface [236,239]. However, in fields that have been mulched for long periods, plastic concentrations tend to increase in deeper soil layers, indicating a slow downward migration of particles over time [212]. In addition, smaller plastic particles became more abundant with longer mulching durations, suggesting ongoing fragmentation of larger pieces [212,240]. This fragmentation might be affected by factors such as film thickness - where thinner films produced more MPs [239] - and local climatic conditions [91].

4. Conclusion & implications

4.1. Methodological recommendation

To fully assess changes of plastics during weathering, we recommend using multimodal approaches, which are already used in many studies (e.g., [30,31,66]). Non-destructive techniques such as spectroscopic methods, light microscopy, X-ray CT and environmental SEM are particularly valuable as they preserve the integrity of the plastic particles (Fig. 9). In contrast, thermal, mechanical and chromatographic methods involve the destruction or modification of the particles, making non-destructive methods preferable as initial tools for property determination, before applying destructive methods. As important as the methods used for the analysis, the extraction can be decisive for a reliable characterisation of plastic weathering. It can damage and modify the polymer structure and may hence lead to an overestimation of plastic weathering. We, therefore, recommend avoiding extraction procedures, but if necessary, using a gentle extraction protocol and additionally using pristine particles during extraction as a control. Furthermore, to obtain more reliable results that account for the heterogeneous conditions within most systems, it is advisable to increase the number of replicates, both in terms of particles analysed and measurements per particle. This will allow more robust statistical evaluation, such as the calculation of CI based on multiple FTIR spectra of different plastic particles [31].

A major challenge is the lack of standard protocols or guidelines which exist for, e.g., tensile testing (ISO and ASTM) [101], but are missing for many commonly used methods. This problem is particularly pronounced in the calculation of indices from FTIR spectra. Even in protocols where CI is used as a parameter to assess biodegradability (e.g., PAS 9017:2020), the calculation method is not clearly defined [72]. As a result, CIs from different studies are hardly comparable [71,72].

For other techniques, such as SEM, standardisation is inherently difficult as optimal settings depend on the research question and type of plastic (Figs. 2–4). To improve reproducibility and comparability, we strongly recommend providing a detailed description of methodology and instrument settings or aligning with existing studies for consistency. In particular, all polymer samples should be coated with a thin layer of carbon (5–10 nm) to enhance electrical conductivity without interfering with elemental detection, ensuring optimal imaging and analysis. In addition, we advocate the use of low-energy SEM with acceleration

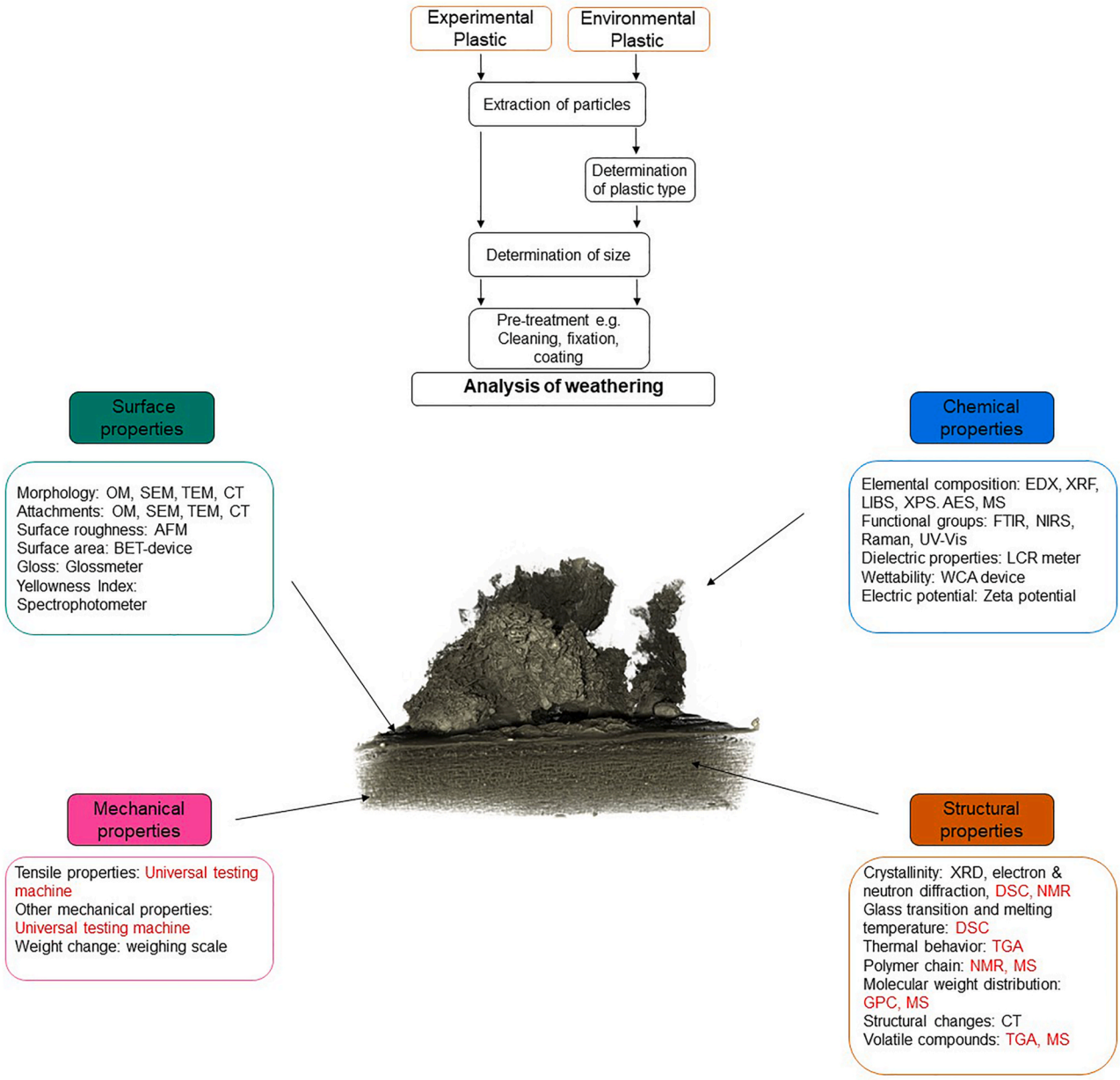

Fig. 9. Idealised workflow and different analysis methods. Destructive methods are highlighted in red. (For interpretation of the references to colour in this figure legend, the reader is referred to the Web version of this article.)

voltages below 5 kV, preferably below 1 kV, to minimise radiation damage when analysing sensitive or non-conductive samples.

4.2. Data availability

Our review shows that the frequency of polymer analysis in existing studies largely correlates with production volumes, with PE and PP being the most commonly studied [2]. However, several other widely produced polymers remain understudied or unstudied in certain terrestrial environments. This highlights the need for a more balanced research focus on commercially significant polymer types. In addition, identification of the specific polymer type in weathering studies is crucial to account for polymer-specific degradation patterns and ensure more accurate assessments of environmental behaviour. A strong geographical imbalance was also evident, with studies from Asia and Europe accounting for over 88 % of the total reviewed. This imbalance is particularly relevant as waste management practices—and consequently the weathering of plastics in landfills, composting and digestion plants, and WWTPs—are influenced by national regulations, prevailing technologies and regional waste compositions, which vary substantially between regions and countries [20,243]. Additionally, when plastics enter soils, climatic factors, like moisture and temperature, play a crucial role in determining the extent and type of weathering [152]. Geographical differences also extend to agricultural practices, particularly in regions where mulch films are commonly used [244]. In arid areas, for example, these films are often exposed to high levels of UV radiation and heat build-up, resulting in accelerated and distinct weathering patterns compared to other environments [198]. This highlights the need for more studies conducted across different geographic regions to fully understand the variability in plastic weathering processes [245].

4.3. Environmental implications

In general, weathering in different terrestrial environments resulted in similar changes in plastics. Surface changes were observed in all plastics regardless of the environment, along with the formation of oxygenated functional groups as detected in FTIR spectra. However, specific functional groups differed depending on the environment: diketone groups were formed in PE during soil surface exposure [66], while cyclic C–*O*–C bonds and CH═CH_2 appeared in BOPP and PP after landfilling [73]. Trends in CI and HI were inconsistent for PP and PE during soil and landfill exposure. An increase in CI was observed for PS after landfilling [84] and for PP after composting [31]. Crystallinity showed different patterns: it increased during soil surface exposure [66], but decreased during composting and digestion for PE [30]. For landfill and soil burial, changes in crystallinity were inconsistent and dependent on the polymer type, exposure time and soil conditions [74,81,85,132]. The mechanical properties of PE and PP also varied significantly between environments. The most significant factor influencing weathering was the thickness of the plastic. Thinner plastics, regardless of the polymer type and environmental system, exhibited more pronounced surface changes [105,106] greater loss of mechanical properties [105] and greater percentual weight loss [106,239], along with higher particle release [106,239]. In addition, thinner PE films showed a greater reduction in bending vibration peaks (1450-1480 cm^{-1}), a reduction in CH_2 and CH_3 peaks [81,105] and a greater loss of crystallinity [74] compared to thicker films. Another factor influencing weathering was the colour of the plastics. PEs with different colours - and consequently dyes with different elemental compositions - showed differences in surface changes [66,98], FTIR peak formation and intensity [66,212], microbial colonisation [80] and variations in DSC thermogram patterns [98]. Our results highlight the limited understanding of plastic weathering, particularly in terrestrial environments.

Plastic weathering in the terrestrial environment is governed by complex conditions that cannot be fully controlled or replicated in laboratory studies [152]. Consequently, common methods for estimating polymer lifetimes, such as Arrhenius extrapolation from accelerated weathering data or extrapolation from initial rates measured under environmentally relevant conditions, have limited validity due to significant and often poorly justified assumptions [16]. Similarly, fragmentation under lab conditions and in the environment varies. Du et al. [246] for instance found that the generation of plastic particles (<20 μm) from weathered, environmentally collected plastic particles (1–5 mm) in laboratory experiments was more than twice as high as in corresponding sediment samples. Long-term studies are essential to elucidate the weathering behaviour of plastics in these environments. Most of the long-term data in the reviewed studies come from landfills, where operational records provide valuable insights into the persistence of plastic particles, with maximum durations of 60 years reported [139]. In contrast, soil exposure studies have analysed plastics buried for a maximum of 32–37 years [93]. Despite the challenges in determining the exact age of plastics in soils, such data are essential for understanding the behaviour of plastics in the environment, particularly as soils act as a major sink for plastic debris [19] and the fate of plastics in soils is more complex than in other environmental systems.

Weathering of plastics typically leads to an increase in surface roughness and surface area [64,84,164], which presents a higher adsorption capacity for the sorption of several toxic organic pollutants [247]. In addition, the formation of new functional groups plays an important role in the accumulation of pollutants, such as heavy metals [64] and the attachment of microorganisms [141], some of which are potential pathogens [44]. The plastisphere [248] on the surface of a weathered particle is a specific ecological niche where microbial communities are distinct from the surrounding terrestrial environment [249,250]. Fragmented particles of smaller size have a higher surface area to volume ratio, leading to an even greater increase in adsorption capacity [109] and an increased function as a 'Trojan horse' when taken up by plants or soil organisms [251].

The fragmentation of larger plastic ultimately leads to the formation of numerous smaller particles, finally down to the submicron range. Especially such submicron plastics are problematic as they harm soil biota, can be taken up by plants and are transported through the food chain, resulting in exposure, and at the same time, adverse effects on humans [252–254]. Research on environmental nanoparticles has shown that the uptake, translocation and accumulation of particles in plants depends on several factors, including the properties of the particle itself (summarised in Jia et al. [255]). The main controlling factor for the uptake of submicron plastics is likely particle size, as small nanoparticles of 20 nm size were more susceptible to plant uptake than larger particles [253,256]. This plant uptake is mainly dependent on size exclusion limits for particles entering whole plants (<30–60 nm) [255] or biological cells of plants with a plant-specific size exclusion limit of, e.g., 10 nm [257,258]. Various studies have confirmed the plant uptake of nanoplastics, such as lettuce and chicory [253,254,256], as recently reviewed by Zhou et al. [259]. Further, the zeta potential influences the uptake and transport of engineered nanoparticles, i.e., the higher the negative charge of the nanoparticle the higher the uptake and translocation by the plant. For plastics, the zeta potential is influenced by polymer type, additives, and surface alterations from weathering. In a laboratory experiment with PET fibres, for example, prolonged exposure to soil led to increased surface negativity over time [108]. Consequently, weathering is expected to enhance the uptake of plastic particles by plants, potentially introducing them into the food chain.

However, plant uptake requires that the particle is bioavailable in soil. Particles, occluded in soil aggregates, might be protected from plant uptake but also from weathering, as not or at least less accessible [260,261]. Hence, such aggregate occlusion might substantially affect the weathering of plastics in soil, with yet unknown consequences.

CRediT authorship contribution statement

Max Groß: Writing – review & editing, Writing – original draft, Visualization, Conceptualization. **Matthias Mail:** Writing – review & editing, Writing – original draft, Resources, Conceptualization. **Rafaela Debastiani:** Writing – review & editing, Writing – original draft, Conceptualization. **Torsten Scherer:** Writing – review & editing, Writing – original draft, Resources, Funding acquisition. **Melanie Braun:** Writing – review & editing, Writing – original draft, Supervision, Funding acquisition, Conceptualization.

Declaration of generative AI and AI-assisted technologies in the writing process

During the preparation of this work the authors used ChatGPT-4 (OpenAI) and DeepL Write (Deepl SE) to enhance readability and clarity. After using this tools/services, the authors reviewed and edited the content as needed and take full responsibility for the content of the publication.

Declaration of competing interest

The authors declare that they have no known competing financial interests or personal relationships that could have appeared to influence the work reported in this paper.

Acknowledgements

This work was funded by the European Research Council (ERC Starting Grant NanoSoil; grant no 101163487) and the European Union's Horizon 2020 - Research and Innovation Framework Programme PAPILLONS (grant agreement no 101000210). This work was partly carried out with the support of the Karlsruhe Nano Micro Facility (KNMFi, www.knmf.kit.edu), a Helmholtz Research Infrastructure at

Karlsruhe Institute of Technology (KIT, www.kit.edu).

Data availability

Data will be made available on request.

References

[1] PlasticsEurope, Plastics - the Facts 2010: an Analysis of European Plastics Production, Demand and Recovery for 2009, 2010.
[2] PlasticsEurope, Plastics – the Fast Facts 2024, 2024.
[3] R. Geyer, J.R. Jambeck, K.L. Law, Production, use, and fate of all plastics ever made, Sci. Adv. 3 (2017) e1700782, https://doi.org/10.1126/sciadv.1700782.
[4] M. Kedzierski, D. Frère, G. Le Maguer, S. Bruzaud, Why is there plastic packaging in the natural environment? Understanding the roots of our individual plastic waste management behaviours, Sci. Total Environ. 740 (2020) 139985, https://doi.org/10.1016/j.scitotenv.2020.139985.
[5] Z. Zhang, S. Zou, P. Li, Aging of plastics in aquatic environments: pathways, environmental behavior, ecological impacts, analyses and quantifications, Environ. Pollut. 341 (2024) 122926, https://doi.org/10.1016/j.envpol.2023.122926.
[6] A.L. Andrady, The plastic in microplastics: a review, Mar. Pollut. Bull. 119 (2017) 12–22, https://doi.org/10.1016/j.marpolbul.2017.01.082.
[7] M. Alexander, How toxic are toxic chemicals in soil? Environ. Sci. Technol. 29 (1995) 2713–2717, https://doi.org/10.1021/es00011a003.
[8] B. Gevao, K.C. Jones, K.T. Semple, A. Craven, P. Burauel, Peer Reviewed: Nonextractable Pesticide Residues in Soil, ACS Publications, 2003.
[9] H. Ciglasch, J. Busche, W. Amelung, S. Totrakool, M. Kaupenjohann, Field aging of insecticides after repeated application to a northern Thailand ultisol, J. Agric. Food Chem. 56 (2008) 9555–9562, https://doi.org/10.1021/jf801545h.
[10] W. He, S. Liu, W. Zhang, K. Yi, C. Zhang, H. Pang, D. Huang, J. Huang, X. Li, Recent advances on microplastic aging: identification, mechanism, influence factors, and additives release, Sci. Total Environ. 889 (2023) 164035, https://doi.org/10.1016/j.scitotenv.2023.164035.
[11] L. Wang, J. Zhang, W. Huang, Y. He, Laboratory simulated aging methods, mechanisms and characteristic changes of microplastics: a review, Chemosphere 315 (2023) 137744, https://doi.org/10.1016/j.chemosphere.2023.137744.
[12] Q. Lu, Y. Zhou, Q. Sui, Y. Zhou, Mechanism and characterization of microplastic aging process: a review, Front. Environ. Sci. Eng. 17 (2023) 100, https://doi.org/10.1007/s11783-023-1700-6.
[13] G. Binda, G. Kalčíková, I.J. Allan, R. Hurley, E. Rødland, D. Spanu, L. Nizzetto, Microplastic aging processes: environmental relevance and analytical implications, TRAC-Trend. Anal. Chem. 172 (2024) 117566, https://doi.org/10.1016/j.trac.2024.117566.
[14] S. Lambert, C. Sinclair, A. Boxall, Occurrence, degradation, and effect of polymer-based materials in the environment, Rev. Environ. Contam. Toxicol. 227 (2014) 1–53, https://doi.org/10.1007/978-3-319-01327-5_1.
[15] A.L. Andrady, Weathering and fragmentation of plastic debris in the ocean environment, Mar. Pollut. Bull. 180 (2022) 113761, https://doi.org/10.1016/j.marpolbul.2022.113761.
[16] A. Chamas, H. Moon, J. Zheng, Y. Qiu, T. Tabassum, J.H. Jang, M. Abu-Omar, S. L. Scott, S. Suh, Degradation rates of plastics in the environment, ACS Sustainable Chem. Eng. 8 (2020) 3494–3511, https://doi.org/10.1021/acssuschemeng.9b06635.
[17] Y. Shi, L. Shi, H. Huang, K. Ye, L. Yang, Z. Wang, Y. Sun, D. Li, Y. Shi, L. Xiao, S. Gao, Analysis of aged microplastics: a review, Environ. Chem. Lett. 22 (2024) 1861–1888, https://doi.org/10.1007/s10311-024-01731-5.
[18] R. Tian, K. Li, Y. Lin, C. Lu, X. Duan, Characterization techniques of polymer aging: from beginning to end, Chem. Rev. 123 (2023) 3007–3088, https://doi.org/10.1021/acs.chemrev.2c00750.
[19] M. Kedzierski, D. Cirederf-Boulant, M. Palazot, M. Yvin, S. Bruzaud, Continents of plastics: an estimate of the stock of microplastics in agricultural soils, Sci. Total Environ. 880 (2023) 163294, https://doi.org/10.1016/j.scitotenv.2023.163294.
[20] S. Kaza, L.C. Yao, P. Bhada-Tata, F. van Woerden, What a Waste 2.0: a Global Snapshot of Solid Waste Management to 2050, World Bank Group, Washington DC, 2018.
[21] M.D. Vaverková, Landfill impacts on the environment—review, Geosciences 9 (2019) 431, https://doi.org/10.3390/geosciences9100431.
[22] L. Canopoli, B. Fidalgo, F. Coulon, S.T. Wagland, Physico-chemical properties of excavated plastic from landfill mining and current recycling routes, Waste Manag. 76 (2018) 55–67, https://doi.org/10.1016/j.wasman.2018.03.043.
[23] O. Wrigley, M. Braun, W. Amelung, Global soil microplastic assessment in different land-use systems is largely determined by the method of analysis: a meta-analysis, Sci. Total Environ. 957 (2024) 177226, https://doi.org/10.1016/j.scitotenv.2024.177226.
[24] S. Peneva, Q.N. Phan Le, D.R. Munhoz, O. Wrigley, G.P.F. Macan, H. Doose, W. Amelung, M. Braun, Plastic input and dynamics in industrial composting, Waste Manag. 193 (2024) 283–292, https://doi.org/10.1016/j.wasman.2024.11.043.
[25] T. Steiner, J.N. Möller, M.G.J. Löder, F. Hilbrig, C. Laforsch, R. Freitag, Microplastic contamination of composts and liquid fertilizers from municipal biowaste treatment plants: effects of the operating conditions, Waste Biomass Valori (2022), https://doi.org/10.1007/s12649-022-01870-2.
[26] J. Sun, X. Dai, Q. Wang, M.C.M. van Loosdrecht, B.-J. Ni, Microplastics in wastewater treatment plants: detection, occurrence and removal, Water Res. 152 (2019) 21–37, https://doi.org/10.1016/j.watres.2018.12.050.
[27] R.R. Hurley, A.L. Lusher, M. Olsen, L. Nizzetto, Validation of a method for extracting microplastics from complex, organic-rich, environmental matrices, Environ. Sci. Technol. 52 (2018) 7409–7417, https://doi.org/10.1021/acs.est.8b01517.
[28] P. Pfohl, C. Roth, L. Meyer, U. Heinemeyer, T. Gruendling, C. Lang, N. Nestle, T. Hofmann, W. Wohlleben, S. Jessl, Microplastic extraction protocols can impact the polymer structure, Micropl.&Nanopl. 1 (2021), https://doi.org/10.1186/s43591-021-00009-9.
[29] I. Schrank, J.N. Möller, H.K. Imhof, O. Hauenstein, F. Zielke, S. Agarwal, M.G. J. Löder, A. Greiner, C. Laforsch, Microplastic sample purification methods - assessing detrimental effects of purification procedures on specific plastic types, Sci. Total Environ. 833 (2022) 154824, https://doi.org/10.1016/j.scitotenv.2022.154824.
[30] A. Alassali, H. Moon, C. Picuno, R. Meyer, K. Kuchta, Assessment of polyethylene degradation after aging through anaerobic digestion and composting, Polym. Degrad. Stabil. 158 (2018) 14–25, https://doi.org/10.1016/j.polymdegradstab.2018.10.014.
[31] M. Groß, M. Mail, O. Wrigley, R. Debastiani, T. Scherer, W. Amelung, M. Braun, Plastic fruit stickers in industrial composting—surface and structural alterations revealed by electron microscopy and computed tomography, Environ. Sci. Technol. (2024), https://doi.org/10.1021/acs.est.3c08734.
[32] S. Rohrbach, G. Gkoutselis, L. Hink, A.R. Weig, M. Obst, A. Diekmann, A. Ho, G. Rambold, M.A. Horn, Microplastic polymer properties as deterministic factors driving terrestrial plastisphere microbiome assembly and succession in the field, Environ. Microbiol. 25 (2023) 2681–2697, https://doi.org/10.1111/1462-2920.16234.
[33] M. Potrykus, V. Redko, K. Głowacka, A. Piotrowicz-Cieślak, P. Szarlej, H. Janik, L. Wolska, Polypropylene structure alterations after 5 years of natural degradation in a waste landfill, Sci. Total Environ. 758 (2021) 143649, https://doi.org/10.1016/j.scitotenv.2020.143649.
[34] S. Peneva, Q.N.P. Le, D.R. Munhoz, O. Wrigley, F. Wille, H. Doose, C. Halsall, P. Harkes, M. Sander, M. Braun, W. Amelung, Microplastic analysis in soils: a comparative assessment, Ecotoxicol. Environ. Saf. 289 (2024) 117428, https://doi.org/10.1016/j.ecoenv.2024.117428.
[35] K. Jarosz, P. Natkański, M. Michalik, Microplastic extraction from the sediment using potassium formate water solution (H2O/KCOOH), Minerals 12 (2022) 269, https://doi.org/10.3390/min12020269.
[36] M.G.J. Löder, H.K. Imhof, M. Ladehoff, L.A. Löschel, C. Lorenz, S. Mintenig, S. Piehl, S. Primpke, I. Schrank, C. Laforsch, G. Gerdts, Enzymatic purification of microplastics in environmental samples, Environ. Sci. Technol. 51 (2017) 14283–14292, https://doi.org/10.1021/acs.est.7b03055.
[37] P.D. Suchi, B. Saha, M. Moniruzzaman, T. Paul, K. Das Karmaker, M.K. Hossain, A. Parvin, A. Parvin, Distribution patterns and ecological risks of microplastics at major waste disposal environments in Dhaka, Bangladesh, Water Air Soil Pollut. 236 (2025), https://doi.org/10.1007/s11270-024-07664-7.
[38] J. Sanderson, Understanding Light Microscopy, Wiley, Hoboken, NJ, 2019.
[39] J. Girkin, A Practical Guide to Optical Microscopy, CRC Press Taylor & Francis Group, Boca Raton, FL, 2019.
[40] G. Berenstein, P. Córdoba, Y.B. Díaz, N. González, M.B. Ponce, J.M. Montserrat, Macro, meso, micro and nanoplastics in horticultural soils in Argentina: Abundance, size distribution and fragmentation mechanism, Sci. Total Environ. 906 (2024) 167672, https://doi.org/10.1016/j.scitotenv.2023.167672.
[41] T. Mumtaz, M.R. Khan, M.A. Hassan, Study of environmental biodegradation of LDPE films in soil using optical and scanning electron microscopy, Micron 41 (2010) 430–438, https://doi.org/10.1016/j.micron.2010.02.008.
[42] M. Mueller, Introduction to Confocal Fluorescence Microscopy, second, SPIE Press, Bellingham, Wash., 2005.
[43] G.C. Cox, Optical Imaging Techniques in Cell Biology, second ed., CRC/Taylor & Francis, Boca Raton, 2012 (Online).
[44] G. Gkoutselis, S. Rohrbach, J. Harjes, M. Obst, A. Brachmann, M.A. Horn, G. Rambold, Microplastics accumulate fungal pathogens in terrestrial ecosystems, Sci. Rep. 11 (2021) 13214, https://doi.org/10.1038/s41598-021-92405-7.
[45] B. Nguyen, N. Tufenkji, Single-particle resolution fluorescence microscopy of nanoplastics, Environ. Sci. Technol. 56 (2022) 6426–6435, https://doi.org/10.1021/acs.est.1c08480.
[46] K.D. Vernon-Parry, Scanning electron microscopy: an introduction, III-Vs review 13, 40–44, https://doi.org/10.1016/S0961-1290(00)80006-X, 2000.
[47] P.W. Hawkes, J.C.H. Spence, Springer Handbook of Microscopy, Springer International Publishing, Cham, 2019.
[48] L. Sabbatini, E. de Giglio, Polymer Surface Characterization, De Gruyter, 2022.
[49] L.C. Sawyer, D.T. Grubb, G.F. Meyers, Polymer microscopy, in: Softcover Version of Original Hardcover Edition, third. ed, Springer New York, New York, NY, 2010.
[50] J.I. Goldstein, D.E. Newbury, J.R. Michael, N.W. Ritchie, J.H.J. Scott, D.C. Joy, Scanning Electron Microscopy and X-Ray Microanalysis, Springer New York, New York, NY, 2018.
[51] B. Qiao, G. Teyssedre, C. Laurent, Electroluminescence and cathodoluminescence from polyethylene and polypropylene films: spectra reconstruction from

elementary components and underlying mechanisms, J. Appl. Phys. 119 (2016) 024103, https://doi.org/10.1063/1.4939824.
[52] E.M. Höppener, M. Shahmohammadi, L.A. Parker, S. Henke, J.H. Urbanus, Classification of (micro)plastics using cathodoluminescence and machine learning, Talanta 253 (2023) 123985, https://doi.org/10.1016/j.talanta.2022.123985.
[53] K. Kanaya, S. Okayama, Penetration and energy-loss theory of electrons in solid targets, J. Phys. D Appl. Phys. 5 (1972) 43–58, https://doi.org/10.1088/0022-3727/5/1/308.
[54] D. Drouin, A.R. Couture, D. Joly, X. Tastet, V. Aimez, R. Gauvin, Casino V2.42: a fast and easy-to-use modeling tool for scanning electron microscopy and microanalysis users, Scanning 29 (2007) 92–101, https://doi.org/10.1002/sca.20000.
[55] L. Hughe, Optimising data acquisition for biological SEM. https://nano.oxinst.com/blogs/optimising-data-acquisition-for-biological-sem, 2021. (Accessed 13 February 2025).
[56] V.T. Breslin, Degradation of starch-plastic composites in a municipal solid waste landfill, J. Polym. Environ. 1 (1993) 127–141, https://doi.org/10.1007/BF01418206.
[57] M. Slouf, J. Kotek, J. Baldrian, J. Kovarova, J. Fencl, T. Bouda, I. Janigova, Comparison of one-step and sequentially irradiated ultrahigh-molecular-weight polyethylene for total joint replacements, J. Biomed. Mater. Res. B Appl. Biomater. 101 (2013) 414–422, https://doi.org/10.1002/jbm.b.32857.
[58] F. Watteau, M.-F. Dignac, A. Bouchard, A. Revallier, S. Houot, Microplastic detection in soil amended with municipal solid waste composts as revealed by transmission electronic microscopy and Pyrolysis/GC/MS, Front. Sustain. Food Syst. 2 (2018) 81, https://doi.org/10.3389/fsufs.2018.00081.
[59] P. Eaton, P. West, Atomic Force Microscopy, Oxford University Press, 2010.
[60] D. Rugar, P. Hansma, Atomic force microscopy, Phys. Today 43 (1990) 23–30, https://doi.org/10.1063/1.881238.
[61] Q. Huang, C. Yang, Z. Cheng, H. Wang, A. Mojiri, N. Zhu, X. Qian, Y. Shen, S. Wu, Z. Lou, Exploring into a light-avoided environment: mechanical-Thermal coupled conditions responsible for the aging behavior of plastic waste in landfills, Water Res. 242 (2023) 120162, https://doi.org/10.1016/j.watres.2023.120162.
[62] M. Abe, Measurement Techniques and Practices of Colloid and Interface Phenomena, Springer Singapore, Singapore, 2019.
[63] K. Higashitani, H. Makino, S. Matsusaka, Powder Technology Handbook, fourth ed., FL Taylor & Francis Group, LLC, Boca Raton, 2020, p. 2019. CRC Press.
[64] X. Li, Q. Mei, L. Chen, H. Zhang, B. Dong, X. Dai, C. He, J. Zhou, Enhancement in adsorption potential of microplastics in sewage sludge for metal pollutants after the wastewater treatment process, Water Res. 157 (2019) 228–237, https://doi.org/10.1016/j.watres.2019.03.069.
[65] J.F. Watts, J. Wolstenholme, An Introduction to Surface Analysis by XPS and AES, Wiley, 2003.
[66] J. Liang, X. Chen, X. Duan, X. Gu, X. Zhao, S. Zha, X. Chen, Natural aging and adsorption/desorption behaviors of polyethylene mulch films: roles of film types and exposure patterns, J. Hazard Mater. 466 (2024) 133588, https://doi.org/10.1016/j.jhazmat.2024.133588.
[67] B.C. Smith, Infrared Spectral Interpretation: a Systematic Approach, firstst ed., CRC Press, Bosa Roca, 1998.
[68] S. Veerasingam, M. Ranjani, R. Venkatachalapathy, A. Bagaev, V. Mukhanov, D. Litvinyuk, M. Mugilarasan, K. Gurumoorthi, L. Guganathan, V.M. Aboobacker, P. Vethamony, Contributions of fourier transform infrared spectroscopy in microplastic pollution research: a review, Crit. Rev. Environ. Sci. Technol. 51 (2021) 2681–2743, https://doi.org/10.1080/10643389.2020.1807450.
[69] I. Noda, Y. Ozaki, Two-Dimensional Correlation Spectroscopy: Applications in Vibrational and Optical Spectroscopy, Wiley, Chichester, Weinheim, 2004.
[70] S. Peng, F. Wang, D. Wei, C. Wang, H. Ma, Y. Du, Application of FTIR two-dimensional correlation spectroscopy (2D-COS) analysis in characterizing environmental behaviors of microplastics: a systematic review, J. Environ. Sci. (China) 147 (2025) 200–216, https://doi.org/10.1016/j.jes.2023.10.004.
[71] J. Almond, P. Sugumaar, M.N. Wenzel, G. Hill, C. Wallis, Determination of the carbonyl index of polyethylene and polypropylene using specified area under band methodology with ATR-FTIR spectroscopy, E-Polymers 20 (2020) 369–381, https://doi.org/10.1515/epoly-2020-0041.
[72] R. S Gomes, A.N. Fernandes, W.R. Waldman, How to measure polymer degradation? An analysis of authors' choices when calculating the carbonyl index, Environ. Sci. Technol. (2024), https://doi.org/10.1021/acs.est.3c10855.
[73] C. Longo, M. Savaris, M. Zeni, R.N. Brandalise, A.M.C. Grisa, Degradation study of polypropylene (PP) and bioriented polypropylene (BOPP) in the environment, Math. Res. 14 (2011) 442–448, https://doi.org/10.1590/S1516-14392011005000080.
[74] Y. Han, M. Wei, X. Shi, D. Wang, X. Zhang, Y. Zhao, M. Kong, X. Song, Z. Xie, F. Li, Effects of tensile stress and soil burial on mechanical and chemical degradation potential of agricultural plastic films, Sustainability 12 (2020) 7985, https://doi.org/10.3390/su12197985.
[75] Y. Ozaki, Near-infrared spectroscopy–its versatility in analytical chemistry, Anal. Sci. 28 (2012) 545–563, https://doi.org/10.2116/analsci.28.545.
[76] P.J. Larkin, Infrared and Raman Spectroscopy: Principles and Spectral Interpretation, second ed., Elsevier, Amsterdam, 2018.
[77] M.G.J. Löder, G. Gerdts, Methodology used for the detection and identification of microplastics—A critical appraisal, in: M. Bergmann, L. Gutow, M. Klages (Eds.), Marine Anthropogenic Litter, Springer International Publishing, Cham, 2015, pp. 201–227.
[78] M. Dong, Q. Zhang, X. Xing, W. Chen, Z. She, Z. Luo, Raman spectra and surface changes of microplastics weathered under natural environments, Sci. Total Environ. 739 (2020) 139990, https://doi.org/10.1016/j.scitotenv.2020.139990.
[79] C.F. Araujo, M.M. Nolasco, A.M.P. Ribeiro, P.J.A. Ribeiro-Claro, Identification of microplastics using raman spectroscopy: latest developments and future prospects, Water Res. 142 (2018) 426–440, https://doi.org/10.1016/j.watres.2018.05.060.
[80] G.P. Macan, M. Anguita-Maeso, C. Olivares-García, Q.N.P. Le, C. Halsall, B. B. Landa, Unravelling the plastisphere-soil and plasticplane microbiome of plastic mulch residues in agricultural soils, Appl. Soil Ecol. 206 (2025) 105900, https://doi.org/10.1016/j.apsoil.2025.105900.
[81] T. Mumtaz, K.M. Mannan, M.R. Khan, Mechanical, chemical and morphological investigations on the degradation of low-density polyethylene films under soil-burial conditions, Int. J. Polym. Mater. 59 (2009) 73–86, https://doi.org/10.1080/00914030903192377.
[82] M. Stamm, Plastics, properties, and testing, in: Ullmann's Encyclopedia of Industrial Chemistry, Wiley-VCH Verlag GmbH & Co. KGaA, Weinheim, Germany, 2000, pp. 1–31.
[83] R. Förch, H. Schönherr, A.T.A. Jenkins, Surface Design: Applications in Bioscience and Nanotechnology, Wiley, 2009.
[84] Q. Huang, Z. Cheng, C. Yang, H. Wang, N. Zhu, X. Cao, Z. Lou, Booming microplastics generation in landfill: an exponential evolution process under temporal pattern, Water Res. 223 (2022) 119035, https://doi.org/10.1016/j.watres.2022.119035.
[85] F. Yu, Z. Wu, J. Wang, Y. Li, R. Chu, Y. Pei, J. Ma, Effect of landfill age on the physical and chemical characteristics of waste plastics/microplastics in a waste landfill sites, Environ. Pollut. 306 (2022) 119366, https://doi.org/10.1016/j.envpol.2022.119366.
[86] J. Yang, K. Song, C. Tu, L. Li, Y. Feng, R. Li, H. Xu, Y. Luo, Distribution and weathering characteristics of microplastics in paddy soils following long-term mulching: a field study in southwest China, Sci. Total Environ. 858 (2023) 159774, https://doi.org/10.1016/j.scitotenv.2022.159774.
[87] M. Kampschulte, A.C. Langheinirch, J. Sender, H.D. Litzlbauer, U. Althöhn, J. D. Schwab, E. Alejandre-Lafont, G. Martels, G.A. Krombach, Nano-computed tomography: technique and applications, Röfo 188 (2016) 146–154, https://doi.org/10.1055/s-0041-106541.
[88] E.L. Ritman, Current status of developments and applications of micro-CT, Annu. Rev. Biomed. Eng. 13 (2011) 531–552, https://doi.org/10.1146/annurev-bioeng-071910-124717.
[89] K. Orhan (Ed.), Micro-Computed Tomography (micro-CT) in Medicine and Engineering, Springer, Cham, Switzerland, 2020.
[90] R.J. Young, Introduction to Polymers, third ed., thirdrd ed., CRC Press, Hoboken, 2011.
[91] G. Xu, Q. Wang, Q. Gu, Y. Cao, X. Du, F. Li, Contamination characteristics and degradation behavior of low-density polyethylene film residues in typical farmland soils of China, J. Environ. Sci. Health B 41 (2006) 189–199, https://doi.org/10.1080/03601230500365069.
[92] B.D. Cullity, S.R. Stock, Pearson India Education Services, Elements of X-ray Diffraction, Pearson India Education Services, 2014.
[93] Y. Otake, T. Kobayashi, H. Asabe, N. Murakami, K. Ono, Biodegradation of low-density polyethylene, polystyrene, polyvinyl chloride, and urea formaldehyde resin buried under soil for over 32 years, J. Appl. Polym. Sci. 56 (1995) 1789–1796, https://doi.org/10.1002/app.1995.070561309.
[94] S.V. Meille, Electron diffraction in polymer crystal structure analysis: some examples, in: D.L. Dorset, S. Hovmöller, X. Zou (Eds.), Electron Crystallography, Springer Netherlands, Dordrecht, 1997, pp. 313–322.
[95] L. Bai, X. Li, H. Li, G. Sun, D. Liu, Z. wu, M. Peng, Z. Zhu, C. Huang, F. Gong, S. Li, A review of small angle scattering, neutron reflection, and neutron diffraction techniques for microstructural characterization of polymer-bonded explosives, Energetic Materials Frontiers 4 (2023) 140–157, https://doi.org/10.1016/j.enmf.2023.01.001.
[96] I.E. Wachs, M.A. Bañares (Eds.), Springer Handbook of Advanced Catalyst Characterization, Springer International Publishing, Cham, 2023.
[97] J.M. Lynch, R.N. Corniuk, K.C. Brignac, M.R. Jung, K. Sellona, J. Marchiani, W. Weatherford, Differential scanning calorimetry (DSC): an important tool for polymer identification and characterization of plastic marine debris, Environ. Pollut. 346 (2024) 123607, https://doi.org/10.1016/j.envpol.2024.123607.
[98] E. Puglisi, F. Romaniello, S. Galletti, E. Boccaleri, A. Frache, P.S. Cocconcelli, Selective bacterial colonization processes on polyethylene waste samples in an abandoned landfill site, Sci. Rep. 9 (2019) 14138, https://doi.org/10.1038/s41598-019-50740-w.
[99] V.K. Ahluwalia, Instrumental Methods of Chemical Analysis, Springer Nature Switzerland, Cham, 2023.
[100] R. Yang, Analytical Methods for Polymer Characterization, CRC Press, Boca Raton, 2018, p. 2018. CRC Press.
[101] A. Shrivastava, Introduction to Plastics Technology, William Andrew, Saint Louis, 2018.
[102] E. Gauthier, M. Nikolić, R. Truss, B. Laycock, P. Halley, Effect of soil environment on the photo-degradation of polyethylene films, J. Appl. Polym. Sci. 132 (2015) 42558, https://doi.org/10.1002/app.42558.
[103] D.M. Wiles, G. Scott, Polyolefins with controlled environmental degradability, Polym. Degrad. Stabil. 91 (2006) 1581–1592, https://doi.org/10.1016/j.polymdegradstab.2005.09.010.
[104] M. Osswald, E. Baur, S. Brinkmann, K. Oberbach, E. Schmachtenberg, International Plastics Handbook: the Resource for Plastics Engineers, fourth. ed., Hanser, Munich, 2006.

[105] X.-B. Xiong, Z.-Y. Zhao, P.-Y. Wang, F. Mo, R. Zhou, J. Cao, S.-T. Liu, F. Zhang, K. Wesly, Y.-B. Wang, X.-W. Fang, H.-Y. Tao, Y.-C. Xiong, Aging rate, environmental risk and production efficiency of the low-density polyethylene (LDPE) films with contrasting thickness in irrigated region, Ecotoxicol. Environ. Saf. 264 (2023) 115399, https://doi.org/10.1016/j.ecoenv.2023.115399.
[106] A. Sholokhova, G. Denafas, J. Ceponkus, R. Kriukiene, Microplastics release from conventional plastics during real open windrow composting, Sustainability 15 (2023) 758, https://doi.org/10.3390/su15010758.
[107] S. Bhattacharjee, DLS and zeta potential - what they are and what they are not? J. Control. Release 235 (2016) 337–351, https://doi.org/10.1016/j.jconrel.2016.06.017.
[108] O. Plohl, A. Erjavec, L. Fras Zemljič, A. Vesel, M. Čolnik, M. Škerget, Y. van Fan, L. Čuček, G. Trimmel, J. Volmajer Valh, Morphological, surface and thermal properties of polylactic acid foils, melamine-etherified resin, and polyethylene terephthalate fabric during (bio)degradation in soil, J. Clean. Prod. 421 (2023) 138554, https://doi.org/10.1016/j.jclepro.2023.138554.
[109] C.B. Crawford, Microplastic Pollutants, Elsevier Science, Kent, 2016.
[110] R. Rial-Otero, M. Galesio, J.-L. Capelo, J. Simal-Gándara, A review of synthetic polymer characterization by Pyrolysis–GC–MS, Chroma 70 (2009) 339–348, https://doi.org/10.1365/s10337-009-1254-1.
[111] V. Gianotti, D. Antonioli, K. Sparnacci, M. Laus, C. Cassino, F. Marsano, G. Seguini, M. Perego, TGA-GC–MS quantitative analysis of phosphorus-end capped functional polymers in bulk and ultrathin films, J. Anal. Appl. Pyrolysis 128 (2017) 238–245, https://doi.org/10.1016/j.jaap.2017.10.005.
[112] G. Montaudo, F. Samperi, M.S. Montaudo, Characterization of synthetic polymers by MALDI-MS, Prog. Polym. Sci. 31 (2006) 277–357, https://doi.org/10.1016/j.progpolymsci.2005.12.001.
[113] J.C. Vickerman, ToF-SIMS—An Overview, ToF-SIMS: Surface Analysis by Mass Spectrometry, 2001, pp. 1–40.
[114] M.C. Biesinger, P.L. Corcoran, M.J. Walzak, Developing ToF-SIMS methods for investigating the degradation of plastic debris on beaches, Surf. Interface Anal. 43 (2011) 443–445, https://doi.org/10.1002/sia.3397.
[115] C. Du, J. Wu, J. Gong, H. Liang, Z. Li, ToF-SIMS characterization of microplastics in soils, Surf. Interface Anal. 52 (2020) 293–300, https://doi.org/10.1002/sia.6742.
[116] K. Liu, Di Tian, C. Li, Y. Li, G. Yang, Y. Ding, A review of laser-induced breakdown spectroscopy for plastic analysis, TRAC-Trend. Anal. Chem. 110 (2019) 327–334, https://doi.org/10.1016/j.trac.2018.11.025.
[117] L. Brunnbauer, M. Mayr, S. Larisegger, M. Nelhiebel, L. Pagnin, R. Wiesinger, M. Schreiner, A. Limbeck, Combined LA-ICP-MS/LIBS: powerful analytical tools for the investigation of polymer alteration after treatment under corrosive conditions, Sci. Rep. 10 (2020) 12513, https://doi.org/10.1038/s41598-020-69210-9.
[118] L. Brunnbauer, S. Larisegger, H. Lohninger, M. Nelhiebel, A. Limbeck, Spatially resolved polymer classification using laser induced breakdown spectroscopy (LIBS) and multivariate statistics, Talanta 209 (2020) 120572, https://doi.org/10.1016/j.talanta.2019.120572.
[119] A. Belhachemi, M. Maatoug, R. Canela-Garayoa, Comparative analysis by UV-vis and FT-IR spectroscopy of the chemical degradation of polyethylene used as greenhouse cover film, J. Elastomers Plast. 54 (2022) 891–905, https://doi.org/10.1177/00952443221077439.
[120] M.P. Seah, A review of the analysis of surfaces and thin films by AES and XPS, Vacuum 34 (1984) 463–478, https://doi.org/10.1016/0042-207X(84)90084-8.
[121] K. Wagatsuma, Spectroscopy for Materials Analysis, Springer Singapore, Singapore, 2021.
[122] B. Gewert, M.M. Plassmann, M. MacLeod, Pathways for degradation of plastic polymers floating in the marine environment, Environ. Sci. Process. Impacts 17 (2015) 1513–1521, https://doi.org/10.1039/c5em00207a.
[123] S. Nanda, F. Berruti, Municipal solid waste management and landfilling technologies: a review, Environ. Chem. Lett. 19 (2021) 1433–1456, https://doi.org/10.1007/s10311-020-01100-y.
[124] L.K. Wang, M.-H.S. Wang, Y.-T. Hung (Eds.), Solid Waste Engineering and Management, 2, first ed., Springer International Publishing; Imprint Springer, Cham, 2022.
[125] I. Wojnowska-Baryła, K. Bernat, M. Zaborowska, Plastic waste degradation in landfill conditions: the problem with microplastics, and their direct and indirect environmental effects, Int. J. Environ. Res. Publ. Health 19 (2022), https://doi.org/10.3390/ijerph192013223.
[126] N.H. Jafari, T.D. Stark, T. Thalhamer, Spatial and temporal characteristics of elevated temperatures in municipal solid waste landfills, Waste Manag. 59 (2017) 286–301, https://doi.org/10.1016/j.wasman.2016.10.052.
[127] E.S. Gould, M. Rado, Homogeneous vs. heterogeneous catalysis oxidation of liquid cyclohexene catalyzed by ions and oxides of transition metals, J. Catal. 13 (1969) 238–244, https://doi.org/10.1016/0021-9517(69)90397-2.
[128] L. Hou, D. Kumar, C.G. Yoo, I. Gitsov, E.L.-W. Majumder, Conversion and removal strategies for microplastics in wastewater treatment plants and landfills, Chem. Eng. J. 406 (2021) 126715, https://doi.org/10.1016/j.cej.2020.126715.
[129] X. Qiu, S. Ma, J. Zhang, L. Fang, X. Guo, L. Zhu, Dissolved organic matter promotes the aging process of polystyrene microplastics under dark and ultraviolet light conditions: the crucial role of reactive oxygen species, Environ. Sci. Technol. 56 (2022) 10149–10160, https://doi.org/10.1021/acs.est.2c03309&ref=pdf.
[130] A.A. Shah, F. Hasan, A. Hameed, S. Ahmed, Biological degradation of plastics: a comprehensive review, Biotechnol. Adv. 26 (2008) 246–265, https://doi.org/10.1016/j.biotechadv.2007.12.005.
[131] N. Lucas, C. Bienaime, C. Belloy, M. Queneudec, F. Silvestre, J.-E. Nava-Saucedo, Polymer biodegradation: mechanisms and estimation techniques, Chemosphere 73 (2008) 429–442, https://doi.org/10.1016/j.chemosphere.2008.06.064.
[132] L. Canopoli, F. Coulon, S.T. Wagland, Degradation of excavated polyethylene and polypropylene waste from landfill, Sci. Total Environ. 698 (2020) 134125, https://doi.org/10.1016/j.scitotenv.2019.134125.
[133] E.M.S. Fernandes, A.G. de Souza, R.F.S. Da Barbosa, D.d.S. Rosa, Municipal park grounds and microplastics contamination, J. Polym. Environ. 30 (2022) 5202–5210, https://doi.org/10.1007/s10924-022-02580-5.
[134] A. Mohammadi, M. Malakootian, S. Dobaradaran, M. Hashemi, N. Jaafarzadeh, Occurrence, seasonal distribution, and ecological risk assessment of microplastics and phthalate esters in leachates of a landfill site located near the marine environment: bushehr port, Iran as a case, Sci. Total Environ. 842 (2022) 156838, https://doi.org/10.1016/j.scitotenv.2022.156838.
[135] Y. Wan, X. Chen, Q. Liu, H. Hu, C. Wu, Q. Xue, Informal landfill contributes to the pollution of microplastics in the surrounding environment, Environ. Pollut. 293 (2022) 118586, https://doi.org/10.1016/j.envpol.2021.118586.
[136] F. Zaman, M.A. Rahman, M.M. Haque, M.A. Akbor, S.M. Tareq, Pervasiveness and classification of microplastics in landfill leachate: impacts, risks, and treatment efficiency, J Hazard. Mater. Adv. 16 (2024) 100502, https://doi.org/10.1016/j.hazadv.2024.100502.
[137] M.A. Rahman, M.M. Haque, S.M. Tareq, Abundance and characteristics of microplastics in the landfill leachate of Amin Bazar, Dhaka: a potential risk to aquatic environments, Phys. Chem. Earth 134 (2024) 103573, https://doi.org/10.1016/j.pce.2024.103573.
[138] E.S. Batarseh, D.R. Reinhart, N.D. Berge, Sustainable disposal of municipal solid waste: post bioreactor landfill polishing, Waste Manag. 30 (2010) 2170–2176, https://doi.org/10.1016/j.wasman.2010.06.015.
[139] V. Redko, L. Wolska, A. Cieślak-Piotrowicz, Alteration and progressive degradation of plastic waste in a polish operational landfill analysed over 60 years, commun, Earth Environ. 5 (2024), https://doi.org/10.1038/s43247-024-01695-y.
[140] R.V. Mankhair, A. Singh, M.K. Chandel, Characterization of excavated plastic waste from an Indian dumpsite: investigating extent of degradation and resource recovery potential, Waste Manag. Res. 734242X231219654 (2024), https://doi.org/10.1177/0734242X231219654.
[141] A. Ammala, S. Bateman, K. Dean, E. Petinakis, P. Sangwan, S. Wong, Q. Yuan, L. Yu, C. Patrick, K.H. Leong, An overview of degradable and biodegradable polyolefins, Prog. Polym. Sci. 36 (2011) 1015–1049, https://doi.org/10.1016/j.progpolymsci.2010.12.002.
[142] J. Tao, Y. Liu, A. Kumar, G. Chen, Y. Sun, J. Li, W. Guo, Z. Cheng, B. Yan, Effect of landfilling time on physico-chemical properties of combustible fractions in excavated waste, Sci. Total Environ. 917 (2024) 170371, https://doi.org/10.1016/j.scitotenv.2024.170371.
[143] J. Chen, L. Huo, Y. Yuan, Y. Jiang, H. Wang, K. Hui, Y. Li, Z. Huang, B. Xi, Interactions between microplastics and heavy metals in leachate: implications for landfill stabilization process, J. Hazard Mater. 480 (2024) 135830, https://doi.org/10.1016/j.jhazmat.2024.135830.
[144] Y. Su, Z. Zhang, D. Wu, L. Zhan, H. Shi, B. Xie, Occurrence of microplastics in landfill systems and their fate with landfill age, Water Res. 164 (2019) 114968, https://doi.org/10.1016/j.watres.2019.114968.
[145] Y. Fu, G. Wu, X. Bian, J. Zeng, Y. Weng, Biodegradation behavior of Poly(Butylene adipate-co-terephthalate) (PBAT), Poly(Lactic acid) (PLA), and their blend in freshwater with sediment, Molecules 25 (2020) 3946, https://doi.org/10.3390/molecules25173946.
[146] A. Sholokhova, G. Denafas, J. Ceponkus, T. Omelianenko, Microplastics in landfill bodies: Abundance, spatial distribution and effect of landfill age, Sustainability 15 (2023) 5017, https://doi.org/10.3390/su15065017.
[147] Y. Zhang, Y. Peng, C. Peng, P. Wang, Y. Lu, X. He, L. Wang, Comparison of detection methods of microplastics in landfill mineralized refuse and selection of degradation degree indexes, Environ. Sci. Technol. 55 (2021) 13802–13811, https://doi.org/10.1021/acs.est.1c02772.
[148] R.E. Day, The role of titanium dioxide pigments in the degradation and stabilisation of polymers in the plastics industry, Polym. Degrad. Stabil. 29 (1990) 73–92, https://doi.org/10.1016/0141-3910(90)90023-Z.
[149] M.J. Jenkins, K.L. Harrison, The effect of crystalline morphology on the degradation of polycaprolactone in a solution of phosphate buffer and lipase, Polym. Adv. Technol. 19 (2008) 1901–1906, https://doi.org/10.1002/pat.1227.
[150] M.S. Rabello, J.R. White, The role of physical structure and morphology in the photodegradation behaviour of polypropylene, Polym. Degrad. Stabil. 56 (1997) 55–73, https://doi.org/10.1016/S0141-3910(96)00202-9.
[151] J.R. White, A.V. Shyichuk, Effect of stabilizer on scission and crosslinking rate changes during photo-oxidation of polypropylene, Polym. Degrad. Stabil. 92 (2007) 2095–2101, https://doi.org/10.1016/j.polymdegradstab.2007.07.013.
[152] G. Grause, M.-F. Chien, C. Inoue, Changes during the weathering of polyolefins, Polym. Degrad. Stabil. 181 (2020) 109364, https://doi.org/10.1016/j.polymdegradstab.2020.109364.
[153] L.F. Diaz (Ed.), Compost Science and Technology, first ed., Elsevier, Amsterdam, 2007.
[154] P. Weiland, Biogas production: current state and perspectives, Appl. Microbiol. Biotechnol. 85 (2010) 849–860, https://doi.org/10.1007/s00253-009-2246-7.
[155] R. Scotti, G. Bonanomi, R. Scelza, A. Zoina, M. Rao, Organic amendments as sustainable tool to recovery fertility in intensive agricultural systems, J. Soil Sci. Plant Nutr. (2015), https://doi.org/10.4067/S0718-95162015005000031, 0.

[156] K.K. Porterfield, S.A. Hobson, D.A. Neher, M.T. Niles, E.D. Roy, Microplastics in composts, digestates, and food wastes: a review, J. Environ. Qual. 52 (2023) 225–240, https://doi.org/10.1002/jeq2.20450.
[157] M. Harrington, Controlling contamination in collected organics. https://www.biocycle.net/controlling-contamination-in-collected-organics/, 2015.
[158] U.S. Environmental Protection Agency, Plastic Contamination: Emerging Issues in Food Waste Management, 2021.
[159] M. Ayilara, O. Olanrewaju, O. Babalola, O. Odeyemi, Waste management through composting: challenges and potentials, Sustainability 12 (2020) 4456, https://doi.org/10.3390/su12114456.
[160] Y. Ding, J. Zhao, J.-W. Liu, J. Zhou, L. Cheng, J. Zhao, Z. Shao, Ç. Iris, B. Pan, X. Li, Z.-T. Hu, A review of China's municipal solid waste (MSW) and comparison with international regions: management and technologies in treatment and resource utilization, J. Clean. Prod. 293 (2021) 126144, https://doi.org/10.1016/j.jclepro.2021.126144.
[161] Z. Li, H. Lu, L. Ren, L. He, Experimental and modeling approaches for food waste composting: a review, Chemosphere 93 (2013) 1247–1257, https://doi.org/10.1016/j.chemosphere.2013.06.064.
[162] J. Gui, Y. Sun, J. Wang, X. Chen, S. Zhang, D. Wu, Microplastics in composting of rural domestic waste: abundance, characteristics, and release from the surface of macroplastics, Environ. Pollut. 274 (2021) 116553, https://doi.org/10.1016/j.envpol.2021.116553.
[163] J. Arutchelvi, M. Sudhakar, A. Arkatkar, M. Doble, S. Bhaduri, P.V. Uppara, Biodegradation of polyethylene and polypropylene, Indian J. Biotechnol. 7 (2008).
[164] M. Tan, Y. Sun, J. Gui, J. Wang, X. Chen, W. Song, D. Wu, Distribution characteristics of microplastics in typical organic solid wastes and their biologically treated products, Sci. Total Environ. 852 (2022) 158440, https://doi.org/10.1016/j.scitotenv.2022.158440.
[165] D. Surendran, G.K. Varghese, C. Zafiu, Characterization and source apportionment of microplastics in Indian composts, Environ. Monit. Assess. 196 (2023) 5, https://doi.org/10.1007/s10661-023-12177-7.
[166] S. As Alariqi, A. A Mutair, Effect of different sterilization methods on biodegradation of biomedical polypropylene, J. Environ. Anal. Toxicol. 6 (2016), https://doi.org/10.4172/2161-0525.1000373.
[167] J.K. Pandey, A.P. Kumar, R.P. Singh, Biodegradation of packaging materials: composting of polyolefins, macromol, Symp. 197 (2003) 411–420, https://doi.org/10.1002/masy.200350735.
[168] E.R. Jones, M.T.H. van Vliet, M. Qadir, M.F.P. Bierkens, Country-level and gridded estimates of wastewater production, collection, treatment and reuse, Earth Syst. Sci. Data 13 (2021) 237–254, https://doi.org/10.5194/essd-13-237-2021.
[169] R. Liu, Z. Tan, X. Wu, Y. Liu, Y. Chen, J. Fu, H. Ou, Modifications of microplastics in urban environmental management systems: a review, Water Res. 222 (2022) 118843, https://doi.org/10.1016/j.watres.2022.118843.
[170] R. Rusidi, I. Rushdi, Mohamed Zin Wan, Mohd Khairul Wan, S. Hamzah, W. Khalik, S. Anuar, N. Abdullah, N. Yahya, A. Abd Rahman Azmi, Microplastics pollution mitigation in wastewater treatment: current practices, challenges, and future perspective, Malays. J. Anal. Sci. 28 (2024) 79–96.
[171] U.S. Environmental Protection Agency, Primer for Municipal Wastewater Treatment Systems, 2004. Washington DC 20460.
[172] W. Elshorbagy (Ed.), Water Treatment, InTech, 2013.
[173] M. von Sperling, Wastewater characteristics, treatment and disposal, Water Intell. Online 6 (2015) 9781780402086, https://doi.org/10.2166/9781780402086, 9781780402086.
[174] A. Joss, S. Zabczynski, A. Göbel, B. Hoffmann, D. Löffler, C.S. McArdell, T. A. Ternes, A. Thomsen, H. Siegrist, Biological degradation of pharmaceuticals in municipal wastewater treatment: proposing a classification scheme, Water Res. 40 (2006) 1686–1696, https://doi.org/10.1016/j.watres.2006.02.014.
[175] T.H. Nafea, A.J. Al-Maliki, I.M. Al-Tameemi, Sources, fate, effects, and analysis of microplastic in wastewater treatment plants: a review, Environ. Eng. Res. 29 (2024) 230040, https://doi.org/10.4491/eer.2023.040, 0.
[176] J. Hu, F.Y. Lim, J. Hu, Characteristics and behaviors of microplastics undergoing photoaging and advanced oxidation processes (AOPs) initiated aging, Water Res. 232 (2023) 119628, https://doi.org/10.1016/j.watres.2023.119628.
[177] M.M. Haque, A.T. Kabir, E.M. Latifi, D.S. Mahmud, M.R. Hossain, H.A. Himu, U. K. Fatema, S.M. Tareq, Microfiber prevalence and removal efficiency of textile effluent treatment plants in Bangladesh, J Hazard. Mater. Adv. 14 (2024) 100436, https://doi.org/10.1016/j.hazadv.2024.100436.
[178] C. Edo, M. González-Pleiter, F. Leganés, F. Fernández-Piñas, R. Rosal, Fate of microplastics in wastewater treatment plants and their environmental dispersion with effluent and sludge, Environ. Pollut. 259 (2020) 113837, https://doi.org/10.1016/j.envpol.2019.113837.
[179] J. Yang, L. Li, R. Li, L. Xu, Y. Shen, S. Li, C. Tu, L. Wu, P. Christie, Y. Luo, Microplastics in an agricultural soil following repeated application of three types of sewage sludge: a field study, Environ. Pollut. 289 (2021) 117943, https://doi.org/10.1016/j.envpol.2021.117943.
[180] X. Li, L. Chen, Q. Mei, B. Dong, X. Dai, G. Ding, E.Y. Zeng, Microplastics in sewage sludge from the wastewater treatment plants in China, Water Res. 142 (2018) 75–85, https://doi.org/10.1016/j.watres.2018.05.034.
[181] H. Kamani, M. Ghayebzadeh, F. Ganji, Tracking and risk assessment of microplastics in a wastewater treatment plant, Water Environ. J. 38 (2024) 613–627, https://doi.org/10.1111/wej.12949.
[182] J. Worek, K. Kawoń, J. Chwiej, K. Berent, R. Rego, K. Styszko, Assessment of the presence of microplastics in stabilized sewage sludge: analysis methods and environmental impact, Appl. Sci. 15 (2025) 1, https://doi.org/10.3390/app15010001.
[183] W. Zhou, J. Xu, B. Fu, Y. Wu, K. Zhang, J. Han, J. Kong, Y. Ma, Microplastic accumulation and transport in agricultural soils with long-term sewage sludge amendments, J. Hazard Mater. 480 (2024) 136263, https://doi.org/10.1016/j.jhazmat.2024.136263.
[184] Y. Ma, Z. Bao, S. Cai, Q. Wang, B. Dou, X. Niu, Q. Meng, P. Li, X. Guo, The pollution characteristics and fate of microplastics in typical wastewater treatment systems in Northern China, Separations 11 (2024) 177, https://doi.org/10.3390/separations11060177.
[185] X.-Y. Li, H.-T. Liu, L.-X. Wang, H.-N. Guo, J. Zhang, D. Gao, Effects of typical sludge treatment on microplastics in China-characteristics, abundance and micro-morphological evidence, Sci. Total Environ. 826 (2022) 154206, https://doi.org/10.1016/j.scitotenv.2022.154206.
[186] A.M. Mahon, B. O'Connell, M.G. Healy, I. O'Connor, R. Officer, R. Nash, L. Morrison, Microplastics in sewage sludge: effects of treatment, Environ. Sci. Technol. 51 (2017) 810–818, https://doi.org/10.1021/acs.est.6b04048.
[187] J. Nylen, M. Sheehan, Review of the integration of drying and thermal treatment processes for energy efficient reduction of contaminants and beneficial reuse of wastewater treatment plant biosolids, Energies 16 (2023) 1964, https://doi.org/10.3390/en16041964.
[188] P.L. Ngo, I.A. Udugama, K.V. Gernaey, B.R. Young, S. Baroutian, Mechanisms, status, and challenges of thermal hydrolysis and advanced thermal hydrolysis processes in sewage sludge treatment, Chemosphere 281 (2021) 130890, https://doi.org/10.1016/j.chemosphere.2021.130890.
[189] D. Adamcová, M. Radziemska, J. Zloch, H. Dvořáčková, J. Elbl, J. Kynický, M. Brtnický, M.D. Vaverková, SEM analysis and degradation behavior of conventional and bio-based plastics during composting, Acta Univ. Agric. Silvic. Mendelianae Brunensis 66 (2018) 349–356, https://doi.org/10.11118/actaun201866020349.
[190] M.G. Iskander, M. Hassan, Accelerated degradation of recycled plastic piling in aggressive soils, J. Compos. Construct. 5 (2001) 179–187, https://doi.org/10.1061/(ASCE)1090-0268(2001)5:3(179.
[191] S. Hajji, M. Ben-Haddad, M.R. Abelouah, N. Rangel-Buitrago, A. Ait Alla, Microplastic characterization and assessment of removal efficiency in an urban and industrial wastewater treatment plant with submarine emission discharge, Sci. Total Environ. 945 (2024) 174115, https://doi.org/10.1016/j.scitotenv.2024.174115.
[192] L.E.P. Real, Weathering of polymers and plastic materials. twentiethtwenty-third, firstst ed., Springer Nature Switzerland; Imprint Springer, Cham, 2023.
[193] L. Miao, X. Deng, X. Qin, Y. Huang, L. Su, T.M. Adyel, Z. Wang, Z. Lu, D. Luo, J. Wu, J. Hou, High-altitude aquatic ecosystems offer faster aging rate of plastics, Sci. Total Environ. 951 (2024) 175827, https://doi.org/10.1016/j.scitotenv.2024.175827.
[194] A.F. Astner, A.B. Gillmore, Y. Yu, M. Flury, J.M. DeBruyn, S.M. Schaeffer, D. G. Hayes, Formation, behavior, properties and impact of micro- and nanoplastics on agricultural soil ecosystems (A review), NanoImpact 31 (2023) 100474, https://doi.org/10.1016/j.impact.2023.100474.
[195] J.M. Ham, G.J. Kluitenberg, W.J. Lamont, Optical properties of plastic mulches affect the field temperature regime, jashs 118 (1993) 188–193, https://doi.org/10.21273/JASHS.118.2.188.
[196] E.B. Rabinovitch, J.G. Quisenberry, J.W. Summers, Predicting heat buildup due to the sun's energy, J. Vinyl Addit. Technol. 5 (1983) 110–115, https://doi.org/10.1002/vnl.730050308.
[197] K. Zhang, A.H. Hamidian, A. Tubić, Y. Zhang, J.K.H. Fang, C. Wu, P.K.S. Lam, Understanding plastic degradation and microplastic formation in the environment: a review, Environ. Pollut. 274 (2021) 116554, https://doi.org/10.1016/j.envpol.2021.116554.
[198] D. Feldman, Polymer weathering: photo-oxidation, J. Polym. Environ. 10 (2002) 163–173, https://doi.org/10.1023/A:1021148205366.
[199] J.R. White, A. Turnbull, Weathering of polymers: mechanisms of degradation and stabilization, testing strategies and modelling, J. Mater. Sci. 29 (1994) 584–613, https://doi.org/10.1007/BF00445969.
[200] P. Gijsman, Review on the thermo-oxidative degradation of polymers during processing and in service, E-Polymers 8 (2008) 65.
[201] B. Cemek, Y. Demir, Testing of the condensation characteristics and light transmissions of different plastic film covering materials, Polym. Test. 24 (2005) 284–289, https://doi.org/10.1016/j.polymertesting.2004.11.007.
[202] G. Bonyadinejad, M. Salehi, A. Herath, Investigating the sustainability of agricultural plastic products, combined influence of polymer characteristics and environmental conditions on microplastics aging, Sci. Total Environ. 839 (2022) 156385, https://doi.org/10.1016/j.scitotenv.2022.156385.
[203] M. Hakkarainen, A.-C. Albertsson, Environmental degradation of polyethylene, in: A.-C. Albertsson (Ed.), Long Term Properties of Polyolefins, Springer Berlin Heidelberg, Berlin, Heidelberg, 2004, pp. 177–200.
[204] A. Holmström, E. Sörvik, Thermal degradation of polyethylene in a nitrogen atmosphere of low oxygen content. III. Structural changes occurring in low-density polyethylene at oxygen contents below 1.2%, J. Appl. Polym. Sci. 18 (1974) 3153–3178, https://doi.org/10.1002/app.1974.070181022.
[205] J. Ge, M. Wang, P. Liu, Z. Zhang, J. Peng, X. Guo, A systematic review on the aging of microplastics and the effects of typical factors in various environmental media, TRAC-Trend. Anal. Chem. 162 (2023) 117025, https://doi.org/10.1016/j.trac.2023.117025.
[206] C. Wang, Z. Xian, X. Jin, S. Liang, Z. Chen, B. Pan, B. Wu, Y.S. Ok, C. Gu, Photo-aging of polyvinyl chloride microplastic in the presence of natural organic acids, Water Res. 183 (2020) 116082, https://doi.org/10.1016/j.watres.2020.116082.

[207] X. Wu, P. Liu, Z. Gong, H. Wang, H. Huang, Y. Shi, X. Zhao, S. Gao, Humic acid and fulvic acid hinder long-term weathering of microplastics in Lake water, Environ. Sci. Technol. 55 (2021) 15810–15820, https://doi.org/10.1021/acs.est.1c04501.
[208] J. Wenk, U. von Gunten, S. Canonica, Effect of dissolved organic matter on the transformation of contaminants induced by excited triplet states and the hydroxyl radical, Environ. Sci. Technol. 45 (2011) 1334–1340, https://doi.org/10.1021/es102212t.
[209] C. Chen, L. Chen, Y. Yao, F. Artigas, Q. Huang, W. Zhang, Organotin release from polyvinyl chloride microplastics and concurrent photodegradation in water: impacts from salinity, dissolved organic matter, and light exposure, Environ. Sci. Technol. 53 (2019) 10741–10752, https://doi.org/10.1021/acs.est.9b03428.
[210] L. Ding, Z. Ouyang, P. Liu, T. Wang, H. Jia, X. Guo, Photodegradation of microplastics mediated by different types of soil: the effect of soil components, Sci. Total Environ. 802 (2022) 149840, https://doi.org/10.1016/j.scitotenv.2021.149840.
[211] L. Ding, X. Yu, X. Guo, Y. Zhang, Z. Ouyang, P. Liu, C. Zhang, T. Wang, H. Jia, L. Zhu, The photodegradation processes and mechanisms of polyvinyl chloride and polyethylene terephthalate microplastic in aquatic environments: important role of clay minerals, Water Res. 208 (2022) 117879, https://doi.org/10.1016/j.watres.2021.117879.
[212] J. Cao, X. Gao, Q. Hu, C. Li, X. Song, Y. Cai, K.H. Siddique, X. Zhao, Distribution characteristics and correlation of macro- and microplastics under long-term plastic mulching in northwest China, Soil Tillage Res. 231 (2023) 105738, https://doi.org/10.1016/j.still.2023.105738.
[213] V. Marturano, P. Cerruti, V. Ambrogi, Polymer additives, Phys. Sci. Rev. 2 (2017), https://doi.org/10.1515/psr-2016-0130.
[214] N.C. Brady, R.R. Weil, The Nature and Properties of Soils, fifteenth ed., global edition, Pearson, Harlow, England, London, New York, 2017.
[215] K. Adhikari, A.F. Astner, J.M. DeBruyn, Y. Yu, D.G. Hayes, B.T. O'Callahan, M. Flury, Earthworms exposed to polyethylene and biodegradable microplastics in soil: microplastic characterization and microbial community analysis, ACS Agr. Sci. Tec. 3 (2023) 340–349, https://doi.org/10.1021/acsagscitech.2c00333.
[216] L. Bhattacharjee, F. Jazaei, M. Salehi, Insights into the mechanism of plastics' fragmentation under abrasive mechanical forces: an implication for agricultural soil health, Clean: Soil, Air, Water 51 (2023) 2200395, https://doi.org/10.1002/clen.202200395.
[217] Y. Li, G. Xu, Y. Yu, Freeze-thaw aged polyethylene and polypropylene microplastics alter enzyme activity and microbial community composition in soil, J. Hazard Mater. 470 (2024) 134249, https://doi.org/10.1016/j.jhazmat.2024.134249.
[218] A. Maqbool, G. Guzmán, P. Fiener, F. Wilken, M.-A. Soriano, J.A. Gómez, Tracing macroplastics redistribution and fragmentation by tillage translocation, J. Hazard Mater. 477 (2024) 135318, https://doi.org/10.1016/j.jhazmat.2024.135318.
[219] S. Chinaglia, E. Esposito, M. Tosin, M. Pecchiari, F. Degli Innocenti, Biodegradation of plastics in soil: the effect of water content, Polym. Degrad. Stabil. 222 (2024) 110691, https://doi.org/10.1016/j.polymdegradstab.2024.110691.
[220] A. Pischedda, M. Tosin, F. Degli-Innocenti, Biodegradation of plastics in soil: the effect of temperature, Polym. Degrad. Stabil. 170 (2019) 109017, https://doi.org/10.1016/j.polymdegradstab.2019.109017.
[221] M. Tosin, A. Pischedda, F. Degli-Innocenti, Biodegradation kinetics in soil of a multi-constituent biodegradable plastic, Polym. Degrad. Stabil. 166 (2019) 213–218, https://doi.org/10.1016/j.polymdegradstab.2019.05.034.
[222] A. Göpferich, Mechanisms of polymer degradation and erosion, Biomaterials 17 (1996) 103–114, https://doi.org/10.1016/0142-9612(96)85755-3.
[223] C. Maraveas, I.V. Kyrtopoulos, K.G. Arvanitis, T. Bartzanas, The aging of polymers under electromagnetic radiation, Polymers 16 (2024), https://doi.org/10.3390/polym16050689.
[224] Z.-Y. Zhao, P.-Y. Wang, Y.-B. Wang, R. Zhou, K. Koskei, A.N. Munyasya, S.-T. Liu, W. Wang, Y.-Z. Su, Y.-C. Xiong, Fate of plastic film residues in agro-ecosystem and its effects on aggregate-associated soil carbon and nitrogen stocks, J. Hazard Mater. 416 (2021) 125954, https://doi.org/10.1016/j.jhazmat.2021.125954.
[225] K. Li, W. Jia, L. Xu, M. Zhang, Y. Huang, The plastisphere of biodegradable and conventional microplastics from residues exhibit distinct microbial structure, network and function in plastic-mulching farmland, J. Hazard Mater. 442 (2023) 130011, https://doi.org/10.1016/j.jhazmat.2022.130011.
[226] A. Wahl, M. Davranche, M. Rabiller-Baudry, M. Pédrot, I. Khatib, F. Labonne, M. Canté, C. Cuisinier, J. Gigault, Condition of composted microplastics after they have been buried for 30 years: vertical distribution in the soil and degree of degradation, J. Hazard Mater. 462 (2023) 132686, https://doi.org/10.1016/j.jhazmat.2023.132686.
[227] J. Liang, X. Chen, S. Zha, X. Chen, Y. Yu, X. Duan, Y. Cao, Y. Liang, Distribution and characteristics of microplastics in agricultural soils around Gehu Lake, China, Water Air Soil Pollut 234 (2023), https://doi.org/10.1007/s11270-023-06546-8.
[228] N. Fierer, J.P. Schimel, P.A. Holden, Variations in microbial community composition through two soil depth profiles, Soil Biol. Biochem. 35 (2003) 167–176, https://doi.org/10.1016/S0038-0717(02)00251-1.
[229] D. Guasconi, J. Juhanson, K.E. Clemmensen, S.A.O. Cousins, G. Hugelius, S. Manzoni, N. Roth, P. Fransson, Vegetation, topography, and soil depth drive microbial community structure in two Swedish grasslands, FEMS Microbiol. Ecol. 99 (2023), https://doi.org/10.1093/femsec/fiad080.
[230] S.-P. Lim, S.-N. Gan, I.K.P. Tan, Degradation of medium-chain-length polyhydroxyalkanoates in tropical forest and mangrove soils, Appl. Biochem. Biotechnol. 126 (2005) 23–33, https://doi.org/10.1007/s12010-005-0003-7.
[231] Z. Xu, C. Hu, X. Wang, L. Wang, J. Xing, X. He, Z. Wang, P. Zhao, Distribution characteristics of plastic film residue in long-term mulched farmland soil, Soil Ecol. Lett. 5 (2023), https://doi.org/10.1007/s42832-022-0144-4.
[232] S. Li, F. Ding, M. Flury, Z. Wang, L. Xu, S. Li, D.L. Jones, J. Wang, Macro- and microplastic accumulation in soil after 32 years of plastic film mulching, Environ. Pollut. 300 (2022) 118945, https://doi.org/10.1016/j.envpol.2022.118945.
[233] T.K.A. Tran, S. Raju, A. Singh, K. Senathirajah, G. Bhagwat-Russell, L. Daggubati, R. Kandaiah, T. Palanisami, Occurrence and distribution of microplastics in long-term biosolid-applied rehabilitation land: an overlooked pathway for microplastic entry into terrestrial ecosystems in Australia, Environ. Pollut. 336 (2023) 122464, https://doi.org/10.1016/j.envpol.2023.122464.
[234] J. Yang, R. Li, Q. Zhou, L. Li, Y. Li, C. Tu, X. Zhao, K. Xiong, P. Christie, Y. Luo, Abundance and morphology of microplastics in an agricultural soil following long-term repeated application of pig manure, Environ. Pollut. 272 (2021) 116028, https://doi.org/10.1016/j.envpol.2020.116028.
[235] J. Zhang, W. Ding, S. Wang, X. Ha, L. Zhang, Y. Zhao, W. Wu, M. Zhao, G. Zou, Y. Chen, Pollution characteristics of microplastics in greenhouse soil profiles with the long-term application of organic compost, Resources, Environment and Sustainability 17 (2024) 100165, https://doi.org/10.1016/j.resenv.2024.100165.
[236] V. Kumar M, M. Sheela A, Effect of plastic film mulching on the distribution of plastic residues in agricultural fields, Chemosphere 273 (2021) 128590, https://doi.org/10.1016/j.chemosphere.2020.128590.
[237] M.S. Islam, Z. Islam, D. Islam, Abundance, source apportionment, and surface characteristics of microplastics in agricultural soil in a flood-prone area of central Bangladesh, Water Air Soil Pollut. 235 (2024), https://doi.org/10.1007/s11270-024-06962-4.
[238] H. Miao, S. Zhang, W. Gao, J. Zhou, H. Cai, L. Wu, J. Liu, Z. Wang, T. Liu, Microplastics occurrence and distribution characteristics in mulched agricultural soils of Guizhou province, Sci. Rep. 14 (2024) 21505, https://doi.org/10.1038/s41598-024-72829-7.
[239] A.G. Uzamurera, P.-Y. Wang, Z.-Y. Zhao, X.-P. Tao, R. Zhou, W.-Y. Wang, X.-B. Xiong, S. Wang, K. Wesly, H.-Y. Tao, Y.-C. Xiong, Thickness-dependent release of microplastics and phthalic acid esters from polythene and biodegradable residual films in agricultural soils and its related productivity effects, J. Hazard Mater. 448 (2023) 130897, https://doi.org/10.1016/j.jhazmat.2023.130897.
[240] R. Bai, H. Liu, J. Cui, Y. Wu, X. Guo, Q. Liu, Q. Liu, H. Gao, C. Yan, W. He, The characteristics and influencing factors of farmland soil microplastic in hetao irrigation district, China, J. Hazard Mater. 465 (2024) 133472, https://doi.org/10.1016/j.jhazmat.2024.133472.
[241] I.H. Craig, J.R. White, A.V. Shyichuk, I. Syrotynska, Photo-induced scission and crosslinking in LDPE, LLDPE, and HDPE, Polym. Eng. Sci. 45 (2005) 579–587, https://doi.org/10.1002/pen.20313.
[242] X. Liu, H. Lin, S. Xu, Y. Yan, R. Yu, G. Hu, Occurrence, distribution, and characteristics of microplastics in agricultural soil around a solid waste treatment center in southeast China, J. Soils Sediments 23 (2023) 936–946, https://doi.org/10.1007/s11368-022-03341-6.
[243] S. Andreasi Bassi, T.H. Christensen, A. Damgaard, Environmental performance of household waste management in Europe - an example of 7 countries, Waste Manag. 69 (2017) 545–557, https://doi.org/10.1016/j.wasman.2017.07.042.
[244] A.H. Demo, G. Asefa Bogale, Enhancing crop yield and conserving soil moisture through mulching practices in dryland agriculture, Front. Agron. 6 (2024) 1361697, https://doi.org/10.3389/fagro.2024.1361697.
[245] Y. Lv, Y. Huang, J. Yang, M. Kong, H. Yang, J. Zhao, G. Li, Outdoor and accelerated laboratory weathering of polypropylene: a comparison and correlation study, Polym. Degrad. Stabil. 112 (2015) 145–159, https://doi.org/10.1016/j.polymdegradstab.2014.12.023.
[246] F. Du, H. Cai, L. Su, W. Wang, L. Zhang, C. Sun, B. Yan, H. Shi, The missing small microplastics: easily generated from weathered plastic pieces in labs but hardly detected in natural environments, Environ. Sci. Adv. 3 (2024) 227–238, https://doi.org/10.1039/d3va00291h.
[247] P.K. Rai, C. Sonne, R.J.C. Brown, S.A. Younis, K.-H. Kim, Adsorption of environmental contaminants on micro- and nano-scale plastic polymers and the influence of weathering processes on their adsorptive attributes, J. Hazard Mater. 427 (2022) 127903, https://doi.org/10.1016/j.jhazmat.2021.127903.
[248] E.R. Zettler, T.J. Mincer, L.A. Amaral-Zettler, Life in the "plastisphere": microbial communities on plastic marine debris, Environ. Sci. Technol. 47 (2013) 7137–7146, https://doi.org/10.1021/es401288x.
[249] U. Zafar, A. Houlden, G.D. Robson, Fungal communities associated with the biodegradation of polyester polyurethane buried under compost at different temperatures, Appl. Environ. Microbiol. 79 (2013) 7313–7324, https://doi.org/10.1128/AEM.02536-13.
[250] M.C. Rillig, S.W. Kim, Y.-G. Zhu, The soil plastisphere, Nat. Rev. Microbiol. 22 (2024) 64–74, https://doi.org/10.1038/s41579-023-00967-2.
[251] M. Zhang, L. Xu, Transport of micro- and nanoplastics in the environment: Trojan-horse effect for organic contaminants, Crit. Rev. Environ. Sci. Technol. 52 (2020) 810–846, https://doi.org/10.1080/10643389.2020.1845531.
[252] R. Lehner, C. Weder, A. Petri-Fink, B. Rothen-Rutishauser, Emergence of nanoplastic in the environment and possible impact on human health, Environ. Sci. Technol. 53 (2019) 1748–1765, https://doi.org/10.1021/acs.est.8b05512.
[253] S. Muccifora, L. Giorgetti, M. Corsini, G. Di Florio, L. Bellani, Nano and submicron fluorescent polystyrene particles internalization and translocation in seedlings of Cichorium endivia L, Environ. Sci. Nano 9 (2022) 4585–4598, https://doi.org/10.1039/D2EN00732K.

[254] Y. Li, X. Lin, J. Wang, G. Xu, Y. Yu, Mass-based trophic transfer of polystyrene nanoplastics in the lettuce-snail food chain, Sci. Total Environ. 897 (2023) 165383, https://doi.org/10.1016/j.scitotenv.2023.165383.
[255] Y. Jia, E. Klumpp, R. Bol, W. Amelung, Uptake of metallic nanoparticles containing essential (Cu, Zn and Fe) and non-essential (Ag, Ce and Ti) elements by crops: a meta-analysis, Crit. Rev. Environ. Sci. Technol. 53 (2023) 1512–1533, https://doi.org/10.1080/10643389.2022.2156225.
[256] L. Li, Y. Luo, R. Li, Q. Zhou, W.J.G.M. Peijnenburg, N. Yin, J. Yang, C. Tu, Y. Zhang, Effective uptake of submicrometre plastics by crop plants via a crack-entry mode, Nat. Sustain. 3 (2020) 929–937, https://doi.org/10.1038/s41893-020-0567-9.
[257] N. Carpita, D. Sabularse, D. Montezinos, D.P. Delmer, Determination of the pore size of cell walls of living plant cells, Science 205 (1979) 1144–1147, https://doi.org/10.1126/science.205.4411.1144.
[258] P. Miralles, T.L. Church, A.T. Harris, Toxicity, uptake, and translocation of engineered nanomaterials in vascular plants, Environ. Sci. Technol. 46 (2012) 9224–9239, https://doi.org/10.1021/es202995d.
[259] P. Zhou, L. Wang, J. Gao, Y. Jiang, M. Adeel, D. Hou, Nanoplastic–plant interaction and implications for soil health, Soil Use Manag. 39 (2023) 13–42, https://doi.org/10.1111/sum.12868.
[260] R. Klíč, M. Kravka, L. Wimmerová, J.L.G. Viruez, M. Válová, M. Miháliková, Microplastics locked in water-stable aggregates of the haplic luvisol and role of land use on their potential mobility, Water Air Soil Pollut. 233 (2022), https://doi.org/10.1007/s11270-022-05499-8.
[261] A. Lehmann, K. Fitschen, M.C. Rillig, Abiotic and biotic factors influencing the effect of microplastic on soil aggregation, Soil Syst. 3 (2019) 21, https://doi.org/10.3390/soilsystems3010021.